

The Riemann Problem for a Weakly Hyperbolic Two-Phase Flow Model of a Dispersed Phase in a Carrier Fluid

Dissertation

zur Erlangung des akademischen Grades

**doctor rerum naturalium
(Dr. rer. nat.)**

von M. Sc. Christoph Matern

geb. am 20.07.1986 in Halle (Saale), Deutschland

genehmigt durch die Fakultät für Mathematik
der Otto-von-Guericke-Universität Magdeburg

Gutachter: PD Dr. Maren Hantke
Prof. Dr. Christiane Helzel
Prof. Dr. Gerald Warnecke

eingereicht am: 10.09.2021

Verteidigung am: 01.02.2022

Ehrenerklärung

Ich versichere hiermit, dass ich die vorliegende Arbeit ohne unzulässige Hilfe Dritter und ohne Benutzung anderer als der angegebenen Hilfsmittel angefertigt habe; verwendete fremde und eigene Quellen sind als solche kenntlich gemacht.

Ich habe insbesondere nicht wissentlich:

- Ergebnisse erfunden oder widersprüchliche Ergebnisse verschwiegen,
- statistische Verfahren absichtlich missbraucht, um Daten in ungerechtfertigter Weise zu interpretieren,
- fremde Ergebnisse oder Veröffentlichungen plagiiert oder verzerrt wiedergegeben.

Mir ist bekannt, dass Verstöße gegen das Urheberrecht Unterlassungs- und Schadenersatzansprüche des Urhebers sowie eine strafrechtliche Ahndung durch die Strafverfolgungsbehörden begründen kann. Die Arbeit wurde bisher weder im Inland noch im Ausland in gleicher oder ähnlicher Form als Dissertation eingereicht und ist als Ganzes auch noch nicht veröffentlicht.

Magdeburg, den 09.09.2021

Christoph Matern

Abstract

We study the two-phase flow model proposed by Dreyer, Hantke and Warnecke [22]. The model describes the evolution of a mixture of a dispersed phase of small ball-shaped bubbles of water vapor, immersed in a carrier fluid, the corresponding liquid water phase. The model was derived from microscopic physical laws using averaging techniques and it is completely in divergence form.

For the mathematical analysis here, we will only consider one space dimension, neglect the phase exchange terms handling phase transitions and assume isothermal flow. In this form, it is a weakly hyperbolic system of conservative partial differential equations.

Since we can not use any of the existing results for the Cauchy problem of systems of conservation laws, we can not solve for arbitrary initial data but only for Riemann initial data.

This thesis includes the first analysis of the Riemann problem of the two-phase flow model considered. We perform the eigenstate analysis on the dispersed phase alone as well as the full two-phase system of equation. The wave types and all possible wave patterns are found. These patterns may contain delta-shocks or vaporless states.

Solutions to the Riemann problem are found by solving highly nonlinear systems of algebraic equations. These solutions are self-similar and uniquely determined by the initial data. All solutions are given implicitly and uniqueness was shown using monotonicity arguments. The final result is a set of inequalities for the relative velocity between the two phases involved. To ensure the uniqueness of the solution, this relative velocity should be a certain amount smaller than the sound speed in the carrier phase. Its explicit value depends on the chosen equation of state and the parameters therein, as well as the initial data used. These bounds on the velocity are not sharp but give a sufficient criterion to ensure the uniqueness of the solution.

We study bubbles in a liquid carrier as well as droplets or dust particles in a vapor carrier. In a gas, the equation of state (EOS) for isothermal flow yields the pressure as a linear function of the density. For a liquid, the simplest realistic assumptions lead to an affine function for the EOS. We extend the usual discussion of a linear equation of state to an affine linear one and therefore include commonly used equations of state like the Tait equation or the stiffened gas equation. The analysis for an affine linear equation of state is much more complicated. This is a key point of this thesis. Nonetheless, all possible wave configurations are discussed, the implicit functions to find a solution are given and the inequalities assuring monotonicity are stated as well.

Numerical simulations for all considered cases were performed using a second-order MUSCL-Hancock type scheme with MINBEE limiters and the HLL approximate Riemann solver. To improve the results, the new GHLL approximate Riemann solver was constructed and tested.

Zusammenfassung

In dieser Arbeit untersuchen wir das zwei-Phasen Modell, welches von Dreyer, Hantke und Warnecke eingeführt wurde [22]. Das Modell beschreibt die zeitliche Entwicklung einer Mischung aus einer gelösten Phase, bestehend aus kleinen kugelförmigen Blasen von Wasserdampf, in zugehöriger Trägerphase aus flüssigem Wasser. Das Modell wurde durch Mittelungstechniken mikroskopischer physikalischer Gesetzmäßigkeiten hergeleitet und ist vollständig in Divergenzform.

Für die mathematische Analyse wurde eine Raumdimension betrachtet, Quellterme vernachlässigt, welche für Phasenübergänge verantwortlich sind und eine isotherme Strömung angenommen. In dieser Form ist das resultierende Modell schwach hyperbolisch und besteht aus speziellen partiellen Differentialgleichungen, sogenannten Erhaltungsgleichungen.

Da die bestehende Theorie zu Cauchy-Problemen für Systeme von Erhaltungsgleichung nicht angewandt werden kann, konstruieren wir Lösungen nicht zu beliebigen Anfangsdaten, sondern nur zu Riemann-Anfangsdaten.

Die vorliegende Arbeit enthält die erste mathematische Analyse des Riemann-Problems für das betrachtete zwei-Phasen Modell. Eine Analyse der Eigenzustände wird für die gelöste Phase, wie auch für das volle zwei-Phasen System durchgeführt. Alle Wellentypen und alle möglicherweise auftretenden Wellenkonfigurationen werden dabei gefunden. Diese Wellenkonfigurationen können delta-Stöße oder gasfreie Zustände enthalten.

Lösungen des Riemann-Problems werden als Lösungen hochgradig nicht-linearer algebraischer Gleichungssysteme gefunden. Diese Lösungen sind selbstähnlich und eindeutig bestimmt durch die Anfangsdaten. Alle Lösungen werden implizit angegeben und Eindeutigkeit wurde mit Hilfe eines Monotoniearguments gezeigt. Im Ergebnis erhält man Ungleichungen für die relative Geschwindigkeit zwischen den beiden Phasen. Um Eindeutigkeit zu garantieren muss diese Relativgeschwindigkeit einen gewissen Betrag kleiner sein als die Schallgeschwindigkeit in der Trägerphase. Der genaue Wert hängt von der gewählten Zustandsgleichung und den darin gewählten Parametern, wie auch von den Anfangsdaten ab. Diese Forderungen an die Geschwindigkeit sind keine scharfen Ungleichungen, aber stellen hinreichende Kriterien für die Eindeutigkeit dar.

Untersucht werden neben Blasen in flüssiger Trägerphase auch Tropfen oder Staubpartikel in gasförmiger Trägerphase. In einer Gasphase wird die Zustandsgleichung durch eine lineare Funktion des Drucks in Abhängigkeit der Dichte gegeben. Für eine Flüssigkeit führt die einfachste realistische Annahme auf eine affin lineare Funktion der Zustandsgleichung. Die Analyse wird auf diese affin linearen Funktionen ausgeweitet und enthält daher die für die Beschreibung von Flüssigkeiten üblicherweise als Zustandsgleichung benutzten Tait-Gleichung und stiffened-gas Gleichung. Die mathematische Analyse dieser affin linearen Zustandsgleichung gestaltet sich deutlich komplizierter. Diese Betrachtungen sind einer der zentralen Punkte dieser Arbeit. Nichtsdestotrotz werden alle möglichen Wellenkonfigurationen diskutiert und die impliziten Funktionen zum Auffinden von Lösungen sowie die

Monotonie garantierenden Ungleichungen angegeben.

Für alle betrachteten Fälle werden numerische Simulationen durchgeführt. Dazu wurde das zweite Ordnung MUSCL-Hancock Schema mit MINBEE Limitern und HLL Riemann-Löser verwendet. Um die numerischen Resultate zu verbessern, wurde der neue GHLL Riemann-Löser konstruiert und getestet.

Contents

Ehrenerklärung	iii
Abstract	v
Zusammenfassung	vii
1 Introduction	1
2 The two-phase Flow Model	7
2.1 The general two-phase flow model	7
2.2 The isothermal model	9
2.3 Equations of state	10
2.4 Lower and upper bounds for carrier phase quantities	12
3 Notions on Nonlinear Hyperbolic Equations	13
3.1 Nonlinear scalar hyperbolic equations	13
3.1.1 Solution along characteristics	15
3.1.2 Rarefaction waves	17
3.1.3 Shock waves	18
3.1.4 Integral form of conservation laws	20
3.1.5 Rankine-Hugoniot jump conditions	22
3.1.6 Non-uniqueness and Lax entropy condition	23
3.2 Nonlinear hyperbolic systems	26
3.2.1 Simple waves	29
3.2.2 The Riemann problem	31
3.2.3 Rarefaction waves and Riemann invariants	31
3.2.4 Shock waves and contact discontinuities	40
3.2.5 General existence and uniqueness results	46
4 Analytical Results for the Two-Phase Flow Model	49
4.1 The dispersed phase equations	49
4.1.1 Linear analysis of the dispersed phase equations	50
4.1.2 The case $v_- = v_+ = v$	51

4.1.3	The case $v_- < v_+$	51
4.1.4	The case $v_- > v_+$	53
	Generalized Rankine-Hugoniot relations for delta-shocks	54
4.2	The carrier phase quantities	58
4.2.1	Linear analysis of the full system	59
4.2.2	Rarefaction waves	60
4.2.3	Shock waves	61
4.3	The carrier phase solution	62
4.4	The case $v_- = v_+ = v$	63
4.4.1	Contact wave	63
4.4.2	Vapor carrier phase	65
4.4.3	Liquid carrier phase	67
4.5	The case $v_- < v_+$	73
4.6	The case $v_- > v_+$	77
5	Numerical Concepts and Results	79
5.1	The finite volume framework - Upwind and central schemes	79
5.1.1	First-order upwind schemes	82
5.1.2	The Godunov method	84
5.1.3	The Roe scheme	86
5.1.4	First-order central schemes	87
5.1.5	First-order finite volume schemes - Summary	89
5.1.6	Second-order finite volume methods	90
5.2	The MUSCL Method	92
5.2.1	The MUSCL-Hancock method	93
5.3	The HLL and HLLC approximate Riemann solvers	95
5.4	The GHLL approximate Riemann solver	98
5.5	Method of modified equation analysis	103
5.6	Numerical simulations	108
6	Conclusion and Outlook	115
A	Calculations	117

Multi-phase flows occur in many natural and engineering applications. Consider the following phases of matter: gas, liquid and solid. We are interested in flows in which one phase is dispersed in a carrier phase. With these phases, the two-phase flows can be separated into three categories: gas-liquid, gas-solid and liquid-solid flows. The first category includes so called "bubbly flows" of gas bubbles in a liquid carrier. One finds these, for example, in chemical reactors. Ship manufacturers are interested to know the effects of bubbles formed in water due to cavitation because they cause substantial damage to propellers. In this category, a second flow form is gas-droplet flows typically found in atmospheric physics, where cloud formation is of considerable interest. It involves liquid water and its vapor, as well as a mixture of other gases. Other examples are sprays with various applications. The second category is gas-solid particle flows. These occur in astrophysics during star formation or in powder applications in the industry. The third category consists of solid-liquid flows, which play an essential role in transport processes like sedimentation. Here, the solid phase should only occur in the role of the dispersed phase. Otherwise, if the solid takes the role of the carrier phase, one has the field of porous media flows, which is quite different in nature. In the beverage industry, coffee beans are sugar-coated using a fluidized bed granulator. This process involves a mixture of solid particles, liquid sprays and gas flow. All such processes are modeled using two-phase or multi-phase flow models.

A central question in the modeling of two-phase flows is the treatment of the interfaces between the two phases. A first approach is to incorporate the interface directly into the model as a free boundary in the flow. The interface itself is a discontinuity in the flow and the mathematical formulation leads to a free-boundary problem. These models are called *sharp-interface models* and they allow the exact determination of the interface position at any time. An extensive study of sharp interface two-phase flows described by the Euler equations can be found in the dissertation of Thein [81]. Even though this formulation is suited for many problems, it also has its limitations. Physically a phase boundary is not a sharp discontinuity. Any internal structure and physical phenomena having a length scale comparable with the width

of the interface region are neglected. Furthermore, topological changes are very hard to describe with these kinds of models. For example, merging or creation of a bubble or a droplet due to condensation or evaporation, respectively, leads to difficulties in the mathematical description of these interfaces.

If one wants to include the internal structure of an interface or consider flows with large interface deformations, a fitting description is given by *diffuse interface models*. Here, a special phase parameter or order parameter is included in the system, which can change continuously between the two states indicating a pure phase. Therefore, the sharp interface is replaced by a thin interfacial layer in which the order parameter, which can be a concentration, rapidly changes its value. Diffuse interface models are well established in the literature for two-phase flows of liquids with identical densities, see for example Hohenberg and Halperin [40]. The model of Hohenberg and Halperin has been modified in a thermodynamically consistent way to allow for different densities. A compressible diffuse interface model for a two-phase flow with non-matching densities was derived by Dreyer, Gieselmann and Kraus [20]. Large differences in densities between liquid and vapor, which are of the order 10^3 , still seem problematic. For details, we would like to refer the reader to an upcoming PhD thesis of Hazem Yaghi.

In the work presented here, we are not particularly interested in the evolution of single bubbles or droplets. Therefore, we would like to describe the evolution of macroscopic quantities. Starting from basic physical laws, there are many techniques to arrive at a macroscopic model. On a macroscopic level, often mixture models are applied. In these models, both phases may be present at any point in space and time. This is taken into account by volume fraction density functions. The equations are usually derived from microscopic considerations using averaging or homogenization techniques, see e.g. Drew and Passman [18], Ishii [41], Nigmatulin [66], Stewart and Wendroff [79], Crowe et al. [13] or Saurel and Abgrall [72]. Alternatively, one may postulate macroscopic balances from basic physical laws, see e.g. Müller and Ruggeri [65] as well as Baer and Nunziato [3].

The theoretical results which we will describe in this thesis were already published in [34, 35]. Some of the following parts of the introduction were taken from these publications.

We study the two-phase flow model proposed by Dreyer, Hantke and Warnecke [22]. The model describes the evolution of a mixture of a dispersed phase of small ball-shaped bubbles of water vapor immersed in a carrier fluid, the corresponding liquid water phase. The model was derived using averaging techniques and it is completely in divergence form, unlike those studied in [3] as well as [79]. For the mathematical analysis here, we will only consider one space dimension, neglect the phase exchange terms handling phase transitions and assume isothermal flow. In this form, we may also consider the case of droplets in vapor. It turns out that, due to the equations of state for the carrier phase, droplets in a gas are mathematically a simpler case than gas bubbles or solids in a liquid.

The assumption of isothermal flow that we make is actually a well justified approximation and simplification for flows with phase transitions. The physical interpretation is that a constant temperature is due to an infinitely fast heat flow. This does not respect the fundamental physical assumption of finite propagation speeds, a flaw it shares with the heat equation. However, it turns out to be a useful approximation. Due to this assumption, the latent heat released or bound in a phase transition can be taken care of. If we used an energy balance, we would need to include a heat flux such as Fourier's law. This would change the mathematical properties of the energy balance. Having an Euler equation type energy conservation leads to inconsistencies in the case of phase transitions, see Hantke and Thein [37].

It is important to note that omission of the source terms, which model phase transitions, leads to the formation of solutions with delta-shocks in certain cases. These are solutions with moving singular point measures. They appear due to the fact that in these physical situations a phase transition would occur. In our model, this generation of the singularity comes along with unphysical values of the volume fractions that are larger than 1 for the vapor and negative for the liquid. These solutions also appear because on the macroscopic scale, modeled by the mixture equations, there is no pressure for the disperse phase. The dispersed phase particles do not exert any forces on each other on the microscopic scale. Only forces due to collisions would lead to a pressure at the macroscopic scale. The pressure in gas dynamics counteracts singularity formation. Analogously, here the phase exchange terms would prevent singularity formation.

The emergence of delta-shocks in our model is quite analogous to the situation in the system of zero pressure or pressureless gas that models for example small dusty particle clouds like a gas in outer space, see e.g. Shandarin and Zeldovich [75, Section VII]. Since the particles do not interact in the form of a Brownian motion on the microscopic scale, there is no pressure force on the macroscopic scale. Due to accretion, these dusty particles can agglomerate to form larger solid particles like planets or a star out of a gas cloud. These are modeled by singular measure solutions to the equations, see e.g. Bouchut [5], Sheng and Zhang [76] or E et al. [25]. This is a kind of phase transition in this model. A similar form of singularity formation due to phase transition in coagulation/agglomeration models is called gelation, see e.g. Ernst et al. [26], Escobedo et al. [27] or Jeon [43].

Another important mathematical feature of multi-phase mixture conservation laws is that they have *weakly hyperbolic states*. By this, we mean that all eigenvalues are real but there is at least one multiple eigenvalue that does not have a full set of eigenvectors. Existence results for hyperbolic systems of conservation laws in one space dimension require strict hyperbolicity, i.e. a full set of distinct real eigenvalues. Therefore, the existing theory does not apply to our system.

One of the most important results concerning the Cauchy problem for systems of conservation laws in one space dimension is obtained using Glimm's scheme, see [29]. Although the Glimm scheme gives a general existence result, we cannot make use of it. To construct a global solution it uses Lax's

theorem for the local solution and therefore needs the system under consideration to be strictly hyperbolic. As we will show in this work, the system under consideration is only weakly hyperbolic. For initial states sufficiently close to each other one more global existence result of solutions to the Cauchy problem for systems of conservation laws was obtained by Bressan [6] using the so called *front tracking algorithm*. But again, to keep track of the wave fronts, one of the crucial requirements for the system of conservation laws under consideration is that it is strictly hyperbolic.

Due to the lack of a general theory, we will consider Riemann problems only and not general initial data. We will analyze the elementary wave structure and use Riemann invariants as well as Rankine-Hugoniot jump conditions to determine a highly nonlinear system of algebraic equations connecting the initial states to each other. We then have to find a solution to these nonlinear systems to provide a solution and use monotonicity arguments to show uniqueness.

Simple models related to our model were studied by Zheng [92]. In the popular Baer-Nunziato mixture model [3] there are some physical states for which weak hyperbolicity occurs, see e.g. Andrianov and Warnecke [2]. In the latter reference, these states were called parabolic degenerate. The term weakly hyperbolic seems to be more adequate. The model we study here is weakly hyperbolic for all states. An advantage of the model considered here is that the equations are in divergence form, whereas the Baer-Nunziato model has non-divergence terms that complicate the handling of discontinuous weak solutions.

We will show the existence of self-similar solutions to the Riemann problem that are uniquely determined by the initial data of the problems. These use the well known self-similarity of conservation laws. Our system (2.5) below has some partial similarities to the Euler equations for which details on the solutions to Riemann problems can be found in Evans [28], Smoller [78], and Toro [83]. In our case, the solutions include classical waves such as rarefactions, shock waves and contact discontinuities. Interestingly, in some cases, it is possible to obtain solutions involving vaporless states as well as the non-classical delta-shock waves already mentioned above.

The vaporless states are analogues of the vacuum in gas dynamics, see e.g. Liu and Smoller [60]. We already mentioned that delta-shocks appear because the equations for the disperse phase are related to zero pressure gas dynamics. Cheng et al. [10] constructed such solutions, see also Li and Zhang [55]. Sheng and Zhang [76] studied the zero pressure gas dynamics model and showed the existence of solutions involving delta-shocks as well as vacuum states. Yang [90] also proved the existence of vacuum states and delta-shocks for a system of conservation laws that has a particular structure generalizing the zero pressure gas. Li and Yang [54] obtained delta-shocks as limits of vanishing viscosity by adding a diffusive term to the system.

Delta-shocks appear in other contexts too. Mazzotti [62] constructed delta-shock solutions for a nonlinear model of chromatography and also proved their existence experimentally in Mazzotti et al. [63]. Tan et al. [80] showed that delta-shocks are limiting solutions for hyperbolic conservation laws with

vanishing viscosity. Keyfitz and Kranzer [45] showed that singular shock solutions for a specific strictly hyperbolic system of conservation laws are well defined in a space of weighted measures and satisfy viscosity limits. We see that delta-shocks are not connected to weak hyperbolicity but due to nonlinear terms that allow singularity formation in finite time while additional terms preventing them are absent.

Our ultimate goal is to construct numerical solutions for two or three dimensional isothermal versions of the system of balance laws (2.1) using splitting methods, see e.g. Toro [83] and the literature cited therein. Such methods involve solving Riemann problems for the homogeneous part of the model. This work exclusively addresses the Riemann problem. Our aim in this thesis is to understand the mathematical structure of the conservation part of the model.

We perform the eigenstate analysis on the dispersed phase alone as well as the full two-phase system of equation. The wave types and all possible wave patterns are found.

Since we can not use any of the existing results for the Cauchy problem of systems of conservation laws, we can not solve for arbitrary initial data but only for Riemann initial data.

Solutions to the Riemann problem are found by solving highly nonlinear systems of algebraic equations. All solutions are given implicitly and uniqueness is shown using monotonicity arguments. The final result is a set of inequalities for the relative velocity between the two phases involved. This relative velocity should be a certain amount smaller than the sound speed in the carrier phase. Its explicit value depends on the chosen equation of state and the parameters therein, as well as the initial data used. These bounds on the velocity are not sharp but give a sufficient criterion to ensure the uniqueness of the solution.

We study bubbles in a liquid carrier as well as droplets or dust particles in a vapor carrier. In a gas, the equation of state (EOS) for isothermal flow yields the pressure as a linear function of the density. For a liquid, the simplest realistic assumptions lead to an affine function for the EOS. Therefore, we extend the usual discussion of a linear equation of state to an affine linear one. The analysis for an affine linear equation of state is much more complicated. This is a key point of this thesis. Nonetheless, all possible wave configurations are discussed, the implicit functions to find a solution are given and the inequalities assuring monotonicity are stated as well.

This thesis includes the first analysis of the two-phase flow model considered. It takes a first step from a linear equation of state towards more general equations of state, which is very important with regard to applications. Commonly used equations of state like the Tait equation or the stiffened gas equation are included in our analysis. It is remarkable how the slight change in the equation of state complicated the analysis considerably.

Initial data are given for all relevant cases. We choose in particular physically reasonable values. Numerical simulations are done with a second-order MUSCL-Hancock type scheme for all the cases mentioned. We construct a

new approximate Riemann solver called GHLL solver, which is an adapted HLL solver for the model considered. In all cases, the analytical and numerical solutions are found to be in very good agreement with each other.

The thesis is organized in the following way:

Chapter 2 contains an overview of the complete system given in [22] as well as the isothermal version. The different choices which are possible for the equation of state are discussed. With the choice of an affine linear equation of state, we included physical relevant descriptions for the liquid phase.

Chapter 3 starts with an introduction to the concepts used to determine the analytical solution of the Riemann problems considered. We start with a short introduction to the nonlinear scalar case to get the basic ideas in a simple setting. The reader familiar with hyperbolic conservation laws may skip this section.

We continue to describe the theory used for systems of conservation laws. Special attention was given to the concepts of Riemann invariants and the Rankine-Hugoniot jump conditions due to their importance in the work below. We show how these relations are derived and used by giving a simple example. A small comment is made that the classical Riemann invariants and the generalized Riemann invariants are in fact the same object.

Chapter 4 contains the main analytical results which were published in [34,35]. In Section 4.1 the analytical solution for the Riemann problem of the dispersed phase is derived. We start from the quasi-linear system and determine wave speeds and wave structures. For all possible cases, we give an exact solution. From Section 4.2 on we discuss the carrier phase equations. Again, we determine wave speeds and wave structures as well as Riemann invariants and jump conditions. These relations allow us to construct a nonlinear system of equations connecting both initial states to each other. This system allows us to calculate a solution for the unknown quantities at least implicitly and the usage of a monotonicity argument to show uniqueness. Again, we discuss all possible wave configurations. Both the cases of vapor and liquid as carrier phases are taken into account.

Chapter 5 contains all aspects regarding numerical simulations. We start with an introduction to first-order finite volume methods. Then, we discuss higher-order methods, especially the MUSCL-Hancock method as our method of choice. Section 5.3 gives a brief overview of the classical HLL and HLLC approximate Riemann solvers. The following Section 5.4 contains the construction of the problem-specific GHLL Riemann solver, which was published in [36]. We then briefly comment on the numerical analysis and try to motivate the choice of the numerical method used in Section 5.5. We conclude this part with numerical simulations of the examples given in Chapter 4 in comparison to the exact solution calculated there.

In **Chapter 6** we give a brief summary of the presented work. Furthermore, we comment on ongoing work and related open problems.

The two-phase Flow Model

We study the two-phase flow model proposed by Dreyer, Hantke and Warnecke [22]. It can describe the evolution of a mixture of a dispersed phase immersed in a carrier fluid. The model was derived using spatial averaging techniques as described in Drew and Passman [18]. A sliding average over a ball of radius $a > 0$ was used, where the diameter $d = 2a$ is the scale at which the macroscopic equations are described. The radii of the dispersed phase bubbles or droplets are assumed to be considerably smaller than a .

The resulting model is completely in divergence form, unlike those studied by Baer and Nunziato [3] as well as Stewart and Wendroff [79]. To avoid the problem of the necessity of closure relations in the final macroscopic model already the microscopic equations for the continuous phase used for the averaging are equipped with equations of state.

We give a complete description of the model for completeness, but we will skip the derivation since this work does not focus on mathematical modeling. The interested reader is referred to the two works of Dreyer, Hantke and Warnecke [19, 22]. The following parts of this chapter are based on the presentation given in [35].

2.1 The general two-phase flow model

Our variables are volume fraction of the dispersed phase c , pressure p , mass density ρ , mean particle radius density R , mass distribution of the dispersed particles m , temperature T , surface tension σ , specific total energy e , heat flux \mathbf{Q} , and velocity components v^j in three space dimensions with $j = 1, 2, 3$. The quantities R and m arise from the modeling of the phase transitions. We will use boldface to represent vectors as well as the subscript C to distinguish the carrier phase from the dispersed phase, the latter one without a subscript. The time and space variables are respectively $t \in \mathbb{R}_{\geq 0}$ and $\mathbf{x} \in \mathbb{R}^3$. We also include the gravitational acceleration \mathbf{g} for completeness of the general model. We will disregard the heat flux in all further considerations below. Gravitational terms are meaningful only if the flow direction is vertical. We will therefore ignore them when we consider horizontal one dimensional flows.

We consider balance equations for the volume fraction of the dispersed phase c , the density ρ , three components of the momentum ρv^j , the total energy e and the radius density R of the dispersed phase as well as density ρ_c , three components of momentum $\rho_c v_c^j$ and total energy e_c for the carrier phase. We assume that the volume is completely filled by both phases. Therefore, the volume fraction of the carrier phase is $c_c = 1 - c$. The pressure p_c will be given as a function of the density ρ_c by an equation of state. This will be discussed in the following subsection. We introduce the mass, volume, momentum and energy transfer terms Π_ρ , Π_c , Π_m^j and Π_e respectively. They will be given below. Then the model in Hantke et al. [22] consists of the following system of partial differential equations

$$\begin{aligned}
\frac{\partial c}{\partial t} + \nabla_{\mathbf{x}} \cdot (c \mathbf{v}) &= \Pi_c \\
\frac{\partial c \rho}{\partial t} + \nabla_{\mathbf{x}} \cdot (c \rho \mathbf{v}) &= \Pi_\rho \\
\frac{\partial c \rho v^j}{\partial t} + \nabla_{\mathbf{x}} \cdot (c \rho v^j \mathbf{v}) - c \rho \mathbf{g}^j &= \Pi_m^j \\
\frac{\partial c \rho e}{\partial t} + \nabla_{\mathbf{x}} \cdot (c \rho e \mathbf{v}) - c \rho \mathbf{g} \cdot \mathbf{v} &= \Pi_e \\
\frac{\partial c R}{\partial t} + \nabla_{\mathbf{x}} \cdot (c R \mathbf{v}) &= \frac{4R}{3} \Pi_c \\
\frac{\partial}{\partial t} [(1-c)\rho_c] + \nabla_{\mathbf{x}} \cdot [(1-c)\rho_c \mathbf{v}_c] &= -\Pi_\rho \\
\frac{\partial}{\partial t} [(1-c)\rho_c v_c^j] + \nabla_{\mathbf{x}} \cdot [(1-c)\rho_c v_c^j \mathbf{v}_c] + \frac{\partial (1-c)p_c}{\partial x_j} - (1-c)\rho_c \mathbf{g}^j &= -\Pi_m^j \\
\frac{\partial}{\partial t} [(1-c)\rho_c e_c] + \nabla_{\mathbf{x}} \cdot [(1-c)(\rho_c e_c + p_c) \mathbf{v}_c + \mathbf{Q}_c] - (1-c)\rho_c \mathbf{g} \cdot \mathbf{v}_c &= -\Pi_e.
\end{aligned} \tag{2.1}$$

Let k be the standard Boltzmann constant, z a constant which depends on the atomic structure of the gas considered, σ the surface tension at the interfaces between the phases and $\dot{\psi}$ represent differentiation of a quantity ψ with respect to time t . Then the transfer terms appearing in system (2.1) are given by

$$\Pi_\rho = \frac{c \dot{m}}{\frac{4}{3}\pi R^3}, \quad \Pi_c = \frac{3c \dot{R}}{R}, \quad \Pi_m^j = -\frac{c \dot{m} v^j}{\frac{4}{3}\pi R^3}, \quad \Pi_e = \frac{c \dot{m} e}{\frac{4}{3}\pi R^3} + c \rho \dot{T} \frac{kz}{m_0} + 6 \frac{c \sigma \dot{R}}{R^2}. \tag{2.2}$$

In order to maintain the nature of the disperse phase in a given carrier phase, the dispersed phase volume fraction should not exceed a certain threshold which should be smaller than one. Otherwise, the assumptions made in deriving the model lose their validity. Although not considered in the derivation of the model, in the limit $c \rightarrow 1$, one obtains a valid model. Setting c identically to 1 makes the first equation trivial and leaves us with an extended zero pressure gas model, see Sheng and Zhang [76]. The carrier phase is eliminated and the phase transition terms become meaningless.

Next we give the expressions for the quantities \dot{R} and \dot{m} appearing in

(2.2). According to Hantke et al. [22], when the liquid is compressible, they are determined from the following system of ODEs

$$\begin{aligned}
\dot{m} &= \frac{4\pi R^2 \rho m_0}{\sqrt{2\pi m_0 k T}} \left[\frac{1}{\rho_c} \left(\frac{\rho k T}{m_0} - \frac{2\sigma}{R} - \bar{p} \right) - \frac{k T}{m_0} \ln \frac{\rho k T}{\bar{p} m_0} - \frac{1}{2} \left(\frac{1}{\rho_c} - \frac{1}{\rho} \right)^2 \left(\frac{\dot{m}}{4\pi R^2} \right)^2 \right] \\
\Phi'(R - a_c t) &= \frac{R}{\rho_c a_c} \left(\frac{\rho k T}{m_0} - \frac{2\sigma}{R} - \left(\frac{1}{\rho_c} - \frac{1}{\rho} \right) \left(\frac{\dot{m}}{4\pi R^2} \right)^2 - p_0 \right) \\
\dot{R} &= -\frac{\Phi(R - a_L t)}{R^2} + \frac{\Phi'(R - a_L t)}{R} + \frac{\dot{m}_B}{4\pi R^2 \rho_L}
\end{aligned} \tag{2.3}$$

where p_0 is the external pressure. This model describes the evolution of mass and radius of a single vapor bubble in liquid water, where phase transition is taken into account. If only small pressure differences appear, the water can be assumed to be incompressible due to the fact that gases have a much higher compressibility than liquids in general. It is shown in [22] that the following incompressible model gives a sufficiently good description of the bubble evolution

$$\begin{aligned}
\dot{m} &= \frac{4\pi R^2 \rho m_0}{\sqrt{2\pi m_0 k T}} \left[\frac{1}{\rho_c} \left(\frac{\rho k T}{m_0} - \frac{2\sigma}{R} - \bar{p} \right) - \frac{k T}{m_0} \ln \frac{\rho k T}{\bar{p} m_0} - \frac{1}{2} \left(\frac{1}{\rho_c} - \frac{1}{\rho} \right)^2 \left(\frac{\dot{m}}{4\pi R^2} \right)^2 \right] \\
\dot{F} &= \frac{F^2}{2R^3} + \frac{R}{\rho_c} \left(\frac{\rho k T}{m_0} - \frac{2\sigma}{R} - \left(\frac{1}{\rho_c} - \frac{1}{\rho} \right) \left(\frac{\dot{m}}{4\pi R^2} \right)^2 - p_0 \right) \\
\dot{R} &= \frac{F}{R^2} + \frac{\dot{m}}{4\pi R^2 \rho_c}.
\end{aligned} \tag{2.4}$$

We will use the last form (2.4) of the ODE system in the numerical investigations of the model in future work.

2.2 The isothermal model

In order to have a tractable model for an analytical study of the model, we make the assumptions that the fluids are isothermal and gravity is ignored. The source terms modeling the phase transitions are dropped. The Riemann problem we want to study is then given by the following system of conservation laws

$$\begin{aligned}
\frac{\partial c}{\partial t} + \frac{\partial}{\partial x} (c v) &= 0 \\
\frac{\partial c \rho}{\partial t} + \frac{\partial}{\partial x} (c \rho v) &= 0 \\
\frac{\partial c \rho v}{\partial t} + \frac{\partial}{\partial x} (c \rho v^2) &= 0 \\
\frac{\partial c R}{\partial t} + \frac{\partial}{\partial x} (c R v) &= 0 \\
\frac{\partial}{\partial t} [(1-c)\rho_c] + \frac{\partial}{\partial x} [(1-c)\rho_c v_c] &= 0 \\
\frac{\partial}{\partial t} [(1-c)\rho_c v_c] + \frac{\partial}{\partial x} [(1-c)\rho_c v_c^2] + \frac{\partial}{\partial x} [(1-c)p_c] &= 0
\end{aligned} \tag{2.5}$$

together with the piecewise constant initial data

$$(c, \rho, v, R, \rho_c, v_c)(t=0, x) = \begin{cases} (c_-, \rho_-, v_-, R_-, \rho_{c-}, v_{c-}) & \text{for } x < 0 \\ (c_+, \rho_+, v_+, R_+, \rho_{c+}, v_{c+}) & \text{for } x > 0. \end{cases} \tag{2.6}$$

The study of this Riemann problem is of great interest, analytically as well as numerically. The above initial data are the simplest, non-trivial initial conditions. Nonetheless, the solution already includes all mathematical and physical properties of the underlying conservation laws. The solution to a general initial value problem can then be seen as a non-linear superposition of solutions of local Riemann problems. One of the rare schemes with a convergence theorem for hyperbolic conservation laws even in one space dimension, the Glimm scheme [29], is based on this idea.

Note that the first four equations of the system (2.5) decouple from the last equations. Therefore we will solve them separately from the rest of the system in the next chapter.

2.3 Equations of state

In this subsection, we briefly want to discuss the equations of state considered to close the system (2.5). We neither want to discuss the derivation nor the application of these equations. Nonetheless, we want to give some attention to the equation of state for the following reason. Almost all analytical results for hyperbolic systems of conservation laws use the simplest possible choice: a linear equation of state, mainly the ideal gas or perfect gas relation. This is a valid choice since the equation of state for isothermal flow yields the pressure as a linear function of the density in a gas. However, for a liquid, the simplest realistic assumptions lead to an affine function for the equation of state. The case of a liquid carrier phase thus leads to a considerable complication in the determination of solutions to the Riemann problem. This will be a key point of the analytical part of this thesis.

The two phases under consideration for the analysis are a vapor and a liquid phase. We will consider both cases, vapor bubbles dispersed in the

liquid phase and liquid droplets in the vapor carrier phase, respectively. The speed of sound a in a fluid is given by

$$a^2 = \frac{\partial p}{\partial \rho}.$$

We may assume an equation of state of the following form throughout the rest of this work

$$p = a^2 \rho + d_0 \quad \text{with} \quad a^2 = \text{const.} \quad (2.7)$$

Taking the vapor phase to be an ideal gas is a valid choice for an equation of state. We use the molecular mass m_0 and the Boltzmann constant k . Then we have

$$p = \frac{kT\rho}{m_0} \quad \text{with} \quad a^2 = \frac{kT}{m_0}, \quad d_0 = 0.$$

For the liquid phase let \bar{p} denote the saturation pressure at temperature T with $\bar{\rho}$ being the corresponding density. The constant \bar{K} is the temperature dependent modulus of compression. These quantities are material constants and can be found in [87]. The pressure of the liquid phase p_L can then be given by the Tait equation of state for $n = 1$

$$p = \bar{p} + \bar{K} \left(\frac{\rho}{\bar{\rho}} - 1 \right). \quad (2.8)$$

A detailed discussion of the Tait equation can be found in [24]. Written in the form of equation (2.7) we have

$$d_0 := \bar{p} - \bar{K}, \quad a_L^2 := \frac{\bar{K}}{\bar{\rho}},$$

where a_L is the speed of sound in the liquid.

It is also possible to use the stiffened gas equation, see e.g. Menikoff and Plohr [64, Section 7], in the isothermal case

$$\frac{p_L + \pi}{c_v \rho_L (\gamma - 1)} = T_L = \text{const.} \quad (2.9)$$

In the form (2.7) it is

$$p_L = T_L c_v (\gamma - 1) \rho_L - \pi, \quad \text{i.e.} \quad a_L^2 = T_L c_v (\gamma - 1), \quad d_0 = -\pi.$$

Note that due to this restriction for the equation of state, the following relation holds in all the cases considered

$$p = p(\rho) \quad \text{with} \quad \frac{dp}{d\rho} = a^2 = \text{const.} \quad (2.10)$$

2.4 Lower and upper bounds for carrier phase quantities

For later purposes, we introduce lower and upper bounds for the concentration of the carrier phase $1 - c_{\max}$ and $1 - c_{\min}$, respectively. Whereas the lower bound for the concentration is given naturally by the absence of the dispersed phase, any upper bound is due to the assumption of isolated bubbles or droplets in the carrier phase. We will not give any explicit number for that bound. Instead, we will assume from here on

$$c_{\min} = 0 \quad \text{and} \quad 0 < c_{\max} \ll 1.$$

In the same way we need to introduce a lower and an upper bound for the carrier densities. In case of an ideal gas equation of state, one gets $\rho > 0$ from the assumption of $p > 0$. In the case of an affine linear equation of state, the condition of positivity of the pressure leads to a lower bound ρ_{\min} for the density, which depends on the chosen equation of state and the parameters therein.¹

We will introduce a quantity ρ_{\max} , too. This can be seen as a maximal density allowed. For a vapor carrier phase, there exists a physical upper bound corresponding to the saturation pressure. For a liquid carrier phase, one has a maximum pressure for an experimental setup or an upper bound coming from the modeling of a real fluid by an affine linear equation of state, which will not be valid up to infinity. Due to this freedom of choice, we will not give any explicit value.

For any application or numerical test, one has to check the inequalities given in Theorem 4.4.1 using explicit values. These inequalities represent bounds for the carrier phase velocity.

¹One can even drop the condition of positivity and allow negative pressures as long as one has a lower bound for the density. This lower bound is necessary only for our later analysis. See [17] for a discussion of negative pressures in water due to acoustic induced cavitation.

Notions on Nonlinear Hyperbolic Equations

In the analytical part of this work, we show that the two-phase flow model that we consider is weakly hyperbolic. Therefore, we want to give a brief introduction to the mathematics of hyperbolic as well as weakly hyperbolic conservation laws. For further reading, we recommend the following books out of an extensive literature on hyperbolic conservation laws. A general introduction to the theory of partial differential equations (PDEs) can be found in the book by Evans [28]. Warnecke [89] gives a detailed introduction and discussion of analytical methods for conservation laws. For a historical survey and a precise mathematical treatment of hyperbolic conservation laws, we refer the reader to the book of Dafermos [16]. The list of references in this book contains almost all significant work in this field of research¹. The book of Smoller [78] is one of the first extensive books on the theory of shock waves and includes reaction-diffusion equations as well. A detailed study of systems of conservation laws and viscous approximations can be found in the books of Serre [73, 74]. An introduction into the mathematical and numerical concepts of hyperbolic balance laws is given in the books of LeVeque [52, 53].

The following section gives a short introduction to the concepts for nonlinear scalar hyperbolic equations. Although one can find them in any of the mentioned textbooks above, they are essential tools in our analysis later and we want to give the reader a self-contained work.

This presentation is based on a lecture given by Prof. Michael Dumbser during the Winter School NUMHYP 2020 in Trento.

3.1 Nonlinear scalar hyperbolic equations

We consider the following first-order nonlinear scalar equation

$$\frac{\partial}{\partial t}u(t, x) + \frac{\partial}{\partial x}f(u(t, x)) = 0 \quad (3.1)$$

¹The bibliography comprises 120 pages.

where $t \in [0, t_{max}) \subseteq \mathbb{R}_{\geq 0}$ denotes the time variable and $x \in \Omega \subseteq \mathbb{R}$ the space variable. The unknown quantity is denoted by $u(t, x)$ with $u : \mathbb{R} \times \mathbb{R} \rightarrow \mathbb{R}$. It is called the *conservative variable* and $f : \mathbb{R} \rightarrow \mathbb{R}$ the *nonlinear flux*. The equation (3.1) is called a *conservation law*. In case of a non-zero source term on the right hand side it is called a *balance law*. The conservation of mass, momentum and energy are classical examples from physics.

For sufficiently regular data, the derivatives in (3.1) are defined and the partial differential equation (PDE) can be written in the so called *quasi-linear* form. With the use of the chain rule, we get

$$\frac{\partial u}{\partial t} + a(u) \frac{\partial u}{\partial x} = 0, \quad \text{with} \quad a(u) = \frac{df}{du} = f'(u). \quad (3.2)$$

The term $a(u)$ is the characteristic velocity and depends on u in general. One distinguishes three different cases of the monotonicity property of $a(u)$:

- Convex flux, for $a(u)$ monotonically increasing

$$\frac{d}{du} a(u) = a'(u) = f''(u) \geq 0, \quad \text{for all } u \in \mathbb{R}.$$

- Concave flux, if $a(u)$ is monotonically decreasing

$$\frac{d}{du} a(u) = a'(u) = f''(u) \leq 0, \quad \text{for all } u \in \mathbb{R}.$$

- General flux, if there exists a $u \in \mathbb{R}$ such that

$$\exists u : \frac{d}{du} a(u) = a'(u) = f''(u) = 0.$$

As an example, we consider the nonlinear Burgers equation.

Example 3.1.1. *The nonlinear Burgers equation is given by*

$$\frac{\partial}{\partial t} u + \frac{\partial}{\partial x} \left(\frac{1}{2} u^2 \right) = 0. \quad (3.3)$$

For the characteristic velocity and its derivative we obtain

$$a(u) = \frac{df}{du} = u, \quad \text{and} \quad a'(u) = f''(u) = 1 \geq 0, \quad \text{for all } u \in \mathbb{R}.$$

Hence, the flux of the Burgers equation is convex.

In the next section, we will see how these concepts are generalized to systems of conservation laws.

3.1.1 Solution along characteristics

To formulate the Cauchy problem, we need to assign an initial condition (IC) to the PDE. Therefore, we consider the following *initial value problem* (IVP):

$$\begin{aligned} \text{PDE : } \quad & \frac{\partial u}{\partial t} + \frac{\partial f}{\partial x} = 0, \\ \text{IC : } \quad & u(0, x) = u_0(x), \end{aligned} \tag{3.4}$$

with a given function $u_0(x) : \mathbb{R} \rightarrow \Omega$. Again, we can write this in quasi-linear form as

$$\frac{\partial u}{\partial t} + a(u) \frac{\partial u}{\partial x} = 0, \quad u(0, x) = u_0(x). \tag{3.5}$$

We assume that the reader is familiar with the method of characteristics for a linear PDE. In the nonlinear case, the characteristic curves are defined by the following ODE

$$\frac{dx}{dt} = a(u(t, x(t))), \quad x(0) = x_0. \tag{3.6}$$

The *total derivative* or *material derivative* of $u(t, x)$ computed along the characteristic curve $x(t)$ is given by

$$\frac{du}{dt} = \frac{\partial u}{\partial t} + \frac{\partial u}{\partial x} \frac{dx}{dt} = \frac{\partial u}{\partial t} + a(u) \frac{\partial u}{\partial x} = 0. \tag{3.7}$$

Hence, even in the nonlinear case, the solution along the characteristic curves remains constant. Therefore, also the characteristic velocity $a(u)$ is constant along the characteristic. With this in mind, we obtain that the characteristic curves are also straight lines, even in the nonlinear case, which might be surprising at first.

From (3.6) together with the initial condition from (3.5) one gets the equation of the characteristic curves as

$$x = x_0 + a(u_0(x_0))t. \tag{3.8}$$

So we end up with an algebraic nonlinear scalar equation for the foot of the characteristic x_0 in terms of t and x , that is $x_0 = h(t, x)$. The solution of the nonlinear PDE (3.4) can then be found easily. We only have to trace back the characteristic to the foot x_0 and evaluate the initial condition there

$$u(t, x) = u_0(x_0(t, x)) = u_0(x - a(u_0(x_0))t). \tag{3.9}$$

We will rewrite (3.8) in the following form

$$0 = x - (x_0 + a(u_0(x_0))t) = g(t, x, x_0).$$

We want to verify that this already provides the solution of the nonlinear PDE with the initial condition $u(0, x) = u_0(x)$, see (3.4). The initial condition is obviously fulfilled. Hence, we compute the derivatives of the function $g(t, x, x_0)$ and keep in mind that x_0 is a function of t and x

$$\begin{aligned}
0 &= \frac{\partial g}{\partial t} = \frac{\partial g}{\partial t} + \frac{\partial g}{\partial x_0} \frac{\partial h}{\partial t} \\
&= -a(u_0(x_0)) - \frac{\partial h}{\partial t} - a'(u_0(x_0))u'_0(x_0) \frac{\partial h}{\partial t} t.
\end{aligned}$$

From this relation, we get the derivative of h with respect to t , which reads

$$\begin{aligned}
(1 + a'(u_0(x_0))u'_0(x_0)t) \frac{\partial h}{\partial t} &= -a(u_0(x_0)) \\
\Rightarrow \frac{\partial h}{\partial t} &= \frac{-a(u_0(x_0))}{1 + a'(u_0(x_0))u'_0(x_0)t}. \tag{3.10}
\end{aligned}$$

Analogously, we get the derivative of h with respect to x from

$$\begin{aligned}
0 &= \frac{\partial g}{\partial x} = \frac{\partial g}{\partial x} + \frac{\partial g}{\partial x_0} \frac{\partial h}{\partial x} \\
&= 1 - \frac{\partial h}{\partial x} - a'(u_0(x_0))u'_0(x_0) \frac{\partial h}{\partial x} t,
\end{aligned}$$

which leads to

$$\frac{\partial h}{\partial x} = \frac{1}{1 + a'(u_0(x_0))u'_0(x_0)t}. \tag{3.11}$$

Substituting (3.10) and (3.11) into (3.7) and using

$$\begin{aligned}
\frac{\partial u}{\partial t} &= u'_0(x_0) \frac{\partial h}{\partial t} \\
\frac{\partial u}{\partial x} &= u'_0(x_0) \frac{\partial h}{\partial x}
\end{aligned}$$

leads to

$$\frac{\partial u}{\partial t} + a(u) \frac{\partial u}{\partial x} = u'_0(x_0) \left(\frac{-a(u_0(x_0))}{1 + a'(u_0(x_0))u'_0(x_0)t} + a \frac{1}{1 + a'(u_0(x_0))u'_0(x_0)t} \right) = 0.$$

Therefore, we verified that (3.9) is indeed a solution of our IVP (3.4).

Note that the solution of (3.4) is given implicitly. To determine x_0 numerically from a given t and x one has to solve

$$g(x_0) = x_0 - x + a(u_0(x_0))t = 0. \tag{3.12}$$

To find the root of this nonlinear equation, it is necessary to use an iterative scheme, such as the bisection or the Newton method.

Finding the solution of the IVP (3.4) also has its limitations. When two characteristics intersect, this method breaks down. Both characteristic curves transport a constant solution along themselves, which means that at the intersection point, we would have two different values of u . Therefore, we would have a *multi-valued solution* at this point. The situation is depicted in

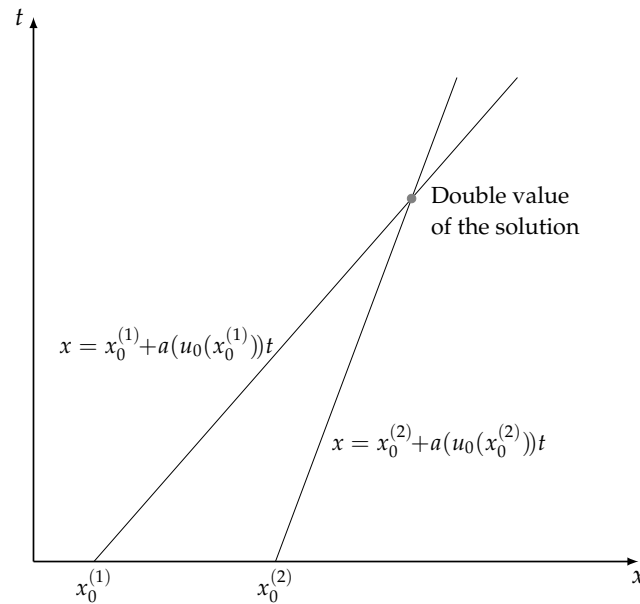


FIGURE 3.1: Multi-valued solution due to intersection of characteristic curves

Fig. 3.1. We will see in the section on shock-waves how to overcome this problem.

3.1.2 Rarefaction waves

Let us consider the following IVP

$$\begin{aligned} \text{PDE: } & u_t + f_x = 0, \quad f'' > 0 \\ \text{IC: } & u(0, x) = u_0(x) = \begin{cases} u_-, & \text{if } x < x_0 \\ u_+, & \text{if } x \geq x_0 \end{cases} \end{aligned} \quad (3.13)$$

with the following property of the characteristic speed

$$a(u_-) \leq a(u_+).$$

Again, the initial condition of the Riemann problem (3.13) consists of two piecewise constant states of the variable u . The solution is given by a so-called *rarefaction wave*. Its borders are defined by the two particular characteristics

$$\begin{aligned} x &= x_0 + a(u_-)t, \\ x &= x_0 + a(u_+)t. \end{aligned}$$

These characteristic curves are called *head* and *tail* of the rarefaction wave with the footpoint located at x_0 . The situation is depicted in Fig. 3.2.

One finds a self-similar solution $u(t, x)$ depending only on one variable $\xi = \frac{x-x_0}{t}$

$$u(t, x) = u(\xi) = u\left(\frac{x-x_0}{t}\right). \quad (3.14)$$

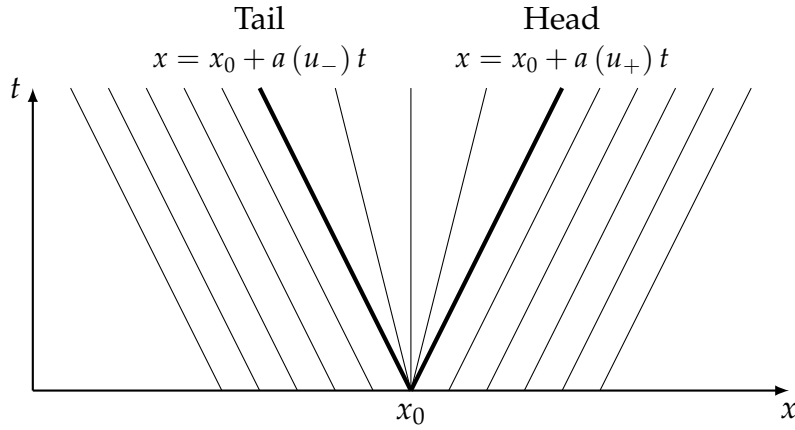


FIGURE 3.2: Characteristic curves of a rarefaction solution of Riemann problem (3.13)

Calculating the derivatives with respect to space and time of the unknown $u(t, x)$ leads

$$\frac{\partial u}{\partial t} = -\frac{x - x_0}{t^2} u', \quad \frac{\partial u}{\partial x} = \frac{1}{t} u',$$

where the prime denotes the derivative with respect to ξ . Substituting these derivatives into (3.13) yields

$$\begin{aligned} & \left(-\frac{x - x_0}{t^2} + a(u(\xi)) \frac{1}{t} \right) u' = 0 \\ \Rightarrow & a(u(\xi)) = \frac{x - x_0}{t} = \xi. \end{aligned}$$

Hence, for the Riemann problem (3.13) the footpoints of the head and tail of the rarefaction coincide with the initial location of the discontinuity at x_0 , see Fig. 3.2. We find the entire solution of the Riemann problem as

$$u(t, x) = \begin{cases} u_-, & \text{if } \frac{x - x_0}{t} < a(u_-) \\ \text{root of } g(u) = a(u) - \frac{x - x_0}{t} = 0, & \text{if } a(u_-) \leq \frac{x - x_0}{t} \leq a(u_+) \\ u_+, & \text{if } \frac{x - x_0}{t} > a(u_+) \end{cases} \quad (3.15)$$

The intermediate states between head and tail of the rarefaction are computed by solving again numerically the nonlinear algebraic equation

$$a(u) = \xi.$$

3.1.3 Shock waves

To get an idea of why the notion of shock waves was introduced into the theory of nonlinear partial differential equations, we want to consider the following IVP for the Burgers equation already mentioned. Its quasi-linear

form reads

$$\begin{aligned} \text{PDE : } & \frac{\partial u}{\partial t} + u \frac{\partial u}{\partial x} = 0 \\ \text{IC: } & u(0, x) = u_0(x) = \begin{cases} 1, & \text{if } x < 0 \\ 1 - x, & \text{if } 0 \leq x \leq 1 \\ 0, & \text{if } x \geq 1. \end{cases} \end{aligned} \quad (3.16)$$

We have already shown that the characteristics are straight lines, even in the nonlinear case. Since the initial condition is constant for $x \leq 0$, all the characteristic curves with footpoint $x_0 \leq 0$ are parallel to each other. The same applies to the characteristic curves with $x_0 \geq 1$. The two limiting characteristics are c_0 and c_1 , which are given by

$$\begin{aligned} c_0 : & x = 0 + 1 \cdot t = t \\ c_1 : & x = 1 + 0 \cdot t = 1 \end{aligned}$$

Between these two curves, the characteristics converge to the intersection point $P = (1, 1)$ and the footpoints of these characteristics are computed from (3.8) and read

$$x = x_0 + a(u_0(x_0))t = x_0 + (1 - x_0)t = x_0(1 - t) + t$$

Hence, we get for the footpoint

$$x_0 = \frac{x - t}{1 - t}.$$

Finally, we can calculate the solution along these characteristics

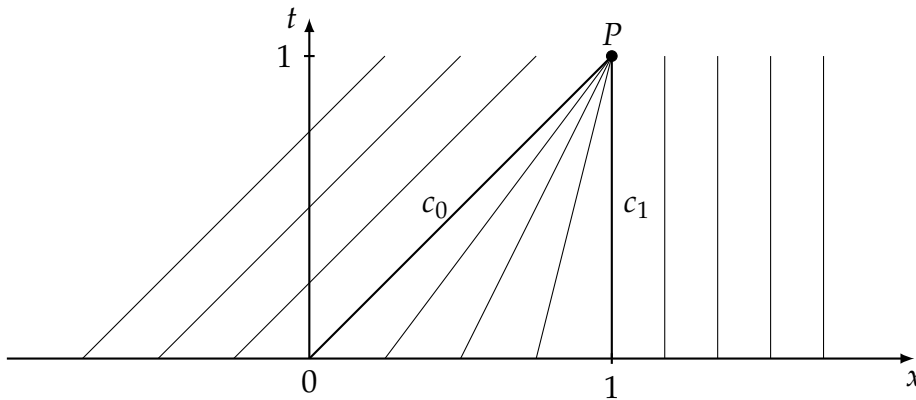
$$u(t, x) = u_0(x_0) = 1 - x_0 = 1 - \frac{x - t}{1 - t}$$

To summarize, we give the solution for all times $t \leq 1$

$$u(t, x) = \begin{cases} 1, & \text{if } x < t \\ \frac{1 - x}{1 - t}, & \text{if } t \leq x \leq 1 \\ 0, & \text{if } x > 1 \end{cases}$$

The characteristics are depicted in Fig. 3.3. The solution itself is shown in Fig. 3.4 for different times. One can see easily that this solution has multiple values for $t \geq 1$. The problem of multi-valued solutions has been solved by Bernhard Riemann already in 1860 [70]. Therein he introduced the concept of *shock waves*, i.e. a *discontinuity* in the solution that guarantees the conservation of the variable u .²

²Riemann himself was skeptical at that time if these purely mathematical concepts would be of any use in physical problems or applications: "Es lassen sich indess für den Fall, dass die anfängliche Bewegung allenthalben in gleicher Richtung stattfindet und in jeder

FIGURE 3.3: Characteristic curves for $t \leq 1$ of problem (3.16)

3.1.4 Integral form of conservation laws

To understand the mathematical structure of shock waves, we need a different notion of conservation laws than the PDE formulation. The conservation of mass, momentum and energy are all derived as integral conservation laws. The time evolution of these integrals is described by means of Reynolds transport theorem, see for example [89]. The PDE formulation is then obtained by assuming an arbitrary control volume and a smooth integrand. Therefore, it is not surprising that any discontinuous solution is not included in this description.

Let us now define a control volume in space $I = [x_L, x_R]$ and integrate the PDE in (3.4) over this spatial control volume

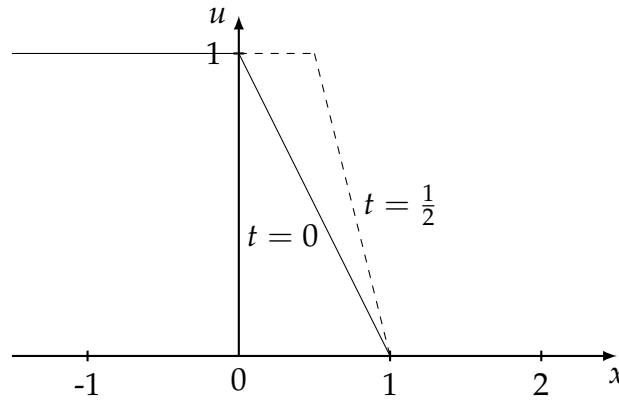
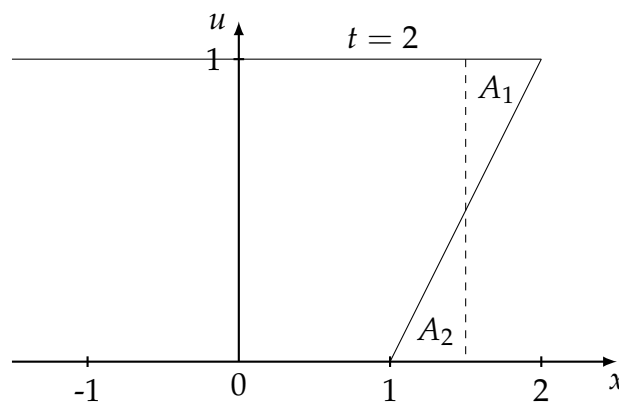
$$\int_{x_L}^{x_R} \frac{\partial u}{\partial t} dx + \int_{x_L}^{x_R} \frac{\partial}{\partial x} f(u) dx = 0$$

Integrating by parts of the second term leads to

$$\frac{\partial}{\partial t} \int_{x_L}^{x_R} u(t, x) dx + f(u(t, x_R)) - f(u(t, x_L)) = 0$$

The change of the conserved quantity $u(t, x)$ inside the spacial interval $I = [x_L, x_R]$ is hence only due to the fluxes at the boundaries of this interval.

auf dieser Richtung senkrechten Ebene Geschwindigkeit und Druck constant sind, die exacten Differentialgleichungen vollständig integriren; und wenn auch zur Erklärung der bis jetzt experimentell festgestellten Erscheinungen die bisherige Behandlung vollkommen ausreicht, so könnten doch, bei den grossen Fortschritten, welche in neuester Zeit durch Helmholtz auch in der experimentellen Behandlung akustischer Fragen gemacht worden sind, die Resultate dieser genaueren Rechnung in nicht allzuferner Zeit vielleicht der experimentellen Forschung einige Anhaltspunkte gewähren; und dies mag, abgesehen von dem theoretischen Interesse, welches die Behandlung nicht linearer partieller Differentialgleichungen hat, die Mittheilung derselben rechtfertigen." From the introduction of [70].

(a) Solution at time $t = 0$ and $t = \frac{1}{2}$ (b) Multiple value solution at $t = 2$. Assuming the equality of A_1 and A_2 the shock can be localized such that conservation of u holds.FIGURE 3.4: Solutions of (3.16) at different times t .

If we consider now a control volume in space *and* in time, that is $V = [t_1, t_2] \times [x_L, x_R]$, the integral form of the conservation law reads

$$\int_{t_1}^{t_2} \int_{x_L}^{x_R} \frac{\partial u}{\partial t} dx dt + \int_{t_1}^{t_2} \int_{x_L}^{x_R} \frac{\partial}{\partial x} f(u) dx dt = 0$$

which is equivalent to

$$\int_{x_L}^{x_R} u(t_2, x) dx = \int_{x_L}^{x_R} u(t_1, x) dx - \int_{t_1}^{t_2} (f(u(t, x_R)) - f(u(t, x_L))) dt \quad (3.17)$$

Thus, the conservative quantity $u(t, x)$ at time t_2 is equal to the conserved quantity at time t_1 minus the difference of the integrals of the fluxes in time on the spatial boundaries of the control volume.

3.1.5 Rankine-Hugoniot jump conditions

To derive the Rankine-Hugoniot relations, we need the integral formulation of the considered PDE. Let us assume a shock wave traveling with velocity s . We do not want to have any other waves near this discontinuity, therefore calling it an isolated discontinuity/shock. This isolated discontinuity separates two piecewise constant states on the left u_- and on the right u_+ from each other. The PDE in integral form is then given by

$$\int_{x_L}^{x_R} (u(t_2, x) - u(t_1, x)) dx + \left(\int_{t_1}^{t_2} (f(u(t, x_R)) - f(u(t, x_L))) dt \right) = 0, \quad (3.18)$$

where we used the control volume $V = [t_1, t_2] \times [x_L, x_R]$ with the following properties: $x_L \leq x_d \leq x_R$ and $x_L \leq x_d + s(t_2 - t_1)$, where x_d denotes the position of the discontinuity at time t_1 . This means, that the shock is entering the control volume at the bottom and leaves it at the top and not on the left or right side, see Fig. 3.5. The integrals in (3.18) can then be evaluated leading

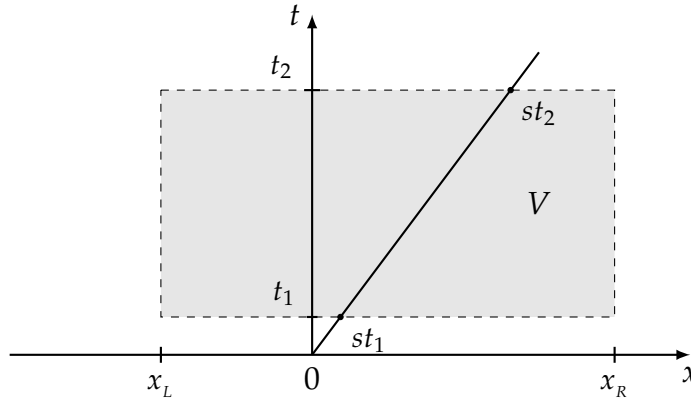


FIGURE 3.5: Control volume V used to derive the Rankine-Hugoniot relation

to

$$u_-(x_d + s(t_2 - t_1)) + u_+(x_R - x_d - s(t_2 - t_1)) - u_-(x_d - x_L) - u_+(x_R - x_d) + (F(u_+) - F(u_-))(t_2 - t_1) = 0$$

Simplification leads to the Rankine-Hugoniot jump condition

$$s(u_+ - u_-) = F(u_+) - F(u_-). \quad (3.19)$$

They relate the jump of the conserved quantity u across a shock wave with the propagation speed s and the jump of the fluxes over the discontinuity. We will see later that this relation has the same structure for systems of conservation laws and in weak formulations.

Example 3.1.2. We want to consider the Burgers equation (3.3) again. It is the simplest nonlinear equation and therefore the standard example for theoretical as well

as numerical purposes. The flux is given by $F(u) = \frac{1}{2}u^2$. The Rankine-Hugoniot relation reads in this case

$$s(u_+ - u_-) = \left(\frac{1}{2}u_+^2 - \frac{1}{2}u_-^2 \right).$$

The shock speed is then

$$s = \frac{1}{2}(u_+ + u_-)$$

In general, for a nonlinear PDE with Riemann initial data

$$\begin{aligned} \text{PDE: } & \frac{\partial u}{\partial t} + \frac{\partial}{\partial x} f(u) = 0 \\ \text{IC: } & u(0, x) = u_0(x) = \begin{cases} u_-, & \text{if } x < x_0 \\ u_+, & \text{if } x \geq x_0 \end{cases} \end{aligned} \quad (3.20)$$

where $a(u_-) > a(u_+)$ is assumed, the solution of the IVP (3.20) is given by

$$u(t, x) = \begin{cases} u_-, & \text{if } \frac{x-x_0}{t} < s, \\ u_+, & \text{if } \frac{x-x_0}{t} \geq s. \end{cases} \quad (3.21)$$

The shock speed s is here determined by the Rankine-Hugoniot relation (3.19). The characteristic curves intersect, they run into each other and form a shock wave. This situation is depicted in Fig. 3.6.

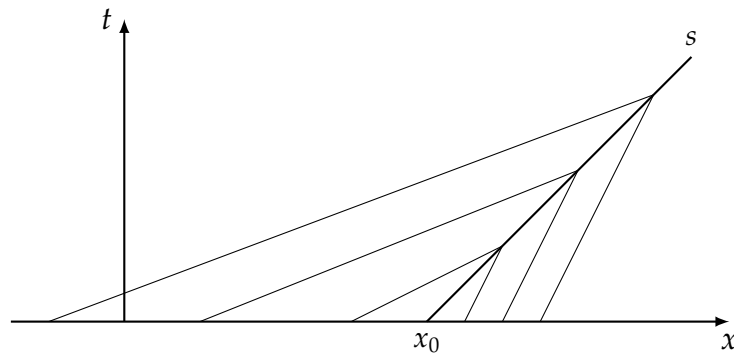


FIGURE 3.6: Shock forming characteristic curves

3.1.6 Non-uniqueness and Lax entropy condition

We have seen in the subsection above that using the integral formulation of our conservation law extends the set of possible solutions. The PDE formulation itself only allows for sufficiently smooth solutions, unlike the integral formulation. Solutions with discontinuities are allowed in this formulation and they are a necessary tool for nonlinear conservation laws to overcome the problem of multi-valued solutions. However, with the extension of the set of possible solutions, the question of uniqueness appears naturally. One has to find further conditions that single out a unique solution for a given

IVP. To show the necessity of further conditions, we want to consider the Burgers equation again.

Example 3.1.3. Consider the following IVP for the Burgers equation

$$\begin{aligned} \text{PDE: } & \frac{\partial u}{\partial t} + u \frac{\partial u}{\partial x} = 0 \\ \text{IC: } & u(0, x) = u_0(x) = \begin{cases} 0, & \text{if } x < 0 \\ 1, & \text{if } x \geq 0 \end{cases} \end{aligned} \quad (3.22)$$

Since $a(u_-) = 0 < 1 = a(u_+)$ we can find a rarefaction solution as shown in Subsection 3.1.2. It is given by

$$u(t, x) = \begin{cases} 0, & \text{if } \frac{x}{t} < 0 \\ \frac{x}{t}, & \text{if } 0 \leq \frac{x}{t} \leq 1 \\ 1, & \text{if } \frac{x}{t} > 1 \end{cases} \quad (3.23)$$

This solution is based on the method of characteristics and satisfies the PDE in its differential form. Since any solution that satisfies the PDE in its differential form also satisfies the PDE in its integral form, it is also a solution of the integral form. But we can construct another solution of the integral form, namely

$$u(t, x) = \begin{cases} 0, & \text{if } \frac{x}{t} < s \\ 1, & \text{if } \frac{x}{t} \geq s \end{cases}, \quad \text{with } s = \frac{1}{2}$$

It is easily shown, that this a solution of (3.22). Using the integral conservation law (3.17) over the space-time control volume $V = [t_1, t_2] \times [x_L, x_R]$, see Fig 3.5, we obtain

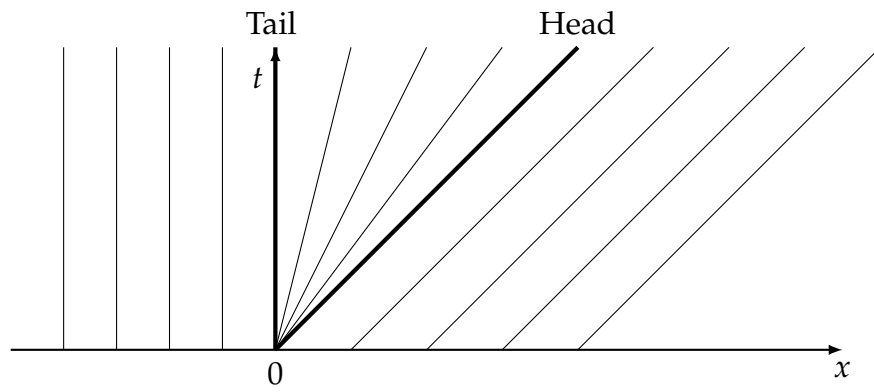
$$x_R - st_2 - (x_R - st_1) + \frac{1}{2} (t_2 - t_1) = 0.$$

With $s = \frac{1}{2} (u_- + u_+) = \frac{1}{2}$ this proves indeed that also the so-called rarefaction shock solution satisfies the integral form of the conservation law. Hence, it is a possible solution of our IVP (3.22). Both solutions are shown in Fig 3.7.

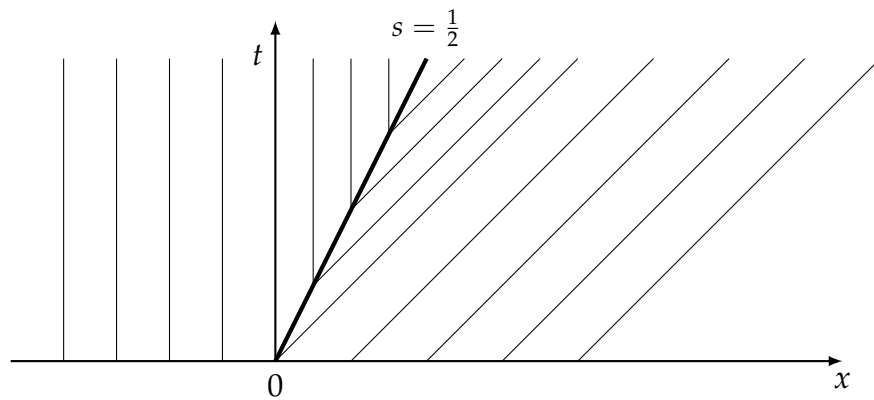
To solve the problem of non-uniqueness in the one dimensional scalar case, we can make use of the famous Lax entropy condition [50]. According to Lax, a solution is admissible if the following relation holds

$$a(u_-) > s > a(u_+)$$

This relation requires that the characteristic curves enter the shock wave from both sides, or in other words, the shock is compressed from both sides. This additional criterion singles out the physically correct solution. The relation is nothing else than the second law of thermodynamics, stating that the mathematical entropy decreases over shocks (the physical entropy increases over a shock). From the point of information entropy, the relation requires that no new information is created by characteristics leaving the shock and hence the second law is satisfied.



(a) Rarefaction fan solution of Burgers equation



(b) Rarefaction shock solution of Burgers equation

FIGURE 3.7: The two possible solutions of (3.22).

Thus, for the example (3.22) only the rarefaction fan solution (3.23) shown in Fig. 3.7(a) is physical admissible and therefore the unique solution to the given IVP.

3.2 Nonlinear hyperbolic systems

“The theory of the scalar balance law, in several spatial dimensions, has reached a state of virtual completeness.” [16, page 175]. We refer the reader to Chapter 6 in this book to get a survey of the existing scalar theory.

In contrast to this situation are systems of balance laws, even in one space dimension. The theory here is far from being understood completely. The successful treatment of the scalar case is based on L^1 and L^∞ estimates. Unfortunately, a similar approach is not possible for systems of conservation laws. This loss of smoothness raises many difficulties, from adequate defining weak solutions to the problem of non-uniqueness. There are many different approaches to overcome these problems, vanishing viscosity limit or the Lax condition in one space dimension, to name only a few. To formulate these criteria for singling out the correct physical solution turns out to be very difficult in general. It is still an open and active field of research to find existence and uniqueness results for systems of hyperbolic partial differential equations.

This section presents many of the basic concepts of the theory of hyperbolic systems of conservation laws in one space dimension used later in this work.

A general system of conservation laws in one space dimension is of the following form

$$\begin{aligned} \frac{\partial}{\partial t} u_1(t, x) + \frac{\partial}{\partial x} f_1(u_1(t, x), \dots, u_m(t, x)) &= 0, \\ &\vdots \\ \frac{\partial}{\partial t} u_m(t, x) + \frac{\partial}{\partial x} f_m(u_1(t, x), \dots, u_m(t, x)) &= 0. \end{aligned} \tag{3.24}$$

Again, $t \in [0, t_{max}) \subseteq \mathbb{R}_{\geq 0}$ denotes the time variable and $x \in \Omega \subseteq \mathbb{R}$ the space variable. We now have a set of unknowns $u_i : \mathbb{R} \times \mathbb{R} \rightarrow \mathbb{R}$ called *conserved quantities* and the functions $f_i : \mathbb{R} \rightarrow \mathbb{R}$ the (*nonlinear*) *fluxes*.

Using $\mathbf{u} = (u_1, \dots, u_m)$ and $\mathbf{f} = (f_1, \dots, f_m)$ we can write (3.24) in a compact form

$$\frac{\partial}{\partial t} \mathbf{u} + \frac{\partial}{\partial x} \mathbf{f}(\mathbf{u}) = 0, \tag{3.25}$$

with $\mathbf{u} : \mathbb{R} \times \mathbb{R} \rightarrow \mathcal{U}$ and $\mathbf{f} : \mathcal{U} \rightarrow \mathbb{R}^m$. Here, the open set $\mathcal{U} \subseteq \mathbb{R}^m$ with $\mathbf{u} \in \mathcal{U}$ is the *state space*. The system (3.25) is completed with suitable initial data

$$\mathbf{u}(0, x) = \mathbf{u}_0(x).$$

If we assume the data to be sufficiently smooth we can make use of the chain rule again and write the system in the *quasi-linear* form³

$$\frac{\partial}{\partial t} \mathbf{u} + \mathbf{A}(\mathbf{u}) \frac{\partial}{\partial x} \mathbf{u} = 0. \quad (3.27)$$

The Matrix $\mathbf{A}(\mathbf{u})$ is the Jacobian of the fluxes \mathbf{f} and thus given by

$$\mathbf{A}(\mathbf{u}) = \mathbf{Df}(\mathbf{u}) = \begin{pmatrix} \frac{\partial f_1}{\partial u_1} & \cdots & \frac{\partial f_1}{\partial u_m} \\ \vdots & & \vdots \\ \frac{\partial f_m}{\partial u_1} & \cdots & \frac{\partial f_m}{\partial u_m} \end{pmatrix} \quad (3.28)$$

with the eigenvalues $\lambda_1(\mathbf{u}) \dots \lambda_m(\mathbf{u})$. The right eigenvectors $\{\mathbf{r}_i(\mathbf{u})\}_{i=1}^m$ are defined by

$$[\mathbf{A}(\mathbf{u}) - \lambda_i(\mathbf{u})\mathbf{I}] \mathbf{r}_i(\mathbf{u}) = 0, \quad (3.29)$$

and correspondingly the left eigenvectors $\{\mathbf{l}_i(\mathbf{u})\}_{i=1}^m$ via

$$\mathbf{l}_i(\mathbf{u}) [\mathbf{A}(\mathbf{u}) - \lambda_i(\mathbf{u})\mathbf{I}] = 0.$$

The eigenvalue $\lambda_i(\mathbf{u})$ is called the *i-th characteristic speed*, compare with the scalar conservation law, where the scalar quantity $a(u)$ was the characteristic speed. The pair $(\lambda_i(\mathbf{u}), \mathbf{r}_i(\mathbf{u}))$ determines the *i-th characteristic field*. We will now give the very important definition of hyperbolicity for systems of conservation laws.

Definition 3.2.1 (Hyperbolicity). *The system (3.25) is hyperbolic at a point (t, x) if the Jacobian $\mathbf{A}(\mathbf{u})$ has m real eigenvalues $\lambda_1(\mathbf{u}) \dots \lambda_m(\mathbf{u})$ and a corresponding set of m linearly independent right eigenvectors $\mathbf{r}_1(\mathbf{u}), \dots, \mathbf{r}_m(\mathbf{u})$. If additionally the eigenvalues $\lambda_i(\mathbf{u})$ are all distinct, the system is called strictly hyperbolic.*

For a hyperbolic system of conservation laws, one can find m left eigenvectors corresponding to the m right eigenvectors satisfying the *bi-orthonormal* restriction

$$\mathbf{l}_i(\mathbf{u}) \cdot \mathbf{r}_k(\mathbf{u}) = \begin{cases} 0, & \text{if } i \neq k \\ 1, & \text{if } i = k \end{cases}.$$

We will comment briefly on the existence and uniqueness results for hyperbolic conservation laws later. Especially the assumption of strict hyperbolicity is a necessary ingredient for almost all results in this field. The strict

³ In general a system of first order partial differential equations of the form

$$\frac{\partial \mathbf{u}}{\partial t} + \mathbf{A} \frac{\partial \mathbf{u}}{\partial x} + \mathbf{B} = 0 \quad (3.26)$$

is called *linear with constant coefficients* if the entries a_{ij} of the matrix \mathbf{A} are all constant and the components b_j of the vector \mathbf{B} are also constant. If they depend on the time and space variables, that is $a_{ij} = a_{ij}(t, x)$ and $b_i = b_i(t, x)$, the system is called *linear with variable coefficients*. The system is still linear if \mathbf{B} depends linearly on \mathbf{u} . If the coefficient matrix $\mathbf{A} = \mathbf{A}(\mathbf{u})$ is a function of the vector of unknowns the system is called *quasi-linear*. For $\mathbf{B} = 0$ it is called *homogeneous*, see [83].

hyperbolicity assures many beneficial properties. For example, the eigenvalues and eigenvectors depend smoothly on \mathbf{u} if the Jacobian is smooth and strictly hyperbolic [28]. Even the solution may not depend continuously on the initial data if the system is not strictly hyperbolic, as shown in [8]. In Chapter 4 one can see how the lack of hyperbolicity of the considered model creates numerous problems.

We will give another very significant definition for our work presented here.

Definition 3.2.2 (Weak Hyperbolicity). *The system (3.25) is weakly hyperbolic at a point (t, x) if the Jacobian $\mathbf{A}(\mathbf{u})$ has m real eigenvalues $\lambda_1(\mathbf{u}) \dots \lambda_m(\mathbf{u})$ but at most $m - 1$ linearly independent right eigenvectors. Therefore, the Jacobian $\mathbf{A}(\mathbf{u})$ is not diagonalizable.*

Note, that this loss of hyperbolicity can be found under the name *parabolic degeneracy* in older Literature, cf. Keyfitz [44], LeFloch [51], Tan [80] or Warnecke [2]. But the term *weakly hyperbolic* seems to be more adequate.

We have already seen in the case of a scalar conservation law that they are distinguished by the mathematical properties of the flux function. If the derivative of the flux function is constant the equation is called linear as for example the *linear advection equation* with $f(u) = au$, $a \in \mathbb{R}$. In the last section we have already seen the *Burgers equation* with $f(u) = u^2/2$ as an example of a nonlinear convex flux ($a(u)$ monotonically increasing).

The notion of linearity/nonlinearity of a scalar conservation law extends to the case of systems in the form of a geometric relation of an eigenvector and the gradient of the corresponding eigenvalue

Definition 3.2.3 (Genuinely Nonlinear/Linearly Degenerate). *The i -th characteristic field $(\lambda_i(\mathbf{u}), \mathbf{r}_i(\mathbf{u}))$ the system of conservation laws (3.25) is*

- genuinely nonlinear iff

$$\nabla_{\mathbf{u}} \lambda_i(\mathbf{u}) \cdot \mathbf{r}_i(\mathbf{u}) \neq 0 \quad \text{for all } u \in \mathcal{U}, \quad (3.30)$$

- linearly degenerate iff

$$\nabla_{\mathbf{u}} \lambda_i(\mathbf{u}) \cdot \mathbf{r}_i(\mathbf{u}) = 0 \quad \text{for all } u \in \mathcal{U}. \quad (3.31)$$

It is a very important property that the notions of hyperbolicity, genuine nonlinearity and linear degeneracy are independent of the chosen variables in system (3.25). Let $\mathbf{u} = \Phi(\mathbf{v})$ be at least a C^1 -diffeomorphism. System (3.25) then becomes

$$\nabla_{\mathbf{v}} \Phi(\mathbf{v}) \frac{\partial \mathbf{v}}{\partial t} + \mathbf{A}(\Phi(\mathbf{v})) \nabla_{\mathbf{v}} \Phi(\mathbf{v}) \frac{\partial \mathbf{v}}{\partial x} = 0,$$

where $\nabla_{\mathbf{v}} \Phi(\mathbf{v})$ is the Jacobian matrix of the given transformation $\mathbf{u} = \Phi(\mathbf{v})$. Using

$$\mathbf{B}(\mathbf{v}) = (\nabla_{\mathbf{v}} \Phi(\mathbf{v}))^{-1} \mathbf{A}(\Phi(\mathbf{v})) \nabla_{\mathbf{v}} \Phi(\mathbf{v}) \quad (3.32)$$

we get

$$\frac{\partial \mathbf{v}}{\partial t} + \mathbf{B}(\mathbf{v}) \frac{\partial \mathbf{v}}{\partial x} = 0.$$

Suppose, that the eigenvalues and associated right eigenvectors of the matrix $\mathbf{B}(\mathbf{u})$ are denoted by $\mu_i(\mathbf{v})$ and $\bar{\mathbf{r}}_i(\mathbf{v})$, respectively. Regarding (3.32) as a similarity transformation one immediately has

$$\mu_i(\mathbf{v}) = \lambda_i(\mathbf{u}) \quad \text{and} \quad \bar{\mathbf{r}}_i(\mathbf{v}) = (\nabla_{\mathbf{v}}\Phi(\mathbf{v}))^{-1}\mathbf{r}_i(\Phi(\mathbf{v})).$$

Therefore, the following relation holds

$$\begin{aligned} \nabla_{\mathbf{u}}\lambda_i(\mathbf{u}) \cdot \mathbf{r}_i(\mathbf{u}) &= \nabla_{\mathbf{u}}\lambda_i(\Phi(\mathbf{v})) \cdot \mathbf{r}_i(\Phi(\mathbf{v})) \\ &= \nabla_{\mathbf{u}}\lambda_i(\Phi(\mathbf{v})) \cdot \nabla_{\mathbf{v}}\Phi(\mathbf{v})\bar{\mathbf{r}}_i(\Phi(\mathbf{v})) \\ &= \nabla_{\mathbf{v}}\mu_i(\mathbf{v}) \cdot \mathbf{r}_i(\Phi(\mathbf{v})) \end{aligned}$$

Due to this property, we can just transform a system of conservation laws into the much simpler primitive variable form to study its characteristic fields.

3.2.1 Simple waves

In this subsection, we follow the presentation given in Evans [28]. To find a solution to the system of conservation laws (3.25) we first search for a solution having a particular form. Assume the solution having the following structure

$$\mathbf{u}(t, x) = \mathbf{v}(w(t, x)),$$

with $\mathbf{v} : \mathbb{R} \rightarrow \mathbb{R}^m$ and $w : [0, \infty) \times \mathbb{R} \rightarrow \mathbb{R}$. Solutions of this form are called *simple waves*. Inserting this ansatz into (3.25) leads to

$$\dot{\mathbf{v}}(w) \frac{\partial}{\partial t} w + \mathbf{Df}(\mathbf{v}(w)) \dot{\mathbf{v}}(w) \frac{\partial}{\partial x} w = 0. \quad (3.33)$$

The task is now to determine the functions \mathbf{v} and w . Equation (3.33) holds if for some $i \in \{1, \dots, m\}$ the function w solves

$$\frac{\partial}{\partial t} w + \lambda_i(\mathbf{v}(w)) \frac{\partial}{\partial x} w = 0 \quad (3.34)$$

and \mathbf{v} solves

$$\frac{d}{ds} \mathbf{v}(s) = \alpha(s) \mathbf{r}_i(\mathbf{v}(s)). \quad (3.35)$$

Here, $\alpha(s) \in \mathbb{R}$ is a scaling factor, since the eigenvectors of $\mathbf{A} = \mathbf{Df}$ are determined only up to a multiplicative constant. But it is convenient to normalize the right eigenvector $\mathbf{r}_i(\mathbf{v}(s))$ such that $\alpha(s) = 1$.

The idea is now to solve (3.35) first. It is an ODE for the vector function \mathbf{v} . This equation gives rise to the following definition.

Definition 3.2.4 (Rarefaction wave curve). *The i -rarefaction wave curve $\mathcal{R}_i(\mathbf{u}_0)$ is defined as the integral curve of the ODE-system*

$$\begin{cases} \dot{\mathbf{v}}(s) = \mathbf{r}_i(\mathbf{v}(s)) \\ \mathbf{v}(s_0) = \mathbf{u}_0 \end{cases}, \quad (3.36)$$

where $\mathbf{u}_0 \in \mathbb{R}^m$ is a given fixed state.

From this definition we see immediately that the i -rarefaction wave curve \mathcal{R}_i is tangent to $\mathbf{r}_i(\mathbf{v}(s))$ everywhere.

Having found a solution \mathbf{v} of (3.35) the equation (3.34) may be regarded as a scalar conservation law for w . We will rewrite this equation in the following form

$$\frac{\partial}{\partial t} w + \frac{\partial}{\partial x} f_i(w) = 0, \quad (3.37)$$

with the flux function given by

$$f_i(s) := \int_0^s \lambda_i(\mathbf{v}(t)) dt \quad \text{for } s \in \mathbb{R}.$$

Calculating the derivatives and using (3.36) leads to

$$\begin{aligned} f_i'(s) &= \lambda_i(\mathbf{v}(s)), \\ f_i''(s) &= \nabla_{\mathbf{v}} \lambda_i(\mathbf{v}(s)) \cdot \dot{\mathbf{v}}(s) = \nabla_{\mathbf{v}} \lambda_i(\mathbf{v}(s)) \cdot \mathbf{r}_i(\mathbf{v}(s)). \end{aligned} \quad (3.38)$$

Hence, the function f_i will be

- convex, if $\nabla_{\mathbf{u}} \lambda_i(\mathbf{u}) \cdot \mathbf{r}_i(\mathbf{u}) > 0 \quad \text{for all } \mathbf{u} \in \mathcal{U}$
- concave, if $\nabla_{\mathbf{u}} \lambda_i(\mathbf{u}) \cdot \mathbf{r}_i(\mathbf{u}) < 0 \quad \text{for all } \mathbf{u} \in \mathcal{U}$
- linear, if $\nabla_{\mathbf{u}} \lambda_i(\mathbf{u}) \cdot \mathbf{r}_i(\mathbf{u}) \equiv 0 \quad \text{for all } \mathbf{u} \in \mathcal{U}$

which should motivate Definition 3.2.3 and shows the analogy to the scalar case, again.

Considering a general curve $s \rightarrow \mathbf{v}(s)$ the change of the eigenvalue along this curve is given by

$$\frac{d}{ds} \lambda_i(\mathbf{v}(s)) = \nabla_{\mathbf{v}} \lambda_i(\mathbf{v}(s)) \dot{\mathbf{v}}(s) = \nabla_{\mathbf{v}} \lambda_i(\mathbf{v}(s)) \mathbf{r}_i(\mathbf{v}(s)).$$

With regard to Definition 3.2.3, an eigenvalue is thus strictly monotone for a genuinely nonlinear characteristic field and it is constant for a linearly degenerated characteristic field along the curve $\mathbf{v}(s)$, which again highlights the connection to the scalar case.

3.2.2 The Riemann problem

The Riemann problem for a system of conservation laws is a specific IVP for the system of conservation laws (3.25). It is given as

$$\begin{aligned} \text{PDE: } & \frac{\partial}{\partial t} \mathbf{u} + \frac{\partial}{\partial x} \mathbf{f}(\mathbf{u}) = 0 \\ \text{IC: } & \mathbf{u}(0, x) = \begin{cases} \mathbf{u}_- & \text{for } x < 0 \\ \mathbf{u}_+ & \text{for } x > 0 \end{cases} \end{aligned} \quad (3.39)$$

with $\mathbf{u} = \mathbf{u}(t, x) \in \mathcal{U}$ and $(t, x) \in (0, t_{\max}) \times \mathbb{R}$. As before \mathbf{u} denotes the vector of unknowns, \mathcal{U} is the state space and the flux is given by a smooth function $\mathbf{f} : \mathcal{U} \rightarrow \mathbb{R}^m$. The initial data consist of two constant states. We will call the given vectors \mathbf{u}_- and \mathbf{u}_+ the left and right *initial states*. The initial data are often called *Riemann (initial) data*.

The Riemann problem is the simplest non-trivial IVP for our system of conservation laws. Its solution still exhibits all the classical nonlinear phenomena. Its solution is not only of analytical interest but also a fundamental building block for numerical schemes. All Godunov-type finite volume schemes require an analytical or approximate solution of the Riemann problem at each cell boundary. We will comment later on these details for numerical approximations, see Chapter 5.

In the following subsections, we will present the fundamental concepts used to find a solution to the Riemann problem (3.39). Therefore we have to consider different strategies for the different wave types as before in the case of a scalar hyperbolic equation.

3.2.3 Rarefaction waves and Riemann invariants

We first note that the Riemann problem for a system of conservation laws (3.39) is invariant under the transformation $(t, x) \mapsto (\alpha t, \alpha x)$. A solution, therefore, is invariant when the space and the time variable are scaled by the same factor α , hence the name *self-similar solutions*. These solutions are of the following form

$$\mathbf{u}(t, x) = \mathbf{v}(\xi) \quad \text{with} \quad \xi := \frac{x}{t}, \quad (3.40)$$

so with respect to the simple wave approach we set $w(t, x) = \xi$. Under this ansatz the Riemann problem (3.39) as an initial value problem transforms into a boundary value problem w.r.t. ξ

$$\begin{aligned} -\mathbf{v}'(\xi)\xi + \mathbf{f}(\mathbf{v}(\xi))' &= 0 \\ \mathbf{v}(-\infty) &= \mathbf{v}_- \\ \mathbf{v}(+\infty) &= \mathbf{v}_+. \end{aligned}$$

Here, the prime denotes the derivative with respect to ξ . Concerning the simple wave ansatz, we can obtain the following important result immediately.

Equation (3.34) reads

$$\frac{\partial}{\partial t}w + \lambda_i(\mathbf{v}(w))\frac{\partial}{\partial x}w = 0. \quad (3.41)$$

In case of $w(t, x) = \frac{x}{t}$ this is equivalent to

$$\lambda_i(\mathbf{v}(\xi)) = \xi. \quad (3.42)$$

We can now draw the important conclusion from the equations above that the characteristic curves $x(t)$ are straight lines, i.e. curves on which the solution is constant. Following the method of characteristics, these curves are defined by

$$\frac{dx}{dt} = \lambda_i(\mathbf{v}(\xi)) = \xi, \quad (3.43)$$

where the index i denotes the number of the characteristic field under consideration. If we fix the value of ξ , the variable $\mathbf{v}(\xi)$ and the eigenvalue $\lambda_i(\mathbf{v}(\xi))$ are constant. In the case of a simple centered rarefaction wave, the solution is thus constant along the characteristic curves. This can also be seen from equation (3.41) with (3.43)

$$\frac{dw}{dt}(t, x(t)) = \frac{\partial}{\partial t}w + \frac{dx}{dt}\frac{\partial}{\partial x}w = 0.$$

We now want to analyze the ansatz (3.40) with regard to Definition 3.2.3, i.e. the distinction between genuinely nonlinear and linearly degenerated fields. Plugging the ansatz (3.40) into the PDE of (3.39) and using $\frac{\partial}{\partial t} = -\frac{\xi}{t}\frac{d}{d\xi}$ and $\frac{\partial}{\partial x} = \frac{1}{t}\frac{d}{d\xi}$ leads to

$$-\frac{\xi}{t}\mathbf{v}'(\xi) + \mathbf{Df}(\mathbf{v}(\xi))\frac{1}{t}\mathbf{v}'(\xi) = 0. \quad (3.44)$$

Note again that the smoothness of the solution is of utter importance in this case to use the chain rule. The term $\mathbf{Df}(\mathbf{u}) = \mathbf{A}(\mathbf{u}) = \frac{\partial \mathbf{f}(\mathbf{u})}{\partial \mathbf{u}}$ is the Jacobian matrix of the flux function $\mathbf{f}(\mathbf{u})$ as before. Equation (3.44) can be rewritten in the following form by multiplying with t

$$[\mathbf{A}(\mathbf{v}) - \xi \mathbf{I}]\mathbf{v}'(\xi) = 0, \quad (3.45)$$

This relation strongly reminds us of equation (3.29) for the right eigenvectors as part of the definition of hyperbolicity of the system (3.25). The trivial solution of (3.45) is

$$\mathbf{v}'(\xi) = 0.$$

Nontrivial solutions are obtained for the case where ξ is an eigenvalue of \mathbf{A} and \mathbf{v}' is parallel to the eigenvector of \mathbf{A} , i.e. when there exists an $i \in \{1, 2, \dots, m\}$ such that

$$\lambda_i(\mathbf{v}(\xi)) = \xi \quad \text{and} \quad \mathbf{v}'(\xi) = \alpha(\xi)\mathbf{r}_i(\mathbf{v}(\xi)).$$

Here $\alpha(\xi)$ can be either seen as the amplitude of the vector $\mathbf{v}(\xi)$ or an appropriate scaling factor since the eigenvectors of \mathbf{A} are only determined up to a multiplicative constant as before. In either way, it is possible and convenient to normalize the right eigenvector $\mathbf{r}_i(\mathbf{v}(\xi))$ such that $\alpha(\xi) = 1$. This leads to

$$\lambda_i(\mathbf{v}(\xi)) = \xi \quad \text{and} \quad \mathbf{v}'(\xi) = \mathbf{r}_i(\mathbf{v}(\xi)). \quad (3.46)$$

Thus from the first relation in (3.46), we obtain

$$\frac{d\lambda_i(\mathbf{v}(\xi))}{d\xi} = \nabla_{\mathbf{v}}\lambda_i(\mathbf{v}(\xi)) \cdot \mathbf{v}'(\xi) = 1. \quad (3.47)$$

Finally, inserting the second relation of (3.46) leads to

$$\nabla_{\mathbf{v}}\lambda_i(\mathbf{v}(\xi)) \cdot \mathbf{r}_i(\mathbf{v}(\xi)) = 1,$$

which implies that the i -th characteristic field is genuinely nonlinear. Note, that by the second relation of (3.46) the self-similar solution $\mathbf{v}(\xi)$ is the integral curve along the field $\mathbf{r}_i(\mathbf{v}(\xi))$. In view of Definition 3.2.4 the i -rarefaction wave curve $\mathcal{R}_i(\mathbf{v}_0)$ is given by

$$\begin{cases} \mathbf{v}'(\xi) = \mathbf{r}_i(\mathbf{v}(\xi)) \\ \mathbf{v}(\xi_0) = \mathbf{v}_0. \end{cases}$$

We have shown that the i -th characteristic field is genuinely nonlinear and determined the i -rarefaction wave curve. These properties allow us to formulate the following theorem, motivated by the presentation given in Evans [28].

Theorem 3.2.1 (Existence of i -rarefaction waves). *Suppose that for some $i \in \{1, 2, \dots, n\}$*

- (i) *the i -th characteristic field $(\lambda_i(\mathbf{u}), \mathbf{r}_i(\mathbf{u}))$ is genuinely nonlinear and*
- (ii) *$\mathbf{u}_+ \in \mathcal{R}_i(\mathbf{u}_-)$ with $\lambda_i(u_-) \leq \lambda_i(u_+)$.*

Then there exists a continuous integral solution \mathbf{u} of the Riemann problem (3.39), which is an i -simple wave that is constant along the lines through the origin.

Proof. Choose $w_-, w_+ \in \mathbb{R}$ such that

$$\mathbf{u}_- = \mathbf{v}(w_-) \quad \text{and} \quad \mathbf{u}_+ = \mathbf{v}(w_+).$$

We will first consider the case $w_- < w_+$. Then one has to solve the Riemann problem (3.37), that is

$$\frac{\partial}{\partial t} w + \frac{\partial}{\partial x} f_i(w) = 0,$$

together with the initial data

$$w_0(x) = \begin{cases} w_- & \text{if } x < 0, \\ w_+ & \text{if } x \geq 0. \end{cases}$$

From (ii) we have $\lambda_i(u_-) \leq \lambda_i(u_+)$ and according to (3.38) this is equivalent to $f'_i(w_-) < f'_i(w_+)$. Together with condition (i) this implies the convexity of f_i . Thus we have a scalar Riemann problem with a convex flux function, compare to (3.13). The unique solution is therefore given by (3.15), which is a continuous rarefaction wave connecting the states w_- and w_+ . In this case it is

$$w(t, x) = \begin{cases} w_- & \text{if } \frac{x}{t} < \lambda_i(\mathbf{v}(w_-)), \\ \text{root of } \lambda_i(\mathbf{v}(\frac{x}{t})) - \frac{x}{t} = 0 & \text{if } \lambda_i(\mathbf{v}(w_-)) \leq \frac{x}{t} \leq \lambda_i(\mathbf{v}(w_+)), \\ w_+ & \text{if } \frac{x}{t} > \lambda_i(\mathbf{v}(w_+)). \end{cases}$$

Therefore $\mathbf{u}(t, x) = \mathbf{v}(w(t, x))$ with \mathbf{v} being an integral curve of the ODE-system (3.35) passing through \mathbf{u}_- is a solution. It is a continuous solution of the Riemann problem (3.39). The case $w_- > w_+$ is treated analogously. \square

Now we have seen how one can determine the solution connecting appropriate states \mathbf{u}_- and \mathbf{u}_+ along a rarefaction wave curve. This solution is constant along lines through the origin. However, to solve the Riemann problem, we need some relations across the different wave structures. In the case of a rarefaction wave, we therefore search for some relations across the rarefaction wave. We already know that the rarefaction wave curve connects the states \mathbf{u}_- and \mathbf{u}_+ across a rarefaction. One very successful ansatz is given by the following definition of Riemann invariants. The idea is to find functions with advantageous properties along the rarefaction wave curve \mathcal{R}_i .

Definition 3.2.5 (Riemann Invariants). *An i -th Riemann invariant is a smooth function $\omega_i : \mathcal{U} \rightarrow \mathbb{R}$ such that*

$$\nabla_{\mathbf{u}}\omega(\mathbf{u}) \cdot \mathbf{r}_i(\mathbf{u}) = 0 \quad \text{for all } \mathbf{u} \in \mathcal{U}. \quad (3.48)$$

The gradient of the function $\omega_i(\mathbf{u})$ is therefore perpendicular to $\mathbf{r}_i(\mathbf{u})$. With regard to Definition 3.2.4 of the rarefaction wave curve this is equivalent to the very important statement that ω_i is constant on the rarefaction wave curve $\mathcal{R}_i(\mathbf{u}_-)$. Indeed we have

$$\frac{d}{d\xi}\omega_i(\mathbf{v}(\xi)) = \nabla_{\mathbf{u}}\omega(\mathbf{u}) \cdot \mathbf{v}'(\xi) = \nabla_{\mathbf{u}}\omega(\mathbf{u}) \cdot \mathbf{r}_i(\mathbf{u}) = 0,$$

due to the definition above. Thus one can say that an i -th Riemann invariant is constant across a simple wave. Smoller [78] used this result as the defining property for simple waves and reversed the argumentation given here.

Note that in general, for $m > 2$, Riemann invariants do not have to exist, see Evans [28]. Only in the strictly hyperbolic case can one guarantee to find $m - 1$ Riemann invariants for characteristic fields that are genuinely nonlinear or linearly degenerated. The gradient of a Riemann invariant belongs to the $m - 1$ dimensional subspace orthogonal to the span of the eigenvector $\mathbf{r}_i(\mathbf{u})$, see (3.48). Therefore one can find $m - 1$ i -th Riemann invariants with linearly independent gradients. The proof can be found e.g. in Smoller [78]. We will not present the proof here and rather turn our attention to finding these Riemann invariants.

In case of a linearly degenerated field one can find a Riemann invariant immediately. Using the definition of linear degeneracy, see Definition 3.2.3

$$\nabla_{\mathbf{u}} \lambda_i(\mathbf{u}) \cdot \mathbf{r}_i(\mathbf{u}) = 0, \quad (3.49)$$

we see that the characteristic speed λ_i is an i -th Riemann invariant.

In general, one can use the Equation (3.35) or, more specifically, in case of a rarefaction wave Equation (3.46)

$$\frac{d}{d\xi} \mathbf{v}(\xi) = \mathbf{r}_i(\mathbf{v}(\xi)) \quad (3.50)$$

to find Riemann invariants. We will show how this can be done in the following example. There is no general method of solving that equation, as this comes down to knowing how to integrate all the differential equations. But in some applications, separation of variables, homogeneity properties or considerations of symmetry enable us to set up an explicit list of Riemann invariants.

Example 3.2.1 (Isothermal Compressible Gas Dynamics). *The governing PDE system consists of the conservation equation of mass and momentum for the fluid*

$$\begin{aligned} \frac{\partial}{\partial t} \rho + \frac{\partial}{\partial x} (\rho u) &= 0 \\ \frac{\partial}{\partial t} (\rho u) + \frac{\partial}{\partial x} (\rho u^2 + p) &= 0. \end{aligned}$$

Here, ρ is the mass density of the fluid, u is the velocity and $p = a^2 \rho$ is the pressure according to the isothermal hypothesis. An equation for the energy conservation is absent which is due to the isothermal property. The nonlinear PDE system can be rewritten as

$$\frac{\partial \mathbf{q}}{\partial t} + \frac{\partial \mathbf{f}(\mathbf{q})}{\partial x} = 0, \quad \mathbf{q}, \mathbf{f} \in \mathbb{R}^2, \quad t \in \mathbb{R}_0^+, \quad x \in \mathbb{R}$$

where we have deliberately chosen the vector of conserved variables to be \mathbf{q} and not \mathbf{u} as usual to avoid confusion with the velocity u . The conserved variables and flux vector are defined as

$$\mathbf{q} = \begin{pmatrix} \rho \\ \rho u \end{pmatrix} = \begin{pmatrix} q_1 \\ q_2 \end{pmatrix}, \quad \mathbf{f} = \begin{pmatrix} \rho u \\ \rho u^2 + p \end{pmatrix} = \begin{pmatrix} q_2 \\ q_2^2/q_1 + a^2 q_1 \end{pmatrix}.$$

One may verify that the Jacobian matrix \mathbf{A} of the flux \mathbf{f} with respect to the vector of conserved variables \mathbf{q} is given by

$$\mathbf{A} = \begin{pmatrix} 0 & 1 \\ -q_2^2/q_1^2 + a^2 & 2q_2/q_1 \end{pmatrix} = \begin{pmatrix} 0 & 1 \\ a^2 - u^2 & 2u \end{pmatrix}.$$

The diagonal matrix of eigenvalues is $\mathbf{\Lambda} = \text{diag}(u - a, u + a)$ and the corresponding matrix of right eigenvectors

$$\mathbf{R} = \begin{pmatrix} 1 & 1 \\ u - a & u + a \end{pmatrix}.$$

We find that the associated characteristic fields for both eigenvalues are genuinely nonlinear since

$$\begin{aligned} \nabla_{\mathbf{q}} \lambda_{1,2} &= \nabla_{\mathbf{q}}(u \mp a) = \frac{\partial}{\partial \mathbf{q}} (q_2/q_1 \mp a) \\ &= \left(-q_2/q_1^2, 1/q_1 \right)^T = (-u/\rho, 1/\rho)^T. \end{aligned} \quad (3.51)$$

This leads to

$$\begin{aligned} \nabla_{\mathbf{q}} \lambda_{1,2} \cdot \mathbf{r}_{1,2} &= (-u/\rho, 1/\rho)^T \cdot (1, u \mp a)^T \\ &= \mp a/\rho \neq 0, \quad \forall Q \in \Omega_Q. \end{aligned} \quad (3.52)$$

These nonlinear waves associated with both eigenvalues can be either a shock wave satisfying the Lax entropy condition in case of compression of the characteristics or else a centered rarefaction wave.

Let us now consider the first characteristic field $\lambda_1 = u - a$ to be a centered rarefaction wave. We can then calculate the Riemann invariants using relation (3.50). Keep in mind that in the simple wave ansatz we set $\mathbf{q}(t, x) = \mathbf{v}(\xi)$. With the vector of unknowns \mathbf{q} and the eigenvector \mathbf{r}_1 given above we get

$$\frac{d}{d\xi} \mathbf{v}(\xi) = \mathbf{r}_1(\mathbf{v}(\xi)), \quad \Rightarrow \quad \frac{d}{d\xi} \begin{pmatrix} \rho \\ \rho u \end{pmatrix} = \begin{pmatrix} 1 \\ u - a \end{pmatrix}.$$

This leads to the following two relations

$$\frac{d\rho}{d\xi} = 1, \quad \frac{d}{d\xi}(\rho u) = u \frac{d\rho}{d\xi} + \rho \frac{du}{d\xi} = u - a.$$

From the first relation we get

$$\int_{\rho_-}^{\rho} dr = \int_0^{\xi} ds, \quad \Rightarrow \quad \rho(\xi) = \rho_- + \xi.$$

Using the first relation the second one is

$$\frac{d}{d\xi}(\rho u) = u + \rho \frac{du}{d\xi} = u - a, \quad \Rightarrow \quad \frac{du}{d\xi} = -\frac{a}{\rho}.$$

Hence, we get

$$\begin{aligned} \int_{u_-}^u du &= \int_0^{\xi} -\frac{a}{\rho(s)} ds = \int_0^1 -\frac{a}{\rho_- + \xi} d\xi \\ \Rightarrow u(\xi) - u_- &= -a (\ln(\rho(\xi)) - \ln(\rho_-)) \\ \Rightarrow u(\xi) &= u_- + a \ln \frac{\rho_-}{\rho(\xi)}. \end{aligned}$$

From this equation we can derive the Riemann invariant for isothermal gas dynamics

$$u(\xi) + a \ln(\rho(\xi)) = u_- + a \ln(\rho_-) := w_1^1 = \text{const.} \quad (3.53)$$

This relation holds across the λ_1 -wave. Here, we used the notation w_j^k to denote the k -th Riemann invariant associated with the j -th characteristic field. Note, that in general for a system of m equations, relation (3.50) gives rise to $m - 1$ Riemann invariants. Hence, in this example, we get one Riemann invariant for each rarefaction wave.

Along the characteristic curves associated with the eigenvalue λ_1 we have $\xi = \lambda_1 = u - a$. Together with equation (3.53) we can calculate the primitive variables in a particular point ξ along the characteristic curves inside the rarefaction fan as

$$u = a + \xi \quad \text{and} \quad \rho = \rho_- \exp\left(\frac{u_- - u}{a}\right). \quad (3.54)$$

We will make use of these techniques later in Chapter 4 to determine the solution to the system of conservation laws considered in the case of rarefaction waves. To calculate the Riemann invariants, we will not use equation (3.50) but instead the following so-called *generalized Riemann invariants*, see Jeffrey [42].

Definition 3.2.6 (Generalized Riemann Invariants). *Let $(\lambda_i, \mathbf{r}_i)$ be the i -th characteristic field of a general hyperbolic system of m conservation laws (3.25). The i -th generalized Riemann invariants are the $m - 1$ ordinary differential equations*

$$\frac{du_1}{r_1^{(i)}} = \frac{du_2}{r_2^{(i)}} = \frac{du_3}{r_3^{(i)}} = \dots = \frac{du_m}{r_m^{(i)}}, \quad (3.55)$$

where $\mathbf{u} = (u_1, u_2, \dots, u_m)^T$ is the vector of dependent variables in some suitable set, which may be the set of conserved variables or primitive variables and $\mathbf{r}_i = (r_1^{(i)}, r_2^{(i)}, \dots, r_m^{(i)})$ the right eigenvector of the i -characteristic field.

The most important observation is that the concepts of Riemann invariants and generalized Riemann invariants are absolutely identical. This can easily be seen by expressing the generalized Riemann invariants in terms of a parameter ξ and thus writing them in the form

$$\frac{du_1}{r_1^{(i)}} = \frac{du_2}{r_2^{(i)}} = \frac{du_3}{r_3^{(i)}} = \dots = \frac{du_m}{r_m^{(i)}} = d\xi.$$

One can then calculate the u_j in terms of ξ by integrating the system

$$\frac{du_j}{d\xi} = r_j^{(i)}, \quad j = 1, \dots, m.$$

Note that this system is identical to equation (3.50) and we have calculated \mathbf{q} in Example 3.2.1 using this relation. The name *generalized Riemann invariants* appeared because Jeffrey [42] introduced the Riemann invariants in the case of 2×2 systems and then generalized this idea to $m \times m$ systems of conservation laws.

As the final part of this section, we want to go back to isothermal gas dynamics. We want to show how the variable transformation to primitive variables is done and how it simplifies the calculations, especially of the Riemann invariants. In this simple example, one might barely spot the simplification in contrast to the system of conservation laws under consideration in Chapter 4.

Example 3.2.2 (Isothermal Compressible Gas Dynamics revisited). *Again, the system of isothermal compressible gas dynamics is given by*

$$\begin{aligned} \frac{\partial}{\partial t} \rho + \frac{\partial}{\partial x} (\rho u) &= 0, \\ \frac{\partial}{\partial t} (\rho u) + \frac{\partial}{\partial x} (\rho u^2 + p) &= 0. \end{aligned}$$

Since, up to this point, we are only looking for smooth solutions, we can use the product rule of differentiation on this system of conservation laws. This leads to

$$\begin{aligned} \frac{\partial}{\partial t} \rho + u \frac{\partial}{\partial x} \rho + \rho \frac{\partial}{\partial x} u &= 0, \\ \rho \frac{\partial}{\partial t} u + u \frac{\partial}{\partial t} \rho + u \frac{\partial}{\partial x} (\rho u) + \rho u \frac{\partial}{\partial x} u + \frac{\partial}{\partial x} p &= 0. \end{aligned}$$

We can then rewrite the second equation as

$$\begin{aligned} \rho \frac{\partial}{\partial t} u + u \underbrace{\left(\frac{\partial}{\partial t} \rho + \frac{\partial}{\partial x} (\rho u) \right)}_{=0} + \rho u \frac{\partial}{\partial x} u + \frac{\partial}{\partial x} (a^2 \rho) &= 0 \\ \Rightarrow \rho \left(\frac{\partial}{\partial t} u + u \frac{\partial}{\partial x} u + \frac{a^2}{\rho} \frac{\partial}{\partial x} \rho \right) &= 0. \end{aligned}$$

where we have used the equation of state $p = a^2 \rho$. Hence, we can write the system in the following quasi-linear primitive variable form with $\mathbf{q} = (\rho, u)^T$ being the vector of primitive variables

$$\frac{\partial}{\partial t} \begin{pmatrix} \rho \\ u \end{pmatrix} + \begin{pmatrix} u & \rho \\ a^2/\rho & u \end{pmatrix} \cdot \frac{\partial}{\partial x} \begin{pmatrix} \rho \\ u \end{pmatrix} = 0.$$

The eigenvalues are therefore given as $\lambda_1 = u - a$ and $\lambda_2 = u + a$ with the corresponding eigenvectors

$$\mathbf{r}_1 = \begin{pmatrix} \rho \\ -a \end{pmatrix} \quad \text{and} \quad \mathbf{r}_2 = \begin{pmatrix} \rho \\ a \end{pmatrix}.$$

Again, we get that the characteristic fields are genuinely nonlinear, see (3.51) and (3.52)

$$\begin{aligned} \nabla_{\mathbf{q}} \lambda_{1,2} \cdot \mathbf{r}_{1,2} &= (-u/\rho, 1/\rho)^T \cdot (1, u \mp a)^T \\ &= \mp a/\rho \neq 0, \quad \forall Q \in \Omega_Q. \end{aligned}$$

If we assume the λ_1 -wave to be a rarefaction wave we can immediately calculate the generalized Riemann invariants without going through all the details in the simple wave ansatz. The generalized Riemann invariant here reads

$$\frac{dq_1}{r_1^{(i)}} = \frac{dq_2}{r_2^{(i)}} \quad \Rightarrow \quad \frac{d\rho}{\rho} = \frac{du}{-a},$$

which can be integrated without any further problem

$$v + a \ln \rho = \text{const.} (= v_- + a \ln \rho_-).$$

Since we know the left state from the initial condition, we can determine the value of this Riemann invariant.

3.2.4 Shock waves and contact discontinuities

In this subsection we want to turn our attention to the cases we have not considered yet, namely $\lambda_i(\mathbf{u}_-) > \lambda_i(\mathbf{u}_+)$ and $\lambda_i(\mathbf{u}_-) = \lambda_i(\mathbf{u}_+)$.

In a first attempt, we would like to use the theory developed so far in these cases, too. Therefore we will start from the simple wave ansatz

$$\mathbf{u}(t, x) = \mathbf{v}(w(t, x)),$$

with $\mathbf{v} : \mathbb{R} \rightarrow \mathbb{R}^m$ and $w : [0, \infty) \times \mathbb{R} \rightarrow \mathbb{R}$, again. We have already seen that this leads to a scalar equation for w , see equation (3.34)

$$\begin{aligned} \frac{\partial w}{\partial t} + \lambda_i(\mathbf{v}(w)) \frac{\partial w}{\partial x} &= 0, \\ w(0, x) &= w_0(x). \end{aligned} \quad (3.56)$$

Since we already know that characteristics are straight lines and the solution is constant along them, we can solve this transport equation immediately and the function w only depends on the choice of the initial data w_0

$$w(t, x) = w_0(x - \lambda_i(\mathbf{v}(t, x))t).$$

Let us assume the i -th characteristic field to be genuinely nonlinear. With proper rescaling, we get

$$\frac{d}{dw} \lambda_i(\mathbf{v}(w)) = \nabla_{\mathbf{v}} \lambda_i(\mathbf{v}(w)) \cdot \mathbf{v}'(w) = 1,$$

compare to equation (3.47). Thus, adapting the initial function w_0 , we can get

$$\lambda_i(\mathbf{v}(w)) = w. \quad (3.57)$$

Hence, equation (3.56) becomes the Burgers equation, which reads

$$\frac{\partial w}{\partial t} + w \frac{\partial w}{\partial x} = 0.$$

Our aim is to solve the Riemann problem with the initial states \mathbf{u}_- and \mathbf{u}_+ . With regard to (3.57) we have for the initial function w_0

$$w_0(x) = \begin{cases} \lambda_i(\mathbf{u}_-) & \text{if } x < 0, \\ \lambda_i(\mathbf{u}_+) & \text{if } x \geq 0. \end{cases}$$

But from Section 3.1 we already know the solution of the Burgers equation in the case $\lambda_i(\mathbf{u}_-) > \lambda_i(\mathbf{u}_+)$ is given by a discontinuous shock

$$w(t, x) = \begin{cases} \lambda_i(\mathbf{u}_-) & \text{if } \frac{x}{t} < s, \\ \lambda_i(\mathbf{u}_+) & \text{if } \frac{x}{t} \geq s, \end{cases}$$

with $s = \frac{\lambda_i(\mathbf{u}_-) + \lambda_i(\mathbf{u}_+)}{2}$ being the shock speed, see Example 3.1.2. Consequently, in case of Riemann initial states \mathbf{u}_- and \mathbf{u}_+ they can not be connected

by a continuous i -simple wave. As we will see, they form a discontinuous shock.

Let us now consider the case that the i -th characteristic field is linearly degenerate. As we have seen in the previous subsection, see (3.49), in this case the eigenvalue λ_i is a Riemann invariant itself, i.e. $\lambda_i(\mathbf{u}_-) = \lambda_i(\mathbf{u}_+)$. Along the i -simple wave the eigenvalue $\lambda_i(\mathbf{u})$ is thus constant. As before, the characteristic curves are straight lines. Since the eigenvalue is constant these are parallel lines $x - \lambda_i t$. The corresponding solution would then be given as

$$\mathbf{u}(t, x) = \mathbf{v}(w_0(x - \lambda_i(\mathbf{v}(t, x))t)).$$

Obviously, the two states \mathbf{u}_- and \mathbf{u}_+ cannot be connected by a continuous i -simple wave if the initial data are discontinuous.

Again, as in the scalar case, we have to turn at least to the integral form of conservation laws to describe discontinuous solutions. For later purposes we would like to extend this idea even further to the so-called *weak formulation*, see for example [16, 78] or [89]. Therefore, let us start with a general initial value problem of a system of conservation laws

$$\begin{aligned} \frac{\partial}{\partial t} \mathbf{u}(t, x) + \frac{\partial}{\partial x} \mathbf{f}(\mathbf{u}(t, x)) &= 0, \\ \mathbf{u}(0, x) &= \mathbf{u}_0(x), \end{aligned} \tag{3.58}$$

with $(t, x) \in (0, t_{\max}) \times \mathbb{R}$.

Following the presentation given in Smoller [78] we assume for the moment that \mathbf{u} is a classical solution of (3.58). We will now multiply this equation with a smooth test function with compact support, that is $\phi \in [C_0^\infty([0, t_{\max}) \times \mathbb{R})]^m$, and integrate over a domain \mathcal{D} . Since ϕ has compact support we can find a suitable large enough rectangle $\mathcal{D} = \{(t, x) \subseteq \mathbb{R}_{\geq 0} \times \mathbb{R} : 0 \leq t \leq t_{\max}, a \leq x \leq b\}$ such that ϕ vanishes outside of the domain \mathcal{D} and on the lines $t = t_{\max}$, $x = a$ and $x = b$. Multiplying (3.58) with ϕ and integrating over $t > 0$ gives

$$\begin{aligned} \iint_{t>0} \left(\frac{\partial}{\partial t} \mathbf{u} + \frac{\partial}{\partial x} \mathbf{f}(\mathbf{u}) \right) \cdot \phi \, dx dt &= \iint_{\mathcal{D}} \left(\frac{\partial}{\partial t} \mathbf{u} + \frac{\partial}{\partial x} \mathbf{f}(\mathbf{u}) \right) \cdot \phi \, dx dt \\ &= \int_0^{t_{\max}} \int_a^b \left(\frac{\partial}{\partial t} \mathbf{u} + \frac{\partial}{\partial x} \mathbf{f}(\mathbf{u}) \right) \cdot \phi \, dx dt = 0. \end{aligned}$$

Integrating by parts leads to

$$\begin{aligned} \int_0^{t_{\max}} \int_a^b \left(\frac{\partial}{\partial t} \mathbf{u} \right) \cdot \boldsymbol{\phi} \, dx dt &= \int_a^b \mathbf{u} \cdot \boldsymbol{\phi} \Big|_{t=0}^{t=t_{\max}} dx - \int_0^{t_{\max}} \int_a^b \mathbf{u} \cdot \left(\frac{\partial}{\partial t} \boldsymbol{\phi} \right) dx dt \\ &= \int_a^b -\mathbf{u}_0(x) \cdot \boldsymbol{\phi}(0, x) dx - \int_0^{t_{\max}} \int_a^b \mathbf{u} \cdot \left(\frac{\partial}{\partial t} \boldsymbol{\phi} \right) dx dt, \end{aligned}$$

and

$$\int_0^{t_{\max}} \int_a^b \left(\frac{\partial}{\partial x} \mathbf{f}(\mathbf{u}) \right) \cdot \boldsymbol{\phi} \, dx dt = \int_0^{t_{\max}} \mathbf{f}(\mathbf{u}) \cdot \boldsymbol{\phi} \Big|_{x=a}^{x=b} dt - \int_0^{t_{\max}} \int_a^b \mathbf{f}(\mathbf{u}) \cdot \left(\frac{\partial}{\partial x} \boldsymbol{\phi} \right) dx dt.$$

Summing up these relations, we finally get

$$\int_0^{t_{\max}} \int_a^b \left(\mathbf{u} \cdot \frac{\partial}{\partial t} \boldsymbol{\phi} + \mathbf{f}(\mathbf{u}) \cdot \frac{\partial}{\partial x} \boldsymbol{\phi} \right) dx dt + \int_a^b \mathbf{u}_0(x) \cdot \boldsymbol{\phi}(0, x) dx = 0. \quad (3.59)$$

So in case of \mathbf{u} being a classical solution, equation (3.59) holds for all $\boldsymbol{\phi} \in [C_0^\infty([0, t_{\max}) \times \mathbb{R})]^m$. Since $\boldsymbol{\phi}$ vanishes outside of \mathcal{D} we can integrate over the whole (t, x) -plane. Furthermore, equation (3.59) makes sense for a much broader class of functions. Thus, we give the following definition.

Definition 3.2.7 (Weak Solution). *A measurable and bounded function $\mathbf{u} : (0, t_{\max}) \times \mathbb{R} \rightarrow \mathbb{R}^m$ is called a weak solution of (3.58) if it satisfies*

$$\int_0^{t_{\max}} \int_{-\infty}^{\infty} \left(\mathbf{u} \cdot \frac{\partial}{\partial t} \boldsymbol{\phi} + \mathbf{f}(\mathbf{u}) \cdot \frac{\partial}{\partial x} \boldsymbol{\phi} \right) dx dt + \int_{-\infty}^{\infty} \mathbf{u}_0(x) \cdot \boldsymbol{\phi}(0, x) dx = 0, \quad (3.60)$$

for every test function $\boldsymbol{\phi} \in [C_0^\infty([0, t_{\max}) \times \mathbb{R})]^m$.

It is easy to verify that when \mathbf{u} satisfies (3.60) and is at least continuously differentiable, it is a classical solution, too. One can perform integration by parts and one gets

$$\iint_{t>0} \left(\frac{\partial}{\partial t} \mathbf{u} + \frac{\partial}{\partial x} \mathbf{f}(\mathbf{u}) \right) \boldsymbol{\phi} \, dx dt = 0,$$

which leads to

$$\frac{\partial}{\partial t} \mathbf{u} + \frac{\partial}{\partial x} \mathbf{f}(\mathbf{u}) = 0,$$

due to the arbitrariness of $\boldsymbol{\phi}$. One also has to check for the initial condition. Therefore one can multiply this last equation by $\boldsymbol{\phi}$ and integrate by parts

again

$$\iint_{t>0} \left(\mathbf{u} \cdot \frac{\partial}{\partial t} \boldsymbol{\phi} + \mathbf{f}(\mathbf{u}) \cdot \frac{\partial}{\partial x} \boldsymbol{\phi} \right) dx dt + \int_{t=0} \mathbf{u}(0, x) \cdot \boldsymbol{\phi}(0, x) dx = 0.$$

Comparing with (3.59) gives

$$\int_{t=0} (\mathbf{u}(0, x) - \mathbf{u}_0(x)) \boldsymbol{\phi}(0, x) dx = 0, \quad (3.61)$$

which gives $\mathbf{u}(0, x) = \mathbf{u}_0(x)$, again due to the arbitrariness of $\boldsymbol{\phi}$ and since \mathbf{u}_0 is assumed to be continuous. Therefore, Definition 3.2.7 is an actual generalization of the classical notion of solutions.

Assume now the situation where we have a region $\mathcal{D} \subset (0, t_{\max}) \times \mathbb{R}$ and let $x = x(t)$ be a smooth curve dividing \mathcal{D} into the two regions \mathcal{D}_- and \mathcal{D}_+ . Further, let \mathbf{u} be a smooth solution in \mathcal{D}_- and \mathcal{D}_+ , i.e. the equation (3.58) holds there respectively. Moreover suppose that \mathbf{u} has a jump discontinuity across $x = x(t)$ and both one-sided limits $\mathbf{u}_- = \mathbf{u}(t, x(t) - 0)$ and $\mathbf{u}_+ = \mathbf{u}(t, x(t) + 0)$ are well defined. With $\boldsymbol{\phi}$ being a test function with compact support in \mathcal{D} and not necessarily vanishing on $x = x(t)$ we get from equation (3.60)

$$\begin{aligned} 0 &= \iint_{\mathcal{D}} \left(\mathbf{u} \cdot \frac{\partial}{\partial t} \boldsymbol{\phi} + \mathbf{f}(\mathbf{u}) \cdot \frac{\partial}{\partial x} \boldsymbol{\phi} \right) dx dt \\ &= \iint_{\mathcal{D}_-} \left(\mathbf{u} \cdot \frac{\partial}{\partial t} \boldsymbol{\phi} + \mathbf{f}(\mathbf{u}) \cdot \frac{\partial}{\partial x} \boldsymbol{\phi} \right) dx dt + \iint_{\mathcal{D}_+} \left(\mathbf{u} \cdot \frac{\partial}{\partial t} \boldsymbol{\phi} + \mathbf{f}(\mathbf{u}) \cdot \frac{\partial}{\partial x} \boldsymbol{\phi} \right) dx dt. \end{aligned}$$

Integrating by parts and using the divergence theorem leads to

$$\begin{aligned} \iint_{\mathcal{D}_-} \left(\mathbf{u} \cdot \frac{\partial}{\partial t} \boldsymbol{\phi} + \mathbf{f}(\mathbf{u}) \cdot \frac{\partial}{\partial x} \boldsymbol{\phi} \right) dx dt &= - \iint_{\mathcal{D}_-} \left(\frac{\partial}{\partial t} \mathbf{u} + \frac{\partial}{\partial x} \mathbf{f}(\mathbf{u}) \right) \cdot \boldsymbol{\phi} dx dt \\ &\quad + \int_{\partial \mathcal{D}_-} \left(\mathbf{u} \nu^{(1)} + \mathbf{f}(\mathbf{u}) \nu^{(2)} \right) \cdot \boldsymbol{\phi} dl. \end{aligned}$$

Here $\boldsymbol{\nu} = (\nu^{(1)}, \nu^{(2)})$ is the outer unit normal of the boundary $\partial \mathcal{D}_-$. Since \mathbf{u} is a smooth solution in \mathcal{D}_- and $\boldsymbol{\phi} = 0$ on $\partial \mathcal{D}$ the integral is only non zero along the curve $x = x(t)$, giving

$$\int_{\partial \mathcal{D}_-} \left(\mathbf{u} \nu^{(1)} + \mathbf{f}(\mathbf{u}) \nu^{(2)} \right) \cdot \boldsymbol{\phi} dl = \int_{x=x(t)} \left(\mathbf{u}_- \nu^{(1)} + \mathbf{f}(\mathbf{u}_-) \nu^{(2)} \right) \cdot \boldsymbol{\phi} dl.$$

Analogously, for the region \mathcal{D}_+ we get

$$\int_{\partial\mathcal{D}_+} \left(\mathbf{u}v^{(1)} + \mathbf{f}(\mathbf{u})v^{(2)} \right) \cdot \boldsymbol{\phi} \, dl = - \int_{x=x(t)} \left(\mathbf{u}_+v^{(1)} + \mathbf{f}(\mathbf{u}_+)v^{(2)} \right) \cdot \boldsymbol{\phi} \, dl,$$

with $-\boldsymbol{\nu}$ being the outer unit normal of the boundary $\partial\mathcal{D}_+$. Hence, we get

$$0 = \int_{x=x(t)} \left[(\mathbf{u}_+ - \mathbf{u}_-)v^{(1)} + (\mathbf{F}(\mathbf{u}_+) - \mathbf{F}(\mathbf{u}_-))v^{(2)} \right] \cdot \boldsymbol{\phi} \, dl.$$

Since this equation holds for all smooth test functions $\boldsymbol{\phi}$ we get

$$0 = (\mathbf{u}_+ - \mathbf{u}_-)v^{(1)} + (\mathbf{F}(\mathbf{u}_+) - \mathbf{F}(\mathbf{u}_-))v^{(2)}.$$

But for a given parametrization $(t, x(t))$ of the discontinuity the specific unit normal to this curve is given by $\boldsymbol{\nu} = (-x'(t), 1) / \sqrt{1 + (x'(t))^2}$. Denoting the propagation speed of the discontinuity as $\sigma = x'(t)$ we finally obtain the Rankine-Hugoniot jump conditions

$$[[\mathbf{f}(\mathbf{u})]] = \sigma[[\mathbf{u}]], \quad (3.62)$$

where we have used the jump bracket $[[\mathbf{u}]] = \mathbf{u}_+ - \mathbf{u}_-$. We have thus shown that not every discontinuity is permissible. Indeed, equation (3.60) implies the Rankine-Hugoniot relations, which are restrictions on the possible curves of discontinuity. In analogy to the rarefaction wave curve, we now define the so called *shock curve*

Definition 3.2.8 (Shock wave curve). *For a given state \mathbf{u}_0 we define the shock set by*

$$\mathcal{S}(\mathbf{u}_0) = \{ \mathbf{u} \mid \sigma(\mathbf{u} - \mathbf{u}_0) = (\mathbf{F}(\mathbf{u}) - \mathbf{F}(\mathbf{u}_0)) \}.$$

The i -th shock wave curve is then given by

$$\mathcal{S}_i(\mathbf{u}_0) = \mathcal{S}_i^+(\mathbf{u}_0) \cup \{ \mathbf{u}_0 \} \cup \mathcal{S}_i^-(\mathbf{u}_0),$$

where $\mathcal{S}_i^+(\mathbf{u}_0)$ and $\mathcal{S}_i^-(\mathbf{u}_0)$ are defined as

$$\begin{aligned} \mathcal{S}_i^+(\mathbf{u}_0) &= \{ \mathbf{u} \in \mathcal{S}(\mathbf{u}) \mid \lambda_i(\mathbf{u}_0) < \sigma < \lambda_i(\mathbf{u}) \}, \\ \mathcal{S}_i^-(\mathbf{u}_0) &= \{ \mathbf{u} \in \mathcal{S}(\mathbf{u}) \mid \lambda_i(\mathbf{u}) < \sigma < \lambda_i(\mathbf{u}_0) \}. \end{aligned}$$

Nonetheless, like in the scalar case, the Rankine-Hugoniot relations are insufficient to single out a unique solution. The physical solution is determined by an additional entropy criterion coming from the second law of thermodynamics. We therefore give the following definition.

Definition 3.2.9 (Shock wave). *Let the i -th characteristic field $(\lambda_i(\mathbf{u}), \mathbf{r}_i(\mathbf{u}))$ of the system of conservation laws (3.25) be genuinely nonlinear and $\mathbf{u}_+ \in \mathcal{S}_i(\mathbf{u}_-)$.*

The discontinuous function

$$\mathbf{u}(t, x) = \begin{cases} \mathbf{u}_- & \text{if } x < \sigma t, \\ \mathbf{u}_+ & \text{if } x \geq \sigma t, \end{cases}$$

is called an *i*-shock wave when satisfying the following entropy inequalities

$$\begin{aligned} \lambda_i(\mathbf{u}_+) &< \sigma < \lambda_{i+1}(\mathbf{u}_+), \\ \lambda_{i-1}(\mathbf{u}_-) &< \sigma < \lambda_i(\mathbf{u}_-), \end{aligned} \tag{3.63}$$

which are also called *Lax entropy conditions*. This implies that $\mathbf{u}_+ \in \mathcal{S}_i^-(\mathbf{u}_-)$ has to hold for physical relevant solutions.

The inequalities (3.63) imply the following inequality often called *Lax entropy condition* as well

$$\lambda_i(\mathbf{u}_+) < \sigma < \lambda_i(\mathbf{u}_-). \tag{3.64}$$

This criterium is often used and sufficient for many cases to single out the unique physical solution. Also in the following chapter, relation (3.64) will be sufficient to find a unique solution for the system of conservation laws considered there. In general, the task of picking the unique physical solution is far from trivial. The theory of entropy criteria is very rich and complex, see for example Liu [56] who extended the notion of Lax entropy conditions or the Dafermos entropy rate admissibility criterion [14]. It states that not only should the physical entropy increase, but in fact, it should be increasing at the maximum rate allowed by the balance laws of mass, momentum and energy. Since these concepts are not necessary for the work presented, we will not give any details here.

We will now turn to the last case, namely the *i*-th characteristic field being linearly degenerate.

Definition 3.2.10. Let the *i*-th characteristic field $(\lambda_i(\mathbf{u}), \mathbf{r}_i(\mathbf{u}))$ of the system of conservation laws (3.25) be linearly degenerate and $\mathbf{u}_+ \in \mathcal{S}_i(\mathbf{u}_-)$. The discontinuous function

$$\mathbf{u}(t, x) = \begin{cases} \mathbf{u}_- & \text{if } x < \sigma t, \\ \mathbf{u}_+ & \text{if } x \geq \sigma t, \end{cases}$$

is called a *contact discontinuity* with

$$\sigma = \lambda_i(\mathbf{u}_+) = \lambda_i(\mathbf{u}_-).$$

The *rarefaction waves*, *shock waves* and *contact discontinuities* are the *elementary waves* of the system of conservation laws (3.25). These concepts can be directly applied to the quasi-linear system (3.27), too.

3.2.5 General existence and uniqueness results

The classical theorem of Kruzhkov [46] provides an estimate of the L^1 distance between any two bounded entropy-admissible solutions of the scalar conservation law in one space dimension. In particular, it guarantees the uniqueness of the entropy solution of the Cauchy problem within a class of L^∞ functions. In his work, he also established the convergence of the method of vanishing viscosity.

For the existence problem of a single scalar conservation law, there are at least five different methods: Hamilton-Jacobi theory, viscosity methods, nonlinear semigroup theory, the layering method and the method of characteristics. The latter we partly presented above. An excellent introduction to the first three methods can be found in Serre [73], the layering method can be found in Dafermos [16].

The uniqueness in the method of Kruzhkov is the consequence of a monotonic property of the flux function. But such a property does not longer exist if one considers systems instead of scalar equations. Therefore the question of uniqueness no longer has a general answer. One alternative method to approach the problem is given by the duality method of Holmgren. Even though it was shown that this method could not work for a broad class of systems, it has given several interesting results. An introduction to this method for a single conservation law can be found in the work of Oleinik [68].

Let us now consider systems of conservation laws. In the previous subsections we have shown how to determine the elementary waves for a single characteristic field $(\lambda_i(\mathbf{u}), \mathbf{r}_i(\mathbf{u}))$. Let us assume now that the system of conservation laws under consideration is strictly hyperbolic, that is the matrix $\mathbf{A}(\mathbf{u}) = \mathbf{Df}(\mathbf{u})$ of the quasi-linear system

$$\frac{\partial}{\partial t} \mathbf{u} + \mathbf{A}(\mathbf{u}) \frac{\partial}{\partial x} \mathbf{u} = 0. \quad (3.65)$$

has n *distinct* real eigenvalues and is diagonalizable, compare to Definition 3.2.1. One of the most important existence result can be found in the very fundamental paper of Lax [50]. For given states \mathbf{u}_- and \mathbf{u}_+ sufficiently close to each other the Riemann problem (3.39) has a weak solution of at most $m + 1$ constant states \mathbf{u}_k , $k = 0, \dots, m$ separated by elementary waves, that is rarefaction waves, shock waves or contact discontinuities.

However, the proof of the whole construction of a solution consisting out of constant states separated by waves and determined by the intersection of the adjacent wave curves breaks down in the case of a non strictly hyperbolic system.

This result was then extended to large total variation of the initial data by Nishida and Smoller [67]. In the case of arbitrary L^∞ data, the problem was solved in the case of the 2×2 p-system in one space dimension by Chen et al. [9]. Other essential works on the Riemann problem for conservation laws are due to Dafermos [14, 15], Liu [56, 57] and many others.

Studying the theory of systems of conservation laws, one of the most important results concerning the Cauchy problem in one space dimension is obtained using Glimm's scheme, see [29]. It is formulated as a convergence theorem of approximate solutions and assures the existence of a weak solution to the given Cauchy problem. The sequence of solutions converges in general but not necessarily to a weak solution when a particular sequence is chosen. The convergence to a weak solution is linked to a random property of the sequence of approximate solutions, hence the name *random choice method*. As in the case of Lax's theorem, the initial data of the Riemann problem need to be sufficiently close to each other since the proof uses the concept of invariant regions and in general, for systems of at least three equations, there does not exist an invariant compact domain for the Riemann problem, see Serre [74, Chapter 8]. The proof of Glimm's theorem is also based on Helly's theorem for the space of functions of bounded variation. This makes generalizations to higher space dimensions very problematic [69]. Nonetheless, the Glimm scheme is one of the only schemes at our disposal for which we have a convergence and therefore an existence theorem in one space dimension. Although the Glimm scheme is a general existence result, we cannot make use of it. To construct a global solution, it uses Lax's theorem for the local solution and therefore needs the system under consideration to be strictly hyperbolic. As we will show in the next chapter, the system under consideration in this work is only weakly hyperbolic.

For initial states sufficiently close to each other, there is one more global existence result of the Cauchy problem for systems of conservation laws based on the so called *front-tracking algorithm* by Bressan [6]. For an introduction to this method, the reader is referred to the textbook of Bressan, see [7]. However, again, to keep track of the wave-fronts, one of the crucial requirements for the system of conservation laws under consideration is that it is strictly hyperbolic. Therefore, it is not suited to treat the system under consideration in this work.

Since we can not use any of the existence and uniqueness results for the Cauchy problem, we will only use the methods presented before in this chapter. Due to the lack of a general theory, we will consider Riemann problems only and not more general initial data. We will analyze the elementary wave structure and use Riemann invariants and Rankine-Hugoniot jump conditions to get a nonlinear system of equations connecting the initial states to each other. We then have to find a solution to these nonlinear systems to provide a solution. To guarantee the uniqueness of a solution, we have to impose some restrictions on the initial data and parameters in the equations of state. This work is carried out in detail in the next chapter for different cases of initial data.

Analytical Results for the Two-Phase Flow Model

In this chapter, we present the main analytical results of this work. We try to find an analytic solution of the Riemann problem for the isothermal two-phase flow model (2.5). The techniques and basic concepts introduced in the last chapter will be used. As we already mentioned in Section 2.2 the first four equations describing the dispersed phase decouple from the last two equations, which describe the carrier phase mass and momentum. Therefore, our strategy is to solve the Riemann problem for the dispersed phase equations separately at first. We start with the analysis of the quasi-linearized equations to determine the wave structure and the characteristic fields. This chapter is based on the publications [34, 35] and extends the presentation of the results therein.

4.1 The dispersed phase equations

As mentioned before, the first four equations of (2.5) can be decoupled from the rest of the system since they do not depend on the carrier phase quantities. Therefore we study as a first step the solution to the Riemann problem for the following subsystem of (2.5)

$$\begin{aligned}
 \frac{\partial c}{\partial t} + \frac{\partial}{\partial x} (c v) &= 0, \\
 \frac{\partial c \rho}{\partial t} + \frac{\partial}{\partial x} (c \rho v) &= 0, \\
 \frac{\partial c \rho v}{\partial t} + \frac{\partial}{\partial x} (c \rho v^2) &= 0, \\
 \frac{\partial c R}{\partial t} + \frac{\partial}{\partial x} (c R v) &= 0,
 \end{aligned} \tag{4.1}$$

together with the piecewise constant initial data

$$(c, \rho, v, R) (t = 0, x) = \begin{cases} (c_-, \rho_-, v_-, R_-) & \text{for } x < 0, \\ (c_+, \rho_+, v_+, R_+) & \text{for } x > 0. \end{cases} \tag{4.2}$$

4.1.1 Linear analysis of the dispersed phase equations

We introduce the vector \mathbf{u} of primitive variables defined by $\mathbf{u} = (c, \rho, v, R)^\top$. For smooth solutions we use the product rule of differentiation on the system (4.1) to obtain the equivalent system

$$\frac{\partial c}{\partial t} + v \frac{\partial c}{\partial x} + c \frac{\partial v}{\partial x} = 0, \quad \frac{\partial \rho}{\partial t} + v \frac{\partial \rho}{\partial x} = 0, \quad \frac{\partial v}{\partial t} + v \frac{\partial v}{\partial x} = 0, \quad \frac{\partial R}{\partial t} + v \frac{\partial R}{\partial x} = 0. \quad (4.3)$$

This gives us the quasi-linear form of our system as

$$\frac{\partial \mathbf{u}}{\partial t} + \mathbf{A}(\mathbf{u}) \frac{\partial \mathbf{u}}{\partial x} = 0, \quad \mathbf{A}(\mathbf{u}) = \begin{pmatrix} v & 0 & c & 0 \\ 0 & v & 0 & 0 \\ 0 & 0 & v & 0 \\ 0 & 0 & 0 & v \end{pmatrix}. \quad (4.4)$$

At this point, we want to remind the reader of Definition 3.2.2, which states that a first-order system of partial differential equations is said to be *weakly hyperbolic* if the matrix \mathbf{A} of the quasi-linear form has all eigenvalues in the real numbers but does not possess a complete set of eigenvectors.

The matrix \mathbf{A} in (4.4) has the repeated eigenvalue $\lambda = v$ of multiplicity four and only three linearly independent right eigenvectors $\mathbf{r}_1, \mathbf{r}_2, \mathbf{r}_4$ as well as the generalized eigenvector \mathbf{r}_3 where

$$\mathbf{r}_1 = \begin{pmatrix} 1 \\ 0 \\ 0 \\ 0 \end{pmatrix}, \quad \mathbf{r}_2 = \begin{pmatrix} 0 \\ 1 \\ 0 \\ 0 \end{pmatrix}, \quad \mathbf{r}_4 = \begin{pmatrix} 0 \\ 0 \\ 0 \\ 1 \end{pmatrix}, \quad \text{and} \quad \mathbf{r}_3 = \begin{pmatrix} 0 \\ 0 \\ 1 \\ 0 \end{pmatrix}.$$

The weak hyperbolicity corresponds to the fact that the first and third equations cannot be decoupled by a linear transformation of the primitive state variables.

The last three equations form a proper hyperbolic system. The third one is the Burgers equation and can be solved in conservative form completely independently of the other equations. For the then given v , the second and fourth equations are linear advection equations with a variable, possibly discontinuous coefficient. In the case of a discontinuous velocity, we see that the first equation would involve a derivative of this velocity. This leads, as we will see, to solutions with singular measures.

Note that the conservative system (4.1) is fully coupled and both systems, the reduced one above and the full model, are weakly hyperbolic. The conservative form (4.1) is relevant for the mathematical treatment of discontinuous solutions.

It is also clear that the characteristic fields are linearly degenerate since the gradient of the eigenvalue $\lambda = v$ with respect to the primitive variables is $\nabla \lambda = \mathbf{r}_3$. This gives

$$\nabla \lambda \cdot \mathbf{r}_1 = \nabla \lambda \cdot \mathbf{r}_2 = \nabla \lambda \cdot \mathbf{r}_4 = 0.$$

It is well known that discontinuities in solutions for conservation laws like (4.1) may develop, even for continuous initial data, as in example (4.13) below. Now suppose that there exists a discontinuity in the solution of (4.1) moving with speed σ . Let us denote the jump in a quantity q between the left state q_- and the right state q_+ across a given discontinuity by $\llbracket q \rrbracket = q_+ - q_-$. Then the Rankine-Hugoniot relations must hold. They are given as

$$\begin{aligned} \sigma \llbracket c \rrbracket - \llbracket c v \rrbracket &= 0, & \sigma \llbracket c \rho \rrbracket - \llbracket c \rho v \rrbracket &= 0, \\ \sigma \llbracket c \rho v \rrbracket - \llbracket c \rho v^2 \rrbracket &= 0. & \sigma \llbracket c R \rrbracket - \llbracket c R v \rrbracket &= 0. \end{aligned} \quad (4.5)$$

Solving these equations, see the Appendix, gives

$$\llbracket v \rrbracket = 0. \quad (4.6)$$

This means that the velocity is continuous across any discontinuity, which fulfills the above jump conditions. Using (4.6) in any equation in (4.5) implies that the speed σ of the discontinuity is given as

$$\sigma = v. \quad (4.7)$$

Therefore any discontinuity will propagate with the local velocity. Such discontinuities are contact discontinuities, as expected from the linear degeneracy above.

Despite the fact that we have (4.6) along a discontinuity, we may consider a jump in v as initial data. We now construct solutions to (4.1) under different conditions on the dispersed phase velocity. We consider three cases namely: $v_- = v_+$, $v_- < v_+$, and $v_- > v_+$.

4.1.2 The case $v_- = v_+ = v$

We observe from (4.3) that in this case the velocity v remains constant while the equations for c and ρ become linear advection equations with constant speed v . Therefore the solution for the Riemann problem (4.2) is given by the contact discontinuity

$$(c, \rho, v, R) = \begin{cases} (c_-, \rho_-, v, R_-) & -\infty < x < vt, \\ (c_+, \rho_+, v, R_+) & vt \leq x < +\infty. \end{cases} \quad (4.8)$$

4.1.3 The case $v_- < v_+$

Putting $\hat{\rho} = c\rho$ the second and third equation of (4.1) are equivalent to the zero pressure gas dynamics model

$$\frac{\partial \hat{\rho}}{\partial t} + \frac{\partial}{\partial x} (\hat{\rho}v) = 0, \quad \frac{\partial}{\partial t} (\hat{\rho}v) + \frac{\partial}{\partial x} (\hat{\rho}v^2) = 0, \quad (4.9)$$

These models, therefore, have a similar structure of solutions under the same conditions for the velocity. Note that vacuum states in the pressureless gas model correspond to vaporless states in our model. In this situation there is no overlap of characteristics and no characteristic passes through the vaporless region $\Omega = \{(x, t) : v_- \leq x/t \leq v_+\}$ in the (x, t) plane, see Figure 4.1(a). Following the results by Sheng and Zhang [76, p. 11] on the zero pressure

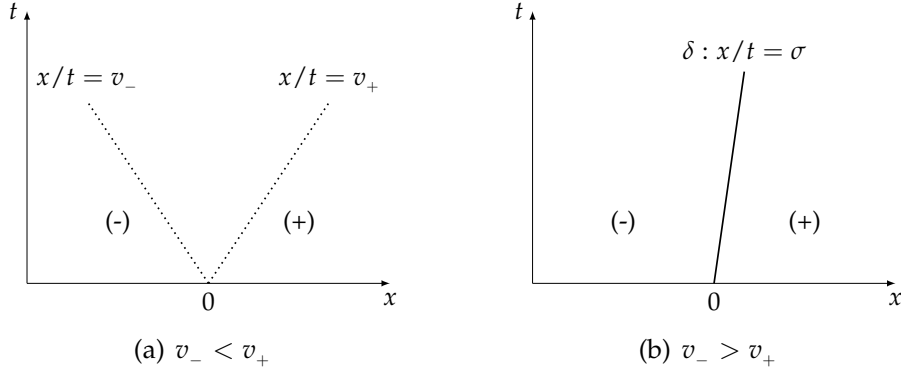


FIGURE 4.1: Wave configurations for system (4.1), cases $v_- \neq v_+$

gas dynamics model, we can construct a solution that consists of two contact discontinuities and a vaporless state, with $c = 0$, between two constant states. We introduce the radial variable $\xi = x/t$ and denote the derivatives with respect to this variable by primes, e.g. c' . Then (4.1) becomes

$$\begin{aligned}
 -\xi c' + (c v)' &= 0, \\
 -\xi (c \rho)' + (c \rho v)' &= 0, \\
 -\xi (c \rho v)' + (c \rho v^2)' &= 0, \\
 -\xi (c R)' + (c R v)' &= 0.
 \end{aligned} \tag{4.10}$$

The initial conditions (4.2) become the asymptotic boundary data

$$\lim_{\xi \rightarrow -\infty} (c, \rho, v, R)(\xi) = (c_-, \rho_-, v_-, R_-), \quad \lim_{\xi \rightarrow \infty} (c, \rho, v, R)(\xi) = (c_+, \rho_+, v_+, R_+).$$

The system corresponds to a two point boundary value problem of first-order ordinary differential equations with boundary data at infinity. For smooth solutions, the system (4.10) is reduced to

$$\begin{pmatrix} v - \xi & 0 & c & 0 \\ 0 & c(v - \xi) & 0 & 0 \\ 0 & 0 & c \rho (v - \xi) & 0 \\ 0 & 0 & 0 & c(v - \xi) \end{pmatrix} \begin{pmatrix} c' \\ \rho' \\ v' \\ R' \end{pmatrix} = 0. \tag{4.11}$$

The third equation is $c\rho(v - \xi)v' = 0$. It is satisfied if either $c\rho = 0$, $v = \xi$ or v is constant. The last case can easily be ruled out. A constant intermediate velocity must be connected to the differing initial data by at least one jump discontinuity. Due to (4.6), the velocity cannot be discontinuous. The system only has contact discontinuities.

We may have the second case $v(\xi) = \xi$ to give the continuous solution linking v_- to v_+ . This corresponds to the usual rarefaction solution to the Burgers equation. With this choice, the second and fourth equations of system (4.11) are automatically satisfied. The variables ρ and R can have arbitrary values and jumps for $\xi \in [v_-, v_+]$, since these would satisfy the Rankine Hugoniot conditions (4.5) with (4.7). In the first equation we are left with the term $0 = cv' = c$ since $v'(\xi) = 1$. This means we have a vaporless intermediate state.

Finally, let us consider the third case $c\rho = 0$. Assuming the intermediate state $\rho = 0$, the second and third equations are satisfied.

Now if we have a vaporless intermediate state $c = 0$ on the interval $[v_-, v_+]$ all four equations (4.11) are satisfied automatically. We choose the function v to be any continuous function satisfying $v(v_-) = v_-$ and $v(v_+) = v_+$. The choice $v(\xi) = \xi$ is the simplest choice. The functions ρ and R are arbitrary. This gives the solution

$$(c, \rho, v, R) = \begin{cases} (c_-, \rho_-, v_-, R_-) & -\infty < \xi \leq v_-, \\ (0, \rho(\xi), v(\xi), R(\xi)) & v_- < \xi < v_+, \\ (c_+, \rho_+, v_+, R_+) & v_+ \leq \xi < +\infty, \end{cases} \quad (4.12)$$

with ρ and R arbitrary functions, v a continuous function satisfying

$$\rho(v_{\pm}) = \rho_{\pm}, \quad v(v_{\pm}) = v_{\pm}, \quad R(v_{\pm}) = R_{\pm}.$$

4.1.4 The case $v_- > v_+$

Looking at the second and third equation of (4.1), which are equivalent to the zero pressure gas dynamics model, we will now illustrate the existence of blow up solutions, even for continuous initial data. Again we put $\hat{\rho} = c\rho$ and start with the initial data for Equations (4.9)

$$\hat{\rho}(0, x) = 1 \quad \text{for all } x \in (-\infty, \infty), \quad \text{and} \quad v(0, x) = \begin{cases} 1 & x \leq 0, \\ 1 - x & 0 < x \leq 1, \\ 0 & \text{otherwise.} \end{cases} \quad (4.13)$$

For smooth solutions, Equations (4.9) can be written as

$$\frac{\partial \hat{\rho}}{\partial t} + v \frac{\partial \hat{\rho}}{\partial x} + \hat{\rho} \frac{\partial v}{\partial x} = 0, \quad \frac{\partial v}{\partial t} + v \frac{\partial v}{\partial x} = 0. \quad (4.14)$$

This system decouples. We first solve the second equation, which is the Burgers equation, for v . Then we use v and v_x to determine the solutions of the first equation. For the given initial data and $t < 1$, we can solve this system by using the method of characteristics where the characteristic equations are given by

$$\frac{dt}{ds} = 1, \quad \frac{dx}{ds} = v, \quad \frac{d\hat{\rho}}{ds} = -\hat{\rho} \frac{\partial v}{\partial x}, \quad \frac{dv}{ds} = 0. \quad (4.15)$$

We differentiate the second equation in (4.14) with respect to x to get

$$\frac{d}{ds} \left(\frac{\partial v}{\partial x} \right) = - \left(\frac{\partial v}{\partial x} \right)^2.$$

For the initial data (4.13) this equation gives for $s \in [0, 1)$

$$\frac{\partial v}{\partial x}(s, x) = \begin{cases} 1/(s-1) & 0 < x \leq 1, \\ 0 & \text{otherwise.} \end{cases} \quad (4.16)$$

We now substitute this result into the equation involving $\hat{\rho}$ in (4.15) and solve the result to obtain for $s \in [0, 1)$

$$\hat{\rho}(s, x) = \begin{cases} 1/(1-s) & 0 < x \leq 1, \\ 1 & \text{otherwise.} \end{cases} \quad (4.17)$$

It is clear from (4.16) and (4.17) that both the density and velocity gradient blow up simultaneously as $s \rightarrow 1$ along the characteristics. Therefore a smooth solution, in this case, is only defined for $s < 1$. For the Burgers equation, we obtain a shock with speed $1/2$. The blow up of v_x leads to the occurrence of a delta-shock wave. This wave is the distributional derivative of the jump discontinuity at the shock. As a consequence, we will immediately have a singularity in the solution to the system (4.1).

Taking the first equation of (4.1) into account, a blow up in $\hat{\rho}$ means a blow up in the concentration c for given initial data with $v_- > v_+$. There is no classical weak solution to the system since this would have to be a contact discontinuity. This means that no solution exists in the space of functions of bounded variation. Instead, solutions exist in the space of distributions that are Borel measures.

Generalized Rankine-Hugoniot relations for delta-shocks

Due to the occurrence of the blow up of c , it is natural to seek solutions in the space of Borel measures. Denote by $BM(\mathbb{R})$ the space of bounded Borel measures on \mathbb{R} . The definition of a measure solution of (4.1) can be given as follows.

Definition 4.1.1 (Yang [90, p. 454]). *A quadruple (c, ρ, v, R) is called a measure solution of (4.1) if it satisfies*

$$(i) \ c \in L^\infty([0, \infty), BM(\mathbb{R})) \cap C([0, \infty), H^{-s}(\mathbb{R})), \quad s > 0,$$

- (ii) $\rho \in L^\infty([0, \infty), L^\infty(\mathbb{R})) \cap C([0, \infty), H^{-s}(\mathbb{R}))$,
- (iii) $v \in L^\infty([0, \infty), L^\infty(\mathbb{R})) \cap C([0, \infty), H^{-s}(\mathbb{R}))$,
- (iv) $R \in L^\infty([0, \infty), L^\infty(\mathbb{R})) \cap C([0, \infty), H^{-s}(\mathbb{R}))$,
- (v) ρ, v and R are measurable with respect to c at almost all $t \geq 0$.

In addition, the conditions

$$\begin{aligned}
\int_0^\infty \int_{\mathbb{R}} (\phi_t + v \phi_x) dc dt + \int_{\mathbb{R}} c(0, x) \phi(0, x) dx &= 0, \\
\int_0^\infty \int_{\mathbb{R}} \rho (\phi_t + v \phi_x) dc dt + \int_{\mathbb{R}} c(0, x) \rho(0, x) \phi(0, x) dx &= 0, \\
\int_0^\infty \int_{\mathbb{R}} \rho v (\phi_t + v \phi_x) dc dt + \int_{\mathbb{R}} c(0, x) \rho(0, x) v(0, x) \phi(0, x) dx &= 0, \\
\int_0^\infty \int_{\mathbb{R}} R (\phi_t + v \phi_x) dc dt + \int_{\mathbb{R}} c(0, x) R(0, x) \phi(0, x) dx &= 0,
\end{aligned} \tag{4.18}$$

hold in the sense of measures for all $\phi \in C_0^\infty([0, \infty) \times \mathbb{R})$.

Definition 4.1.2. A two dimensional weighted delta functional $w(t)\delta_L$, $w \in C^1([a, b])$, supported on a smooth curve L parametrized by $t = s$, $x = x(s)$ for $a \leq s \leq b$ is defined by

$$\langle w(t)\delta_L, \varphi \rangle = \int_a^b w(s) \varphi(t(s), x(s)) ds$$

for all $\varphi \in C_0^\infty(\mathbb{R}^2)$.

Now we propose to find a solution of (4.1), with a discontinuity at $x = x(t)$, of the form

$$(c, \rho, v, R)(t, x) = \begin{cases} (c_-, \rho_-, v_-, R_-) & x < x(t), \\ (w(t)\delta_{x(t)}, \rho_\delta(t), v_\delta(t), R_\delta(t)) & x = x(t), \\ (c_+, \rho_+, v_+, R_+) & x > x(t), \end{cases} \tag{4.19}$$

where $x(t) \in C^1$ and δ_x is the standard Dirac measure with all mass at $x \in \mathbb{R}$. Note that we use the notations ρ_δ, v_δ and R_δ for the exceptional values taken by these physical states along the path of the singular measure.

Theorem 4.1.1. *The solution (c, ρ, v, R) defined in (4.19) satisfies (4.1) in the sense of measures if the following relations hold:*

$$\begin{aligned}
\frac{dx}{dt} &= v_\delta, \\
\frac{dw}{dt} &= v_\delta \llbracket c \rrbracket - \llbracket c v \rrbracket, \\
\frac{d(w\rho_\delta)}{dt} &= v_\delta \llbracket c \rho \rrbracket - \llbracket c \rho v \rrbracket, \\
\frac{d(w\rho_\delta v_\delta)}{dt} &= v_\delta \llbracket c \rho v \rrbracket - \llbracket c \rho v^2 \rrbracket, \\
\frac{d(wR_\delta)}{dt} &= v_\delta \llbracket c R \rrbracket - \llbracket c R v \rrbracket.
\end{aligned} \tag{4.20}$$

Proof. The first equation in system (4.20) follows directly from the characteristic equations and (4.7) as well as the value for v at the discontinuity given in (4.19), to be determined later. We will assume that $\phi \in C_0^\infty([0, \infty) \times \mathbb{R})$ and also use d/dt the convective derivative given by $d/dt = \partial/\partial t + v_\delta \partial/\partial x$ along $x(t)$. A function $\phi(t, x)$ has compact support if it vanishes outside some bounded set. To prove the second equation in (4.20) we split the integration of the first equation in (4.18) into the two regions separated by the discontinuity at $x = x(t)$ to get

$$\begin{aligned}
0 &= \int_0^\infty \int_{-\infty}^{x(t)} (\phi_t + v_- \phi_x) c_- dx dt + \int_0^\infty \int_{x(t)}^\infty (\phi_t + v_+ \phi_x) c_+ dx dt + \int_0^\infty w(t) (\phi_t + v_\delta \phi_x) dt \\
&\quad + \int_{-\infty}^{x(0)} c_- \phi(0, x) dx + \int_{x(0)}^\infty c_+ \phi(0, x) dx.
\end{aligned}$$

Integration by parts leads to

$$\begin{aligned}
&= \int_0^\infty \int_{-\infty}^{x(t)} ((c_- \phi)_t + (c_- v_- \phi)_x) dx dt + \int_0^\infty \int_{x(t)}^\infty ((c_+ \phi)_t + (c_+ v_+ \phi)_x) dx dt \\
&\quad - \int_0^\infty \int_{-\infty}^{x(t)} ((c_-)_t + (c_- v_-)_x) \phi dx dt - \int_0^\infty \int_{x(t)}^\infty ((c_+)_t + (c_+ v_+)_x) \phi dx dt \\
&\quad + \int_0^\infty w(t) \frac{d\phi}{dt} dt + \int_{-\infty}^{x(0)} c_- \phi(0, x) dx + \int_{x(0)}^\infty c_+ \phi(0, x) dx,
\end{aligned}$$

the third and fourth integral vanish and with use of Green's Theorem for the first two terms we get

$$\begin{aligned}
&= \oint_{x(t)} (-c_- \phi) dx + (c_- v_- \phi) dt - \oint_{x(t)} (-c_+ \phi) dx + (c_+ v_+ \phi) dt \\
&\quad + \int_{-\infty}^{x(0)} (-c_- \phi) dx + (c_- v_- \phi) dt + \int_{x(0)}^\infty (-c_+ \phi) dx + (c_+ v_+ \phi) dt \\
&\quad - \int_0^\infty \frac{dw(t)}{dt} \phi(t, x(t)) dt + \int_{-\infty}^{x(0)} c_- \phi(0, x) dx + \int_{x(0)}^\infty c_+ \phi(0, x) dx.
\end{aligned}$$

Again two terms vanish and furthermore the boundary terms cancel, which leads to

$$\begin{aligned}
&= \oint_{x(t)} (-c_- \phi) dx + (c_- v_- \phi) dt - \oint_{x(t)} (-c_+ \phi) dx + (c_+ v_+ \phi) dt - \int_0^\infty \frac{dw(t)}{dt} \phi(t, x(t)) dt \\
&= \int_0^\infty -(c_- \phi)(t, x(t)) x'(t) dt + \int_0^\infty (c_- v_- \phi)(t, x(t)) dt - \int_0^\infty -(c_+ \phi)(t, x(t)) x'(t) dt \\
&\quad - \int_0^\infty (c_+ v_+ \phi)(t, x(t)) dt - \int_0^\infty \frac{dw(t)}{dt} \phi(t, x(t)) dt \\
&= \int_0^\infty \left(v_\delta \llbracket c \rrbracket - \llbracket c v \rrbracket - \frac{dw(t)}{dt} \right) \phi(t, x(t)) dt.
\end{aligned}$$

Since ϕ is arbitrary, the second equation in (4.20) must hold. The third, fourth and fifth equations in (4.20) can be proved analogously. The conditions (4.20) are referred to as the generalized Rankine-Hugoniot relations. They describe the relationships among the location, propagation speed, weight and assignments of ρ , v as well as R on the discontinuity. \square

In order to obtain a physical relevant solution, the discontinuity must satisfy the Lax entropy condition $\lambda(v_+) < \sigma < \lambda(v_-)$ or equivalently

$$v_+ < v_\delta < v_-. \quad (4.21)$$

The Riemann problem is now reduced to solving (4.20) with the initial data

$$x(0) = 0, \quad w(0) = 0,$$

under the entropy condition (4.21). Like Yang [90] we assume a delta-shock of the form

$$x(t) = \sigma t = v_\delta t, \quad w(t) = c_\delta t, \quad v_\delta(t) = v_\delta, \quad \text{and} \quad \rho_\delta(t) = \rho_\delta.$$

Substituting these forms into (4.20) gives the system

$$\begin{aligned}
c_\delta &= v_\delta \llbracket c \rrbracket - \llbracket c v \rrbracket, \\
c_\delta \rho_\delta &= v_\delta \llbracket c \rho \rrbracket - \llbracket c \rho v \rrbracket, \\
c_\delta \rho_\delta v_\delta &= v_\delta \llbracket c \rho v \rrbracket - \llbracket c \rho v^2 \rrbracket, \\
c_\delta R_\delta &= v_\delta \llbracket c R \rrbracket - \llbracket c R v \rrbracket.
\end{aligned} \quad (4.22)$$

Multiplying the second equation with v_δ and subtracting the result from the third equation leads to a quadratic equation in v_δ written as

$$-\llbracket c \rho \rrbracket v_\delta^2 + 2 \llbracket c \rho v \rrbracket v_\delta - \llbracket c \rho v^2 \rrbracket = 0.$$

This equation possesses the solutions

$$v_\delta = \frac{v_- \sqrt{c_- \rho_-} \pm v_+ \sqrt{c_+ \rho_+}}{\sqrt{c_- \rho_-} \pm \sqrt{c_+ \rho_+}}.$$

We can easily show by use of (4.21) that the entropy solution to our Riemann problem must satisfy

$$v_\delta = \frac{v_- \sqrt{c_- \rho_-} + v_+ \sqrt{c_+ \rho_+}}{\sqrt{c_- \rho_-} + \sqrt{c_+ \rho_+}}. \quad (4.23)$$

Now substituting this solution into (4.22) we obtain

$$c_\delta = \left(\frac{c_+ \sqrt{c_- \rho_-} + c_- \sqrt{c_+ \rho_+}}{\sqrt{c_- \rho_-} + \sqrt{c_+ \rho_+}} \right) (v_- - v_+), \quad (4.24)$$

and

$$R_\delta = \frac{c_+ R_+ \sqrt{c_- \rho_-} + c_- R_- \sqrt{c_+ \rho_+}}{c_+ \sqrt{c_- \rho_-} + c_- \sqrt{c_+ \rho_+}}, \quad \rho_\delta = \frac{c_+ \rho_+ \sqrt{c_- \rho_-} + c_- \rho_- \sqrt{c_+ \rho_+}}{c_+ \sqrt{c_- \rho_-} + c_- \sqrt{c_+ \rho_+}}. \quad (4.25)$$

In summary, we have the following existence result.

Theorem 4.1.2 (Existence). *Let $v_- > v_+$. The Riemann problem (4.1) and (4.2) admits an entropy measure solution of the form*

$$(c, \rho, v, R)(t, x) = \begin{cases} (c_-, \rho_-, v_-, R_-) & x < v_\delta t, \\ (c_\delta t \delta_{x(t)}, \rho_\delta, v_\delta, R_\delta) & x = v_\delta t, \\ (c_+, \rho_+, v_+, R_+) & x > v_\delta t, \end{cases}$$

where $v_\delta, c_\delta, R_\delta$ and $\rho_{B\delta}$ are given in (4.23) - (4.25).

Note that the solution $c_\delta t \delta_{x(t)}$ has the physical dimension of a dimensionless volume fraction. By (4.24) c_δ has the dimension of a velocity but we are multiplying by t and $\delta_{x(t)}$ has the dimension of x^{-1} , because this is the dimension of approximate delta functions giving the measure δ in the limit.

4.2 The carrier phase quantities

We are now ready to determine the carrier phase density and velocity by solving the last two equations of (2.5). They are coupled to the dispersed phase variables through the volume fraction c . We consider the subsystem obtained from the second and last two equations of (2.5). This system has a similar structure to the continuity and momentum Euler equations modeling flow in ducts of variable cross-section area. These were studied by Liu [58, 59], Andrianov and Warnecke [1], as well as Han et al. [33]. A complete solution to the Riemann problem for these specific flows was given in the latter, including the resonant cases.

We include the mass and momentum balance equations for the dispersed phase since they are necessary to determine the velocity v completely. The

subsystem can be written as

$$\frac{\partial}{\partial t} \begin{pmatrix} c \\ c\rho \\ c\rho v \\ (1-c)\rho_c \\ (1-c)\rho_c v_c \end{pmatrix} + \frac{\partial}{\partial x} \begin{pmatrix} c\rho \\ c\rho v \\ c\rho v^2 \\ (1-c)\rho_c v_c \\ (1-c)(\rho_c v_c^2 + p_c) \end{pmatrix} = 0. \quad (4.26)$$

4.2.1 Linear analysis of the full system

To understand the mathematical characteristics of this model, we calculate the characteristic speeds and characteristic fields of the PDE system. Again we introduce a vector \mathbf{u} of primitive variables, this time defined as $\mathbf{u} = (c, \rho, v, \rho_c, v_c)^\top$. The system (4.26) can then be written in the quasi-linear form as

$$\frac{\partial \mathbf{u}}{\partial t} + \mathbf{B}(\mathbf{u}) \frac{\partial \mathbf{u}}{\partial x} = 0,$$

which reads in detail

$$\frac{\partial}{\partial t} \begin{pmatrix} c \\ \rho \\ v \\ \rho_c \\ v_c \end{pmatrix} + \begin{pmatrix} v & 0 & c & 0 & 0 \\ 0 & v & 0 & 0 & 0 \\ 0 & 0 & v & 0 & 0 \\ \frac{\rho_c(v-v_c)}{1-c} & 0 & \frac{\rho_c c}{1-c} & v_c & \rho_c \\ -\frac{p_c}{\rho_c(1-c)} & 0 & 0 & \frac{a_c^2}{\rho_c} & v_c \end{pmatrix} \cdot \frac{\partial}{\partial x} \begin{pmatrix} c \\ \rho \\ v \\ \rho_c \\ v_c \end{pmatrix} = 0.$$

The eigenvalues of the matrix \mathbf{B} are

$$\lambda_1 = v_c - a_c, \quad \lambda_2 = \lambda_3 = \lambda_4 = v, \quad \lambda_5 = v_c + a_c.$$

There are only four corresponding right eigenvectors

$$\mathbf{r}_1 = \begin{pmatrix} 0 \\ 0 \\ 0 \\ \rho_c \\ -a_c \end{pmatrix}, \quad \mathbf{r}_2 = \begin{pmatrix} 0 \\ 1 \\ 0 \\ 0 \\ 0 \end{pmatrix}, \quad \mathbf{r}_3 = \begin{pmatrix} (1-c)(a_c^2 - (v_c - v)^2) \\ 0 \\ 0 \\ p_c - \rho_c(v_c - v)^2 \\ (v_c - v)(a_c^2 - p_c/\rho_c) \end{pmatrix}, \quad \mathbf{r}_5 = \begin{pmatrix} 0 \\ 0 \\ 0 \\ \rho_c \\ a_c \end{pmatrix}.$$

Additionally, we have the relations

$$\nabla \lambda_1 \cdot \mathbf{r}_1 \neq 0, \quad \nabla \lambda_2 \cdot \mathbf{r}_2 = \nabla \lambda_3 \cdot \mathbf{r}_3 = 0 \quad \text{and} \quad \nabla \lambda_5 \cdot \mathbf{r}_5 \neq 0.$$

From these relations, we conclude that the λ_1 and λ_5 characteristic fields are genuinely nonlinear. On the other hand, the λ_2 and λ_3 characteristic fields are linearly degenerate. Therefore solutions may contain rarefaction waves or shock waves that result from the genuinely nonlinear characteristic fields

and contact discontinuities that arise from the linearly degenerate characteristic field. The structure of the system also admits constant solutions. Note further that the system additionally allows for delta-shock and vacuum-type solutions with phase extinction as shown in Chapter 4.3.

4.2.2 Rarefaction waves

Across a left rarefaction wave, the generalized Riemann invariants are obtained by solving

$$-\frac{a_c}{\rho_c} d\rho_c = dv_c, \quad c = \text{const.}, \quad \rho = \text{const.}, \quad v = \text{const.}$$

Integrating the first equation gives

$$v_c + a_c \ln \rho_c = \text{const.}$$

In this case, we have the relations

$$c_-^* = c_-, \quad \rho_-^* = \rho_-, \quad v_-^* = v_-, \quad \text{and} \quad v_{c_-}^* = v_{c_-} - a_c \ln \left(\frac{\rho_{c_-}^*}{\rho_{c_-}} \right). \quad (4.27)$$

For a left rarefaction wave, the head speed is given by $v_{c_-} - a_c$ whereas the tail speed is given by $v_{c_-}^* - a_c$. The slope inside the rarefaction fan is such that

$$\frac{dx}{dt} = \frac{x}{t} = v_c - a_c. \quad (4.28)$$

Using (4.27), the solution \mathbf{u} inside the fan is given by

$$\mathbf{u}_{\text{-fan}} = \begin{cases} v_c = a_c + \frac{x}{t}, \\ \rho_c = \rho_{c_-} \exp \left(\frac{v_{c_-} - v_c}{a_c} \right). \end{cases} \quad (4.29)$$

On the other hand, across a right rarefaction wave, the Riemann invariants are obtained from

$$\frac{a_c}{\rho_c} d\rho_c = dv_c, \quad c = \text{const.}, \quad \rho = \text{const.}, \quad v = \text{const.},$$

giving

$$c = \text{const.}, \quad \rho = \text{const.}, \quad v = \text{const.}, \quad \text{and} \quad v_c - a_c \ln \rho_c = \text{const.}$$

These imply that

$$c_+^* = c_+, \quad \rho_+^* = \rho_+, \quad v_+^* = v_+, \quad \text{and} \quad v_{c_+}^* = v_{c_+} + a_c \ln \left(\frac{\rho_{c_+}^*}{\rho_{c_+}} \right). \quad (4.30)$$

Here we have the head speed $v_{c+} + a_c$ and tail speed $v_{c+}^* + a_c$. The solution inside the fan is given by

$$\mathbf{u}_{+\text{fan}} = \begin{cases} v_c = -a_c + \frac{x}{t}, \\ \rho_c = \rho_{c+} \exp\left(\frac{v_c - v_{c+}}{a_c}\right). \end{cases} \quad (4.31)$$

4.2.3 Shock waves

We use Rankine-Hugoniot jump conditions to derive relations across shock waves. Suppose the left shock moves with a speed σ_- . Like e.g. Toro [83] we consider a frame of reference where the shock speed is zero. We therefore consider the new transformed states

$$\hat{v}_{c-} = v_{c-} - \sigma_- \quad \text{and} \quad \hat{v}_{c-}^* = v_{c-}^* - \sigma_-. \quad (4.32)$$

The Rankine-Hugoniot jump conditions in the new reference frame are then written as

$$\rho_{c-} \hat{v}_{c-} = \rho_{c-}^* \hat{v}_{c-}^*, \quad \rho_{c-} \hat{v}_{c-}^2 + a_c^2 \rho_{c-} = \rho_{c-}^* \hat{v}_{c-}^{*2} + a_c^2 \rho_{c-}^*. \quad (4.33)$$

We introduce the mass flux Q_- . The first equation in (4.33) gives

$$Q_- = \rho_{c-} \hat{v}_{c-} = \rho_{c-}^* \hat{v}_{c-}^*, \quad Q_- > 0, \quad (4.34)$$

while the second equation leads to

$$Q_- = -a_c^2 \frac{\rho_{c-}^* - \rho_{c-}}{\hat{v}_{c-}^* - \hat{v}_{c-}} = -a_c^2 \frac{\rho_{c-}^* - \rho_{c-}}{v_{c-}^* - v_{c-}}. \quad (4.35)$$

Equivalently, this equation can be written as

$$v_{c-}^* = v_{c-} - a_c^2 \frac{\rho_{c-}^* - \rho_{c-}}{Q_-}. \quad (4.36)$$

We use (4.34) to rewrite the velocities in terms of the mass flux as well as densities. Then we substitute the results into (4.35) to get

$$Q_- = \sqrt{a_c^2 \rho_{c-}^* \rho_{c-}}. \quad (4.37)$$

We now substitute this result into (4.36) to obtain

$$v_{c-}^* = v_{c-} - a_c \frac{\rho_{c-}^* - \rho_{c-}}{\sqrt{\rho_{c-}^* \rho_{c-}}}. \quad (4.38)$$

Finally, from (4.32), (4.34), and (4.37) we determine the speed of the left shock wave as

$$\sigma_- = v_{c_-} - a_c \sqrt{\frac{\rho_{c_-}^*}{\rho_{c_-}}}.$$

Similarly, the mass flux Q_+ for a right shock wave is given by

$$Q_+ = -\rho_{c_+} \hat{v}_{c_+} = -\rho_{c_+}^* \hat{v}_{c_+}^*, \quad Q_+ > 0.$$

Suppose σ_+ is the speed of the right shock wave. Analogous calculations give

$$v_{c_+}^* = v_{c_+} + a_c \frac{\rho_{c_+}^* - \rho_{c_+}}{\sqrt{\rho_{c_+}^* \rho_{c_+}}} \quad \text{and} \quad \sigma_+ = v_{c_+} + a_c \sqrt{\frac{\rho_{c_+}^*}{\rho_{c_+}}}. \quad (4.39)$$

4.3 The carrier phase solution

In the next subsections we will determine values for ρ_c and v_c under the two conditions $v_- = v_+$ and $v_- < v_+$ that were already studied in Subsections 4.1.2 and 4.1.3 for the gas phase. The case $v_- > v_+$ has a blow up leading to a singular measure. In the process of the blow up the volume fraction c takes values larger than 1, which implies that $c_c = 1 - c < 0$. This case corresponds physically to a phase transition which is not modeled in the system of equations under consideration. Nevertheless, we give a solution for this case, too.

In all three cases, we give initial data and determine the exact solution. We want to emphasize the possibility of choosing physically relevant values for the involved quantities. Therefore, we assumed the carrier phase to be liquid water and used a Tait equation of state (2.8) with the corresponding parameters from [87]. The initial data are given by

	c	$\rho \left[\frac{\text{kg}}{\text{m}^3} \right]$	$v \left[\frac{\text{m}}{\text{s}} \right]$	R	$\rho_c \left[\frac{\text{kg}}{\text{m}^3} \right]$	$v_c \left[\frac{\text{m}}{\text{s}} \right]$	$p \text{ [Pa]}$
Left state	0.05	0.5863	10	0.001	998.2081	5	100000
Right state	0.001	0.5584	10	0.0005	998.1715	5.2887	20000

(4.40)

	c	$\rho \left[\frac{\text{kg}}{\text{m}^3} \right]$	$v \left[\frac{\text{m}}{\text{s}} \right]$	R	$\rho_c \left[\frac{\text{kg}}{\text{m}^3} \right]$	$v_c \left[\frac{\text{m}}{\text{s}} \right]$	$p \text{ [Pa]}$
Left state	0.05	0.5573	-20	0.0005	993.6919	5	100000
Right state	0.001	0.5307	40	0.001	993.7095	3.6612	140000

(4.41)

	c	$\rho \left[\frac{\text{kg}}{\text{m}^3} \right]$	$v \left[\frac{\text{m}}{\text{s}} \right]$	R	$\rho_c \left[\frac{\text{kg}}{\text{m}^3} \right]$	$v_c \left[\frac{\text{m}}{\text{s}} \right]$	$p \text{ [Pa]}$
Left state	0.02	0.6879	10	0.0008	965.3410	20	145000
Right state	0.008	0.5503	-20	0.0006	966.0308	21	1655149.1033

(4.42)

where we have assumed temperatures of 293.15 K, 309.15 K and 363.15 K, respectively. We give a set of initial data for a vapor carrier phase as well. In this case the carrier phase is assumed to be water vapor with an ideal gas equation of state at a temperature of 309.15 K. The initial data are the following

	c	$\rho \left[\frac{\text{kg}}{\text{m}^3} \right]$	$v \left[\frac{\text{m}}{\text{s}} \right]$	R	$\rho_c \left[\frac{\text{kg}}{\text{m}^3} \right]$	$v_c \left[\frac{\text{m}}{\text{s}} \right]$	$p \text{ [Pa]}$
Left state	0.05	993.6941	-20	0.0005	0.5307	5	100000
Right state	0.001	993.6919	40	0.001	0.7430	-180.3256	140000

(4.43)

All these examples fulfill the inequalities given later in this chapter.

4.4 The case $v_- = v_+ = v$

From the results in Section 4.1.2, we know that the velocity v in the dispersed phase remains constant while the volume fraction c and the density ρ are advected with constant speed v . The possible wave configurations are depicted in Figure 4.2.

4.4.1 Contact wave

In this first case we consider a contact wave in the dispersed phase. The jump conditions for the two carrier phase equations at this contact read

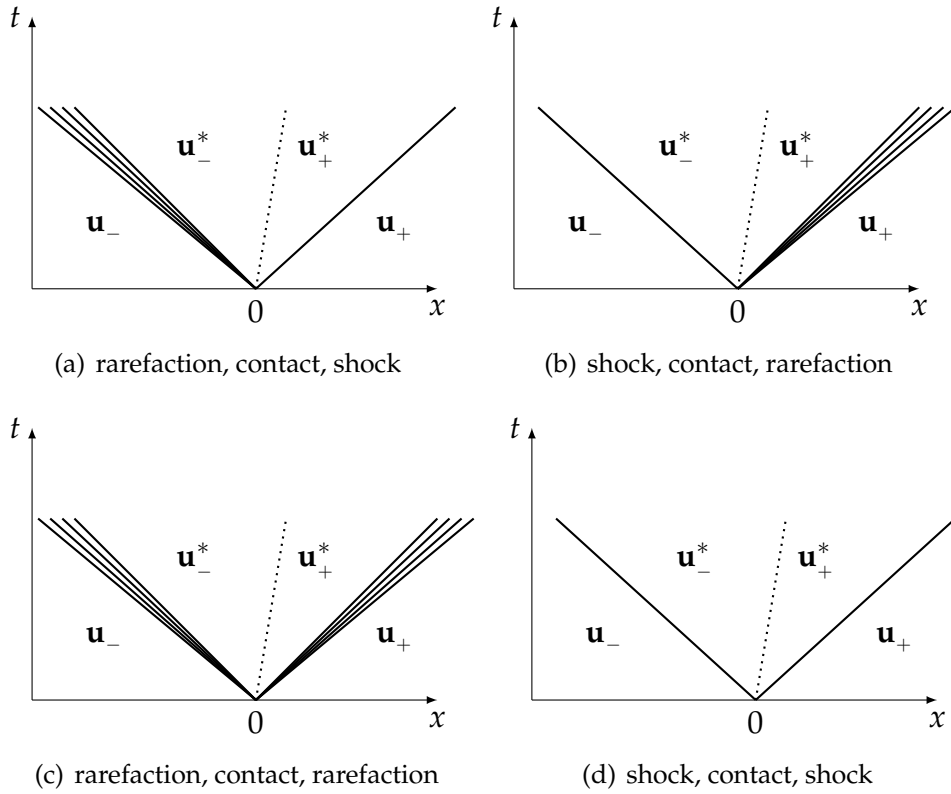
$$0 = v[(1-c)\rho_c] - [(1-c)\rho_c v_c], \quad (4.44)$$

$$0 = v[(1-c)\rho_c v_c] - [(1-c)\rho_c v_c^2 + (1-c)p_c]. \quad (4.45)$$

These relations mean that the solutions \mathbf{u}_-^* and \mathbf{u}_+^* in Figure 4.2 are related by the equations

$$(1-c_+^*)\rho_{c_+}^*(v_{c_+}^* - v) = (1-c_-^*)\rho_{c_-}^*(v_{c_-}^* - v),$$

$$(1-c_+^*)\left[\rho_{c_+}^*((v_{c_+}^*)^2 - v v_{c_+}^*) + p_c(\rho_{c_+}^*)\right] = (1-c_-^*)\left[\rho_{c_-}^*((v_{c_-}^*)^2 - v v_{c_-}^*) + p_c(\rho_{c_-}^*)\right].$$

FIGURE 4.2: Wave configurations in the case $v_- = v_+$

Now using (4.29) and (4.31) for v^* and c_{\pm}^* and the equation of state gives the system

$$(1-c_+) \rho_{c_+}^* (v_{c_+}^* - v) = (1-c_-) \rho_{c_-}^* (v_{c_-}^* - v),$$

$$(1-c_+) \left[\rho_{c_+}^* \left((v_{c_+}^*)^2 - v v_{c_+}^* \right) + \left(a_c^2 \rho_{c_+}^* + d_0 \right) \right] = (1-c_-) \left[\rho_{c_-}^* \left((v_{c_-}^*)^2 - v v_{c_-}^* \right) + \left(a_c^2 \rho_{c_-}^* + d_0 \right) \right].$$

Multiplying the first equation by v and adding it to the second equation leads to

$$(1-c_+) \rho_{c_+}^* (v_{c_+}^* - v) = (1-c_-) \rho_{c_-}^* (v_{c_-}^* - v),$$

$$(1-c_+) \rho_{c_+}^* \left[\left(v_{c_+}^* - v \right)^2 + a_c^2 \right] - c_+ d_0 = (1-c_-) \rho_{c_-}^* \left[\left(v_{c_-}^* - v \right)^2 + a_c^2 \right] - c_- d_0.$$

Introducing $\Delta v_{c_{\pm}}^* = v_{c_{\pm}}^* - v$ allows us to solve this system easily. We describe the values with index $+$ as functions of the values with index $-$. Due to the

quadratic nature of these equations, we get two solutions

$$\begin{aligned} \Delta v_{c_+(1,2)}^* &= \frac{(1-c_-)\rho_{c_-}^* \left((\Delta v_{c_-}^*)^2 + a_c^2 \right) + d_0(c_+ - c_-)}{2(1-c_-)\rho_{c_-}^* \Delta v_{c_-}^*} \\ &\pm \frac{\sqrt{\left((1-c_-)\rho_{c_-}^* \left((\Delta v_{c_-}^*)^2 + a_c^2 \right) + d_0(c_+ - c_-) \right)^2 - 4\left((1-c_-)\rho_{c_-}^* (\Delta v_{c_-}^*)^2 a_c^2 \right)^2}}{2(1-c_-)\rho_{c_-}^* \Delta v_{c_-}^*}, \\ (1-c_+)\rho_{c_+(1,2)}^* &= \frac{(1-c_-)\rho_{c_-}^* \left((\Delta v_{c_-}^*)^2 + a_c^2 \right) + d_0(c_+ - c_-)}{2a_c^2} \\ &\mp \frac{\sqrt{\left((1-c_-)\rho_{c_-}^* \left((\Delta v_{c_-}^*)^2 + a_c^2 \right) + d_0(c_+ - c_-) \right)^2 - 4\left((1-c_-)\rho_{c_-}^* (\Delta v_{c_-}^*)^2 a_c^2 \right)^2}}{2a_c^2}. \end{aligned} \quad (4.46)$$

Note that the following Prandtl-type relation holds

$$\Delta v_{c_+(1)}^* \Delta v_{c_+(2)}^* = a_c^2.$$

We assume the square root in these expressions being positive. Then, depending on the sign in front of the quotient, we have a unique solution for the carrier phase density and velocity in the *-region that is subsonic. Note that subsonic here means that the relative velocity between the carrier and dispersed phase is subsonic. We are not aware of any application where one would move bubbles at supersonic speed through a liquid. Such a situation would also violate basic assumptions of the model, such as assuming that the bubbles are of almost spherical shape. Therefore, we will discuss only the unique subsonic solutions and drop the subscript (1) or (2) in the following discussion.

4.4.2 Vapor carrier phase

We will now consider the carrier phase as a vapor. Taking this vapor phase to be an ideal gas is a valid choice for an equation of state, see Section 2. Starting from the linear equation of state $p = a^2 \rho + d_0$ this leads to

$$d_0 = 0$$

for an ideal gas.

Note that in this case the relations (4.46) holding at the contact wave simplify in the subsonic case to the following form

$$\begin{aligned} \Delta v_{c_+}^* &= \Delta v_{c_-}^* \\ (1-c_+)\rho_{c_+}^* &= (1-c_-)\rho_{c_-}^*. \end{aligned}$$

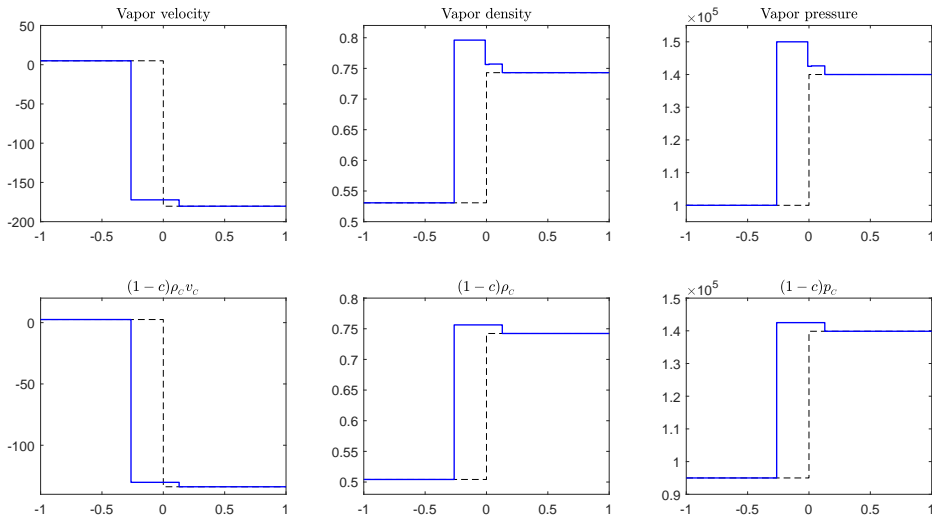


FIGURE 4.3: Initial data (dashed lines) and exact solution (solid lines) for a vapor carrier phase. Note the difference between primitive and conserved variables in their behavior at the middle wave in accordance with (4.47). Initial data is given by (4.43)

Again we put $\hat{\rho}_c = (1 - c) \rho_c$ and we get

$$\begin{aligned} \llbracket \Delta v_c^* \rrbracket &= 0, \\ \llbracket \hat{\rho}_c^* \rrbracket &= 0. \end{aligned} \quad (4.47)$$

The carrier phase quantities v_c^* and the transformed $\hat{\rho}_c^*$ are constant over the contact wave. This fact can be seen in Figure 4.3. There is no jump of these quantities, whereas one can clearly see the jump in the primitive variables ρ_c and p_c . Note that the jump only appears due to the back transformation of $\hat{\rho}_c^*$ where the factor $(1 - c)$ appears. The jump in the concentration c of the dispersed phase leads to the jump of the primitive variables of the carrier phase. Therefore, in the conserved quantities, one has only two acoustic waves and none of those quantities appear in the dispersed phase relations. This is equivalent to the statement that the subsystem of these new carrier phase equations decouples from the rest of the system (4.26). Hence the carrier phase equations can be solved independently. They read

$$\begin{aligned} \frac{\partial}{\partial t} (\hat{\rho}_c) + \frac{\partial}{\partial x} (\hat{\rho}_c v_c) &= 0, \\ \frac{\partial}{\partial t} (\hat{\rho}_c v_c) + \frac{\partial}{\partial x} (\hat{\rho}_c v_c^2 + \tilde{p}_c) &= 0. \end{aligned}$$

This is the well known system of the isothermal Euler equations. We omit the solution. A detailed discussion of the isothermal Euler equations may be found in [21] or [83].

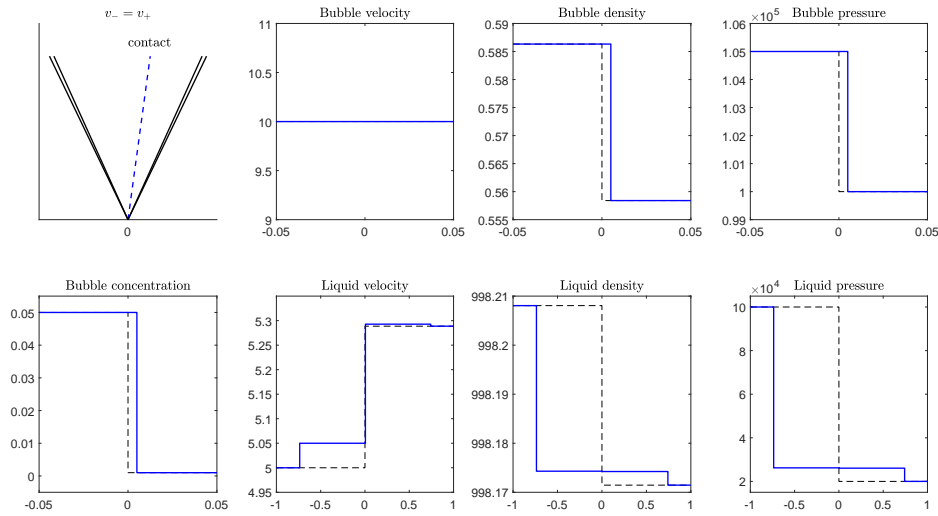


FIGURE 4.4: Initial data (dashed lines) and exact solution (solid lines) for a liquid carrier phase. The middle wave is a contact wave. Initial data are given by (4.40)

4.4.3 Liquid carrier phase

Having a liquid carrier phase the solution is much more complex. To model a liquid we use the general linear equation of state $p = a^2 \rho + d_0$ with

$$d_0 \neq 0.$$

This leads to

$$\begin{aligned} \llbracket \Delta v_c^* \rrbracket &\neq 0, \\ \llbracket \hat{\rho}_c^* \rrbracket &\neq 0. \end{aligned} \quad (4.48)$$

A set of initial data and the exact solution in this case are depicted in Figure 4.4. For the four unknown quantities of the carrier phase in the *-region we have four relations. In the previous parts of this section we derived the relations which hold over the acoustic waves and determined the relations at the contact wave, see (4.38) and (4.39) in case of a shockwave, (4.29) and (4.31) in case of a rarefaction wave, as well as (4.44) for contact waves. Therefore, we have to solve a nonlinear system to find the solution in the *-region. In this case it is given by

$$0 = v \llbracket (1-c) \rho_c^* \rrbracket - \llbracket (1-c) \rho_c^* v_c^* \rrbracket, \quad (4.49)$$

$$0 = v \llbracket (1-c) \rho_c^* v_c^* \rrbracket - \llbracket (1-c) \rho_c^* v_c^{*2} + (1-c) p_c^* \rrbracket, \quad (4.50)$$

$$v_{C\pm}^* = v_{C\pm} \pm \begin{cases} a_c \frac{\rho_{C\pm}^* - \rho_{C\pm}}{\sqrt{\rho_{C\pm}^* \rho_{C\pm}}} & \rho_{C\pm}^* > \rho_{C\pm} \quad (\text{shock}), \\ a_c \ln \frac{\rho_{C\pm}^*}{\rho_{C\pm}} & \rho_{C\pm}^* \leq \rho_{C\pm} \quad (\text{rarefaction}). \end{cases} \quad (4.51)$$

We will describe the $C+$ -quantities on the right side of the contact in terms of the $C-$ -quantities on the left side of the contact in the $*$ -region. Using again $\Delta v_{C\pm}^* = v_{C\pm}^* - v$ and $\hat{\rho} = c \rho$ the functions

$$\Delta v_{C+}^* = V \left(\Delta v_{C-}^*, \hat{\rho}_{C-}^* \right), \quad (4.52)$$

$$\hat{\rho}_{C+}^* = P \left(\Delta v_{C-}^*, \hat{\rho}_{C-}^* \right) \quad (4.53)$$

are given by equations (4.46). Alternatively, we can use (4.51) to describe $\Delta v_{C\pm}^*$ in terms of $\hat{\rho}_{C\pm}$

$$\Delta v_{C\pm}^* = W_{\pm} \left(\hat{\rho}_{C\pm}^* \right). \quad (4.54)$$

We now try to give an idea of the solution strategy before we state the main result. We rewrite (4.46) by subtracting Δv_{C+}^* . Using the other relations from the nonlinear system (4.49) - (4.51) we can further reduce the number of unknown quantities in this function. To see this, we introduce the following notation

$$\begin{aligned} A &= \left[(1-c_-) \rho_{C-}^* \left((\Delta v_{C-}^*)^2 + a_c^2 \right) + d_0 (c_+ - c_-) \right], \\ B &= \left((1-c_-) \rho_{C-}^* \left((\Delta v_{C-}^*)^2 + a_c^2 \right) + d_0 (c_+ - c_-) \right)^2 - 4 \left((1-c_-) \rho_{C-}^* (\Delta v_{C-}^*)^2 a_c^2 \right)^2. \end{aligned} \quad (4.55)$$

Hence the first equation of (4.46) can be rewritten in the following form

$$\begin{aligned} 0 &= -\Delta v_{C+}^* + \frac{A - \sqrt{B}}{2\hat{\rho}_{C-}^* \Delta v_{C-}^*} \\ &= F \left(\hat{\rho}_{C-}^*, \Delta v_{C-}^*, \Delta v_{C+}^* \right) \\ &= F \left(\hat{\rho}_{C-}^*, W_- \left(\hat{\rho}_{C-}^* \right), W_+ \left(\hat{\rho}_{C+}^* \right) \right) \\ &= F \left(\hat{\rho}_{C-}^*, W_- \left(\hat{\rho}_{C-}^* \right), W_+ \left(P \left(\hat{\rho}_{C-}^*, W_- \left(\hat{\rho}_{C-}^* \right) \right) \right) \right), \end{aligned}$$

where we have used (4.52) - (4.54) to eliminate the dependencies on unknown quantities. The function F is now an implicit function of only one unknown variable $\hat{\rho}_{C-}^*$. Any root of this function is a solution for $\hat{\rho}_{C-}^*$ from which we can then calculate all the other unknown quantities. The solution is unique if the function F is strictly monotone. The analysis of this function and its first derivative leads to the following result.

Theorem 4.4.1. *A solution of the carrier phase equations of system (4.26) in the case $v_- = v_+$ is the root of the function*

$$F \left(\hat{\rho}_{C-}^*, W_- \left(\hat{\rho}_{C-}^* \right), W_+ \left(P \left(\hat{\rho}_{C-}^*, W_- \left(\hat{\rho}_{C-}^* \right) \right) \right) \right) = -\Delta v_{C+}^* + \frac{A - \sqrt{B}}{2\hat{\rho}_{C-}^* \Delta v_{C-}^*} \quad (4.56)$$

and it is unique if F is strictly monotone w.r.t. $\hat{\rho}_{C-}^*$. This is fulfilled for $B > 0$ and under the following conditions for the absolute value of the carrier velocity

$$\begin{aligned}
(1) \quad \Delta v_{\max} &< a_C \\
(2) \quad \Delta v_{\max} &< a_C + \frac{d_0 c_{\max}}{a_C (1 - c_{\max}) \rho_{\min}} \\
(3) \quad \Delta v_{\max} &< a_C \frac{(1 - c_{\max}) \rho_{\min}}{2\rho_{\max} - (1 - c_{\max}) \rho_{\min}} \\
(4) \quad \Delta v_{\max} &< -\frac{|d_0| c_{\max} \sqrt{\rho_{\max} \rho_{\min}}}{a_C (1 - c_{\max}) \rho_{\min} (\rho_{\max} + \rho_{\min})} \\
&\quad + \sqrt{\left(\frac{|d_0| c_{\max} \sqrt{\rho_{\max} \rho_{\min}}}{a_C (1 - c_{\max}) \rho_{\min} (\rho_{\max} + \rho_{\min})} \right)^2 + a_C^2} \\
(5) \quad \Delta v_{\max} &< -a_C \frac{\rho_{\max} + \rho_{\min}}{2\sqrt{\rho_{\max} \rho_{\min}}} \frac{\rho_{\max} - \rho_{\min}}{2\rho_{\max} - \rho_{\min}} \\
&\quad + \sqrt{\left(a_C \frac{\rho_{\max} + \rho_{\min}}{2\sqrt{\rho_{\max} \rho_{\min}}} \frac{\rho_{\max} - \rho_{\min}}{2\rho_{\max} - \rho_{\min}} \right)^2 + \frac{\rho_{\min} a_C}{2\rho_{\max} - \rho_{\min}}}
\end{aligned} \tag{4.57}$$

These conditions state that the relative velocities between the carrier and dispersed phase should be only a certain amount smaller than the sound speed. Note further that d_0 is negative for fluids. To give an example we have $d_0 \approx -0.5 * 10^9$ for liquid water at 293.15 K, see [87].

Proof. To find a solution for the four unknown carrier phase quantities $\rho_{C\pm}^*$ and $v_{C\pm}^*$ one uses the Riemann invariants and Rankine-Hugoniot jump conditions to get the four relations (4.49) - (4.51). The first two equations

$$\begin{aligned}
0 &= v \llbracket (1 - c) \rho_C^* \rrbracket - \llbracket (1 - c) \rho_C^* v_C^* \rrbracket, \\
0 &= v \llbracket (1 - c) \rho_C^* v_C^* \rrbracket - \llbracket (1 - c) \rho_C^* v_C^{*2} + (1 - c) p_C^* \rrbracket
\end{aligned}$$

possess a unique subsonic solution $\Delta v_{C+}^* = V(\Delta v_{C-}^*, \hat{\rho}_{C-}^*)$ and $\hat{\rho}_{C+}^* = P(\Delta v_{C-}^*, \hat{\rho}_{C-}^*)$ given by (4.46). Rewriting the first expression of (4.46) in the form

$$0 = F(\hat{\rho}_{C-}^*, \Delta v_{C-}^*, \Delta v_{C+}^*) = -\Delta v_{C+}^* + V(\Delta v_{C-}^*, \hat{\rho}_{C-}^*)$$

and using $\Delta v_{C\pm}^* = W_{\pm}(\hat{\rho}_{C\pm}^*)$, obtained from (4.51)

$$\Delta v_{C\pm}^* = \Delta v_{C\pm} \pm \begin{cases} a_C \frac{\hat{\rho}_{C\pm}^* - \hat{\rho}_{C\pm}}{\sqrt{\hat{\rho}_{C\pm}^* \hat{\rho}_{C\pm}}} & \hat{\rho}_{C\pm}^* > \hat{\rho}_{C\pm} \quad (\text{shock}), \\ a_C \ln \frac{\hat{\rho}_{C\pm}^*}{\hat{\rho}_{C\pm}} & \hat{\rho}_{C\pm}^* \leq \hat{\rho}_{C\pm} \quad (\text{rarefaction}), \end{cases}$$

we can reduce the number of unknown quantities. Note that in the case with the + sign we will replace $\hat{\rho}_{C+}^*$ by the function $P(\hat{\rho}_{C-}^*, W_-(\hat{\rho}_{C-}^*))$. The

function F is a function of $\hat{\rho}_{c-}^*$ only. A solution is then determined by

$$0 = F \left(\hat{\rho}_{c-}^*, W_- \left(\hat{\rho}_{c-}^* \right), W_+ \left(P \left(\hat{\rho}_{c-}^*, W_- \left(\hat{\rho}_{c-}^* \right) \right) \right) \right).$$

To verify uniqueness of solutions one checks the strict monotonicity of F , that is

$$\frac{dF}{d\hat{\rho}_{c-}^*} < 0. \quad (4.58)$$

The derivative of F reads

$$\frac{dF}{d\hat{\rho}_{c-}^*} = \frac{\partial F}{\partial \hat{\rho}_{c-}^*} + \frac{\partial F}{\partial W_-} \frac{\partial W_-}{\partial \hat{\rho}_{c-}^*} + \frac{\partial F}{\partial W_+} \left[\frac{\partial W_+}{\partial P} \left(\frac{\partial P}{\partial \hat{\rho}_{c-}^*} + \frac{\partial P}{\partial W_-} \frac{\partial W_-}{\partial \hat{\rho}_{c-}^*} \right) \right].$$

We omit the calculation details of all these terms and just state the result. Using the abbreviations (4.55) the partial derivatives are

$$\frac{\partial F}{\partial \hat{\rho}_{c-}^*} = \frac{(-\sqrt{B} + A) d_0 (c_+ - c_-)}{B 2 (\hat{\rho}_{c-}^*)^2 \Delta v_{c-}^*}, \quad (4.59)$$

$$\frac{\partial F}{\partial W_-} = \frac{-(-\sqrt{B} + A) \left(\hat{\rho}_{c-}^* (W_-^2 - a_c^2) - d_0 (c_+ - c_-) \right)}{B 2 \hat{\rho}_{c-}^* W_-^2}, \quad (4.60)$$

$$\frac{\partial W_-}{\partial \hat{\rho}_{c-}^*} = \begin{cases} -a_c \frac{\hat{\rho}_{c-}^* + \hat{\rho}_{c-}}{2 \hat{\rho}_{c-}^* \sqrt{\hat{\rho}_{c-}^* \hat{\rho}_{c-}}} & \hat{\rho}_{c-}^* > \hat{\rho}_{c-} \quad (\text{shock}), \\ -a_c \frac{1}{\hat{\rho}_{c-}^*} & \hat{\rho}_{c-}^* \leq \hat{\rho}_{c-} \quad (\text{rarefaction}), \end{cases} \quad (4.61)$$

$$\frac{\partial F}{\partial W_+} = -1. \quad (4.62)$$

Further, using $\hat{\rho}_{c+}^* = P \left(\hat{\rho}_{c-}^*, W_- \left(\hat{\rho}_{c-}^* \right) \right)$ we have

$$\frac{\partial W_+}{\partial P} = \begin{cases} a_c \frac{P + \hat{\rho}_{c+}^*}{2P \sqrt{P \hat{\rho}_{c+}^*}} & P > \hat{\rho}_{c+} \quad (\text{shock}), \\ a_c \frac{1}{P} & P \leq \hat{\rho}_{c+} \quad (\text{rarefaction}), \end{cases} \quad (4.63)$$

$$\frac{\partial P}{\partial \hat{\rho}_{c-}^*} = \frac{1}{2a_c} \left[\frac{W_-^2 + a_c^2}{\sqrt{B}} (A + \sqrt{B}) - \frac{4a_c^2 \hat{\rho}_{c-}^* W_-^2}{\sqrt{B}} \right], \quad (4.64)$$

$$\frac{\partial P}{\partial W_-} = \frac{1}{2a_c} \left[\frac{2\hat{\rho}_{c-}^* W_-}{\sqrt{B}} (A + \sqrt{B}) - \frac{4a_c^2 (\hat{\rho}_{c-}^*)^2 W_-}{\sqrt{B}} \right]. \quad (4.65)$$

Note that the derivative (4.63) is always positive. Hence there is no dependency on whether the right going wave is a shock or a rarefaction. Nonetheless, we have to discuss the different cases for the left going acoustic wave.

In the case of the left moving acoustic wave being a rarefaction wave with $\hat{\rho}_{c_-}^* > \hat{\rho}_{c_-}$ one can simplify the derivative by combining some terms together. One gets

$$\frac{\partial F}{\partial \hat{\rho}_{c_-}^*} + \frac{\partial F}{\partial W_-} \frac{\partial W_-}{\partial \hat{\rho}_{c_-}^*} = \frac{1}{B \hat{\rho}_{c_-}^*} \frac{\Delta v_{c_+}^*}{\Delta v_{c_-}^*} (\Delta v_{c_-}^* - a_c) \left(d_0 (c_+ - c_-) + a_c \hat{\rho}_{c_-}^* (a_c + \Delta v_{c_-}^*) \right).$$

This leads to two conditions to satisfy (4.58), namely

$$(i) \quad \Delta v_{c_-}^* - a_c \stackrel{!}{<} 0,$$

$$(ii) \quad d_0 (c_+ - c_-) + a_c \hat{\rho}_{c_-}^* (a_c + \Delta v_{c_-}^*) \stackrel{!}{>} 0.$$

One sees immediately that the conditions (i) and (1) are equivalent. An estimate on the quantities in (ii) shows that for monotonicity of F we need

$$d_0 (c_+ - c_-) + a_c \hat{\rho}_{c_-}^* (a_c + \Delta v_{c_-}^*) \geq d_0 c_{\max} + a_c (1 - c_{\max}) \rho_{\min} (a_c - \Delta v_{\max}) \stackrel{!}{>} 0.$$

This leads to

$$(2) \quad \Delta v_{\max} < a_c + \frac{d_0 c_{\max}}{a_c (1 - c_{\max}) \rho_{\min}}.$$

The terms of the derivative of F which are left over combine in the following way

$$\frac{\partial P}{\partial \hat{\rho}_{c_-}^*} + \frac{\partial P}{\partial W_-} \frac{\partial W_-}{\partial \hat{\rho}_{c_-}^*} = \frac{1}{B} (a_c - \Delta v_{c_-}^*) \left((a_c - \Delta v_{c_-}^*) \hat{\rho}_{c_+}^* + 2 \hat{\rho}_{c_-}^* \Delta v_{c_-}^* \right).$$

This leads to the further condition

$$(iii) \quad (a_c - \Delta v_{c_-}^*) \hat{\rho}_{c_+}^* + 2 \hat{\rho}_{c_-}^* \Delta v_{c_-}^* \stackrel{!}{>} 0.$$

Similar estimates of the quantities involved give

$$\begin{aligned} (a_c - \Delta v_{c_-}^*) \hat{\rho}_{c_+}^* + 2 \hat{\rho}_{c_-}^* \Delta v_{c_-}^* &= a_c \hat{\rho}_{c_+}^* + \Delta v_{c_-}^* (2 \hat{\rho}_{c_-}^* - \hat{\rho}_{c_+}^*) \\ &\geq a_c (1 - c_{\max}) \rho_{\min} - \Delta v_{\max} (2 \rho_{\max} - (1 - c_{\max}) \rho_{\min}) \\ &\stackrel{!}{>} 0, \end{aligned}$$

which is equivalent to condition (3).

In case of a left moving shock wave the combined terms of the derivative of F read

$$\begin{aligned} \frac{\partial F}{\partial \hat{\rho}_{c-}^*} + \frac{\partial F}{\partial W_-} \frac{\partial W_-}{\partial \hat{\rho}_{c-}^*} &= \frac{1}{\sqrt{B} \hat{\rho}_{c-}^*} \frac{\Delta v_{c+}^*}{\Delta v_{c-}^*} \left(d_0 (c_+ - c_-) \left(\Delta v_{c-}^* - a_c \frac{\hat{\rho}_{c-}^* + \hat{\rho}_{c-}}{2\sqrt{\hat{\rho}_{c-}^* \hat{\rho}_{c-}}} \right) \right. \\ &\quad \left. + a_c \hat{\rho}_{c-}^* (\Delta v_{c-}^* - a_c) (\Delta v_{c-}^* + a_c) \frac{\hat{\rho}_{c-}^* + \hat{\rho}_{c-}}{2\sqrt{\hat{\rho}_{c-}^* \hat{\rho}_{c-}}} \right), \\ \frac{\partial R}{\partial \hat{\rho}_{c-}^*} + \frac{\partial R}{\partial W_-} \frac{\partial W_-}{\partial \hat{\rho}_{c-}^*} &= \frac{1}{\sqrt{B}} \left(\hat{\rho}_{c+}^* \left(a_c^2 + (\Delta v_{c-}^*)^2 - 2a_c \Delta v_{c-}^* \frac{\hat{\rho}_{c-}^* + \hat{\rho}_{c-}}{2\sqrt{\hat{\rho}_{c-}^* \hat{\rho}_{c-}}} \right) \right. \\ &\quad \left. + 2\hat{\rho}_{c-}^* \Delta v_{c-}^* \left(a_c \frac{\hat{\rho}_{c-}^* + \hat{\rho}_{c-}}{2\sqrt{\hat{\rho}_{c-}^* \hat{\rho}_{c-}}} - \Delta v_{c-}^* \right) \right). \end{aligned}$$

Again, to satisfy condition (4.58) this leads to two conditions

$$\begin{aligned} (iv) \quad & d_0 (c_+ - c_-) \left(\Delta v_{c-}^* - a_c \frac{\hat{\rho}_{c-}^* + \hat{\rho}_{c-}}{2\sqrt{\hat{\rho}_{c-}^* \hat{\rho}_{c-}}} \right) + a_c \hat{\rho}_{c-}^* (\Delta v_{c-}^* - a_c) (\Delta v_{c-}^* + a_c) \frac{\hat{\rho}_{c-}^* + \hat{\rho}_{c-}}{2\sqrt{\hat{\rho}_{c-}^* \hat{\rho}_{c-}}} \\ & < -|d_0| c_{\max} \left(-\Delta v_{\max} - a_c \frac{\rho_{\max} + \rho_{\min}}{2\sqrt{\rho_{\max} \rho_{\min}}} \right) \\ & \quad + a_c (1 - c_{\max}) \rho_{\min} \left((\Delta v_{c-}^*)^2 - a_c^2 \right) \frac{\rho_{\max} + \rho_{\min}}{2\sqrt{\rho_{\max} \rho_{\min}}} \\ & = a_c (1 - c_{\max}) \rho_{\min} \frac{\rho_{\max} + \rho_{\min}}{2\sqrt{\rho_{\max} \rho_{\min}}} \\ & \quad \left((\Delta v_{\max})^2 + \frac{2|d_0| c_{\max} \sqrt{\rho_{\max} \rho_{\min}}}{a_c (1 - c_{\max}) \rho_{\min} (\rho_{\max} + \rho_{\min})} \Delta v_{\max} + \frac{|d_0| c_{\max}}{(1 - c_{\max}) \rho_{\min}} - a_c^2 \right) \\ & \stackrel{!}{<} 0, \\ (v) \quad & \hat{\rho}_{c+}^* \left(a_c^2 + (\Delta v_{c-}^*)^2 - a_c \Delta v_{c-}^* \frac{\hat{\rho}_{c-}^* + \hat{\rho}_{c-}}{\sqrt{\hat{\rho}_{c-}^* \hat{\rho}_{c-}}} \right) \\ & \quad + 2\hat{\rho}_{c-}^* \Delta v_{c-}^* \left(a_c \frac{\hat{\rho}_{c-}^* + \hat{\rho}_{c-}}{2\sqrt{\hat{\rho}_{c-}^* \hat{\rho}_{c-}}} - \Delta v_{c-}^* \right) \stackrel{!}{>} 0. \end{aligned}$$

Again, we have used similar estimates than before. The two relations are simple quadratic expressions in Δv_{c-}^* . One sees that satisfying (4) and (5) is sufficient for (iv) and (v), which proves the theorem. \square

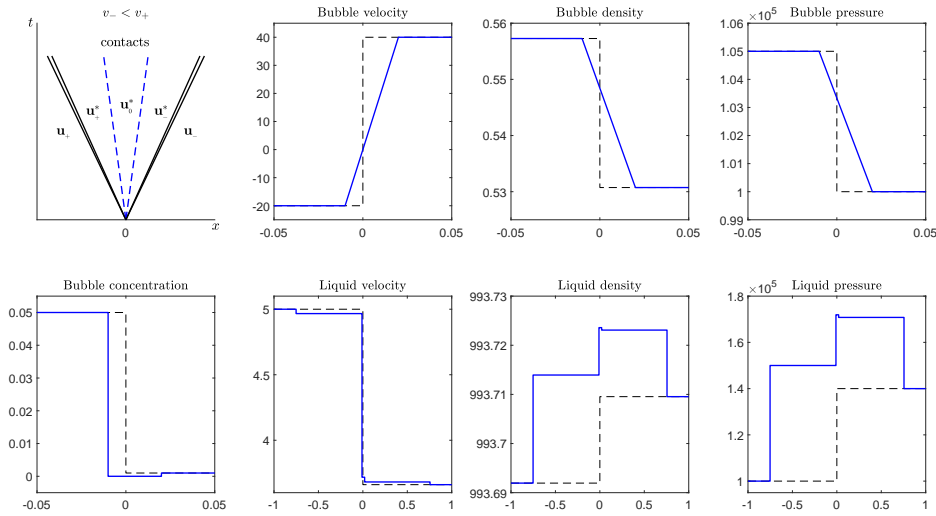


FIGURE 4.5: Initial data (dashed lines) and exact solution (solid lines) for a liquid carrier phase. The middle wave splits in two contacts. Initial data is given by (4.41)

4.5 The case $v_- < v_+$

In this case, the middle wave consists out of two contact waves with velocities v_- and v_+ and a vaporless state between these two contact waves. Detailed results for the dispersed phase can be found in Section 4.1.3. The wave configuration, initial data and the corresponding exact solution is depicted in Figure 4.5. Note that in the first row, we show only a part of the x-Axis to highlight the bubble free region, which is barely noticeable in the second row. Starting again from the relations which hold over the acoustic waves, as well as over a contact wave we get our nonlinear system of equations. In this case the six relations read

$$0 = v_+ \llbracket (1-c) \rho_c^* \rrbracket - \llbracket (1-c) \rho_c^* v_c^* \rrbracket, \quad (4.66)$$

$$0 = v_+ \llbracket (1-c) \rho_c^* v_c^* \rrbracket - \llbracket (1-c) \rho_c^* v_c^{*2} + (1-c) p_c^* \rrbracket, \quad (4.67)$$

$$0 = v_- \llbracket (1-c) \rho_c^* \rrbracket - \llbracket (1-c) \rho_c^* v_c^* \rrbracket, \quad (4.68)$$

$$0 = v_- \llbracket (1-c) \rho_c^* v_c^* \rrbracket - \llbracket (1-c) \rho_c^* v_c^{*2} + (1-c) p_c^* \rrbracket, \quad (4.69)$$

$$v_{c\pm}^* = v_{c\pm} \pm \begin{cases} a_c \frac{\rho_{c\pm}^* - \rho_{c\pm}}{\sqrt{\rho_{c\pm}^* \rho_{c\pm}}} & \rho_{c\pm}^* > \rho_{c\pm} \quad (\text{shock}), \\ a_c \ln \frac{\rho_{c\pm}^*}{\rho_{c\pm}} & \rho_{c\pm}^* \leq \rho_{c\pm} \quad (\text{rarefaction}). \end{cases} \quad (4.70)$$

for the six unknown carrier phase quantities $\rho_{c-}^*, v_{c-}^*, \rho_{c+}^*, v_{c+}^*$ and ρ_{c0}^*, v_{c0}^* . For both contact waves we follow the approach of Section 4.4.1. The jump conditions over the right moving contact wave, the first two equations (4.66)

and (4.67) respectively, read

$$(1-c_0)\rho_{c_0}^*(v_{c_0}^*-v_+) = (1-c_+)\rho_{c_+}^*(v_{c_+}^*-v_+),$$

$$(1-c_0)\rho_{c_0}^*\left[(v_{c_0}^*-v_+)^2+a_c^2\right]-c_0d_0 = (1-c_+)\rho_{c_+}^*\left[(v_{c_+}^*-v_+)^2+a_c^2\right]-c_+d_0.$$

Following the approach from Section 4.4.1 we get two functions

$$v_{c_+}^* = V_{0+}(v_{c_0}^*, \rho_{c_0}^*),$$

$$\rho_{c_+}^* = P_{0+}(v_{c_0}^*, \rho_{c_0}^*).$$

These functions are given by (compare with (4.46))

$$v_{c_+}^* = v_+ + \frac{(1-c_0)\rho_{c_0}^*((v_{c_0}^*-v_+)^2+a_c^2)+d_0(c_+-c_0)}{2(1-c_0)\rho_{c_0}^*(v_{c_0}^*-v_+)}$$

$$- \frac{\sqrt{((1-c_0)\rho_{c_0}^*((v_{c_0}^*-v_+)^2+a_c^2)+d_0(c_+-c_0))^2-4((1-c_0)\rho_{c_0}^*(v_{c_0}^*-v_+)^2a_c^2)}}{2(1-c_0)\rho_{c_0}^*(v_{c_0}^*-v_+)}, \quad (4.71)$$

$$(1-c_+)\rho_{c_+}^* = \frac{(1-c_0)\rho_{c_0}^*((v_{c_0}^*-v_+)^2+a_c^2)+d_0(c_+-c_0)}{2a_c^2}$$

$$+ \frac{\sqrt{((1-c_0)\rho_{c_0}^*((v_{c_0}^*-v_+)^2+a_c^2)+d_0(c_+-c_0))^2-4((1-c_0)\rho_{c_0}^*(v_{c_0}^*-v_+)^2a_c^2)}}{2a_c^2}. \quad (4.72)$$

The jump conditions over the left moving contact (4.68) and (4.69) read in detail

$$(1-c_0)\rho_{c_0}^*(v_{c_0}^*-v_-) = (1-c_-)\rho_{c_-}^*(v_{c_-}^*-v_-),$$

$$(1-c_0)\rho_{c_0}^*\left[(v_{c_0}^*-v_-)^2+a_c^2\right]-c_0d_0 = (1-c_-)\rho_{c_-}^*\left[(v_{c_-}^*-v_-)^2+a_c^2\right]-c_-d_0,$$

from those relations we can determine the two functions

$$v_{c_0}^* = V_{-0}(v_{c_-}^*, \rho_{c_-}^*),$$

$$\rho_{c_0}^* = P_{-0}(v_{c_-}^*, \rho_{c_-}^*),$$

which we will not state in detail. They have a similar structure like (4.71) and (4.72). Furthermore, we use the relations over the acoustic waves (4.51) from the previous chapter, given by (4.70), to define $v_{c_{\pm}}^* = W_{\pm}(\hat{\rho}_{c_{\pm}}^*)$ again.

Again we write (4.71) in the form

$$0 = G(\rho_{c_0}^*, v_{c_0}^*, v_{c_+}^*) = -v_{c_+}^* + V_{0+}(v_{c_0}^*, \rho_{c_0}^*),$$

and use the other relations to reduce the number of unknown quantities. The function G can be written as function of $\rho_{c_-}^*$ only.

$$\begin{aligned} 0 &= G\left(\rho_{c_0}^*, v_{c_0}^*, v_{c_+}^*\right) \\ &= G\left(P_{-0}\left(\rho_{c_-}^*, W_{-}\left(\rho_{c_-}^*\right)\right), V_{-0}\left(\rho_{c_-}^*, W_{-}\left(\rho_{c_-}^*\right)\right), \dots \right. \\ &\quad \left. \dots V_{0+}\left(P_{0+}\left(P_{-0}\left(\rho_{c_-}^*, W_{-}\left(\rho_{c_-}^*\right)\right), V_{-0}\left(\rho_{c_-}^*, W_{-}\left(\rho_{c_-}^*\right)\right)\right)\right)\right) \end{aligned} \quad (4.73)$$

A solution $\rho_{c_-}^*$ of system (4.26) is now implicitly given by this equation (4.73). It is unique, if G is a strict monotone function of $\rho_{c_-}^*$. The derivative is given by

$$\begin{aligned} \frac{dG}{d\rho_{c_-}^*} &= \frac{\partial G}{\partial P_{-0}} \left(\frac{\partial P_{-0}}{\partial \rho_{c_-}^*} + \frac{P_{-0}}{\partial W_{-}} \frac{\partial W_{-}}{\partial \rho_{c_-}^*} \right) + \frac{\partial G}{\partial V_{-0}} \left(\frac{\partial V_{-0}}{\partial \rho_{c_-}^*} + \frac{\partial V_{-0}}{\partial W_{-}} \frac{\partial W_{-}}{\partial \rho_{c_-}^*} \right) \\ &\quad + \frac{\partial G}{\partial V_{0+}} \left[\frac{\partial V_{0+}}{\partial P_{0+}} \left(\frac{\partial P_{0+}}{\partial P_{-0}} \left(\frac{\partial P_{-0}}{\partial \rho_{c_-}^*} + \frac{P_{-0}}{\partial W_{-}} \frac{\partial W_{-}}{\partial \rho_{c_-}^*} \right) + \frac{\partial P_{0+}}{\partial V_{-0}} \left(\frac{\partial V_{-0}}{\partial \rho_{c_-}^*} + \frac{\partial V_{-0}}{\partial W_{-}} \frac{\partial W_{-}}{\partial \rho_{c_-}^*} \right) \right) \right]. \end{aligned} \quad (4.74)$$

We will use the following notation

$$\begin{aligned} A_{0+} &= [(1-c_0)\rho_{c_0}^* ((v_{c_0}^* - v_+)^2 + a_c^2) + d_0(c_+ - c_0)], \\ B_{0+} &= ((1-c_0)\rho_{c_0}^* ((v_{c_0}^* - v_+)^2 + a_c^2) + d_0(c_+ - c_0))^2 - 4((1-c_0)\rho_{c_0}^* (v_{c_0}^* - v_+)^2 a_c^2)^2, \\ B_{-0} &= ((1-c_-)\rho_{c_-}^* ((v_{c_-}^* - v_-)^2 + a_c^2) + d_0(c_0 - c_-))^2 - 4((1-c_-)\rho_{c_-}^* (v_{c_-}^* - v_-)^2 a_c^2)^2. \end{aligned}$$

to shorten the following expressions. We state the terms of the derivative explicitly. Compare with (4.59) - (4.65) from Section 4.4.3.

$$\frac{\partial G}{\partial V_{0+}} = -1 \quad (4.75)$$

$$\frac{\partial V_{0+}}{\partial P_{0+}} = \begin{cases} a_c \frac{P_{0+} + \rho_{c+}}{2P_{0+} \sqrt{P_{0+} \rho_{c+}}} & P_{0+} > \rho_{c+} \quad (\text{shock}) \\ a_c \frac{1}{P_{0+}} & P_{0+} \leq \rho_{c+} \quad (\text{rarefaction}) \end{cases} \quad (4.76)$$

$$\frac{\partial P_{0+}}{\partial P_{-0}} = \frac{(1-c_0)}{2(1-c_+) a_c} \left[\frac{(V_{-0} - v_+)^2 + a_c^2}{\sqrt{B_{0+}}} (A_{0+} + \sqrt{B_{0+}}) - \frac{4a_c^2 (1-c_0) P_{-0} (V_{-0} - v_+)^2}{\sqrt{B_{0+}}} \right] \quad (4.77)$$

$$\frac{P_{0+}}{\partial V_{-0}} = \frac{(1-c_0)}{2(1-c_+) a_c} \left[\frac{2P_{-0} (V_{-0} - v_+)}{\sqrt{(R)}} (A_{0+} + \sqrt{B_{0+}}) - \frac{4a_c^2 (1-c_0) (P_{-0})^2 (V_{-0} - v_+)}{\sqrt{B_{0+}}} \right] \quad (4.78)$$

$$\frac{\partial G}{\partial \rho_{c-}^*} = \frac{(-\sqrt{B_{0+}} + A_{0+}) d_0 (c_+ - c_0)}{\sqrt{B_{0+}} 2(1-c_0) (P_{-0})^2 (W_- - v_+)^2} \quad (4.79)$$

$$\frac{\partial G}{\partial V_{-0}} = \frac{-(-\sqrt{B_{0+}} + A_{0+}) ((1-c_0) P_{-0} ((V_{-0} - v_+)^2 - a_c^2) - d_0 (c_+ - c_0))}{\sqrt{B_{0+}} 2(1-c_0) \rho_{c-}^* (W_- - v_+)^2} \quad (4.80)$$

Again, we can combine some of these terms and resubstitute the quantities to get some estimates later on

$$\frac{\partial P_{-0}}{\partial \rho_{c-}^*} + \frac{P_{-0}}{\partial W_-} \frac{\partial W_-}{\partial \rho_{c-}^*} = \frac{(1-c_-)}{2(1-c_0) \sqrt{B_{-0}}} \left(a_c - (v_{c-}^* - v_-) \right) \quad (4.81)$$

$$\left((a_c - (v_{c-}^* - v_-)) (1-c_0) \rho_{c_0}^* + 2(1-c_-) \rho_{c-}^* (v_{c-}^* - v_-) \right),$$

$$\frac{\partial v_{c_0}^*}{\partial \rho_{c-}^*} + \frac{\partial v_{c_0}^*}{\partial v_{c-}^*} \frac{\partial v_{c-}^*}{\partial \rho_{c-}^*} = \frac{1}{\rho_{c-}^* \sqrt{B_{-0}}} \frac{v_{c_0}^* - v_-}{v_{c-}^* - v_-} \left((v_{c-}^* - v_-) - a_c \right) \quad (4.82)$$

$$\left(d_0 (c_0 - c_-) + a_c (1-c_-) \rho_{c-}^* \left((v_{c-}^* - v_-) - a_c \right) \right).$$

We have stated the case of the left moving acoustic wave being a rarefaction wave only. The derivatives are completely similar to the derivatives from the previous chapter. Conditions (1) - (3) from Theorem 4.4.1 are therefore sufficient to have the appropriate sign in each term. Conditions (4) and (5) are sufficient in case of a left moving shock wave.

There exists only one difficult term, namely (4.78). Due to the structure of the derivative of G we can not combine this terms directly as in the previous

chapter. Hence we need to formulate the condition

$$\frac{2\rho_{c_0}^*(v_{c_0}^* - v_+)}{\sqrt{(R)}} \left(A_{0+} + \sqrt{B_{0+}} \right) - \frac{4a_c^2 (1-c_0) (\rho_{c_0}^*)^2 (v_{c_0}^* - v_+)}{\sqrt{B_{0+}}} \stackrel{!}{<} 0. \quad (4.83)$$

Even though we are pretty sure that this condition is redundant, we cannot prove it. Therefore we formulate the result in the following form:

Theorem 4.5.1. *Any solution of system (4.26) in the case $v_- < v_+$ is implicitly given by*

$$0 = G \left(\rho_{c_0}^* \left(\rho_{c_-}^*, v_{c_-}^* \left(\rho_{c_-}^* \right) \right), v_{c_0}^* \left(\rho_{c_-}^*, v_{c_-}^* \left(\rho_{c_-}^* \right) \right), \dots \right. \\ \left. \dots v_{c_+}^* \left(\rho_{c_+}^* \left(\rho_{c_0}^* \left(\rho_{c_-}^*, v_{c_-}^* \left(\rho_{c_-}^* \right) \right), v_{c_0}^* \left(\rho_{c_-}^*, v_{c_-}^* \left(\rho_{c_-}^* \right) \right) \right) \right) \right).$$

The solution is unique if G is strictly monotone, that is

$$\frac{dG}{d\rho_{c_-}^*} \leq 0.$$

which is satisfied under the conditions (1) - (5) from Theorem 4.4.1 and (4.83) additionally.

4.6 The case $v_- > v_+$

In this case the middle wave is a delta-shock as shown in Section 4.1.4. Hence we can apply the Rankine-Hugoniot jump conditions. Together with the relations over the acoustic waves they read

$$0 = v_\delta \llbracket (1-c) \rho_c^* \rrbracket - \llbracket (1-c) \rho_c^* v_c^* \rrbracket, \\ 0 = v_\delta \llbracket (1-c) \rho_c^* v_c^* \rrbracket - \llbracket (1-c) \rho_c^* v_c^{*2} + (1-c) p_c^* \rrbracket, \\ v_{c_\pm}^* = v_{c_\pm} \pm \begin{cases} a_c \frac{\rho_{c_\pm}^* - \rho_{c_\pm}}{\sqrt{\rho_{c_\pm}^* \rho_{c_\pm}}} & \rho_{c_\pm}^* > \rho_{c_\pm} \quad (\text{shock}), \\ a_c \ln \frac{\rho_{c_\pm}^*}{\rho_{c_\pm}} & \rho_{c_\pm}^* \leq \rho_{c_\pm} \quad (\text{rarefaction}). \end{cases}$$

This is exactly the system of nonlinear equations from Section 4.4.3 with the substitution $v \rightarrow v_\delta$ only. The solution is therefore equivalent to the solution given in the previous sections with v_δ given by (4.23) instead of v .

Theorem 4.6.1. *Any solution of system (4.26) in the case $v_- > v_+$ is given by Theorem 4.4.1 with the substitution $v \rightarrow v_\delta$ in $\Delta v_{c_\pm}^* = v_{c_\pm}^* - v$.*

The wave configuration and an exact solution is depicted in Figure 4.6.

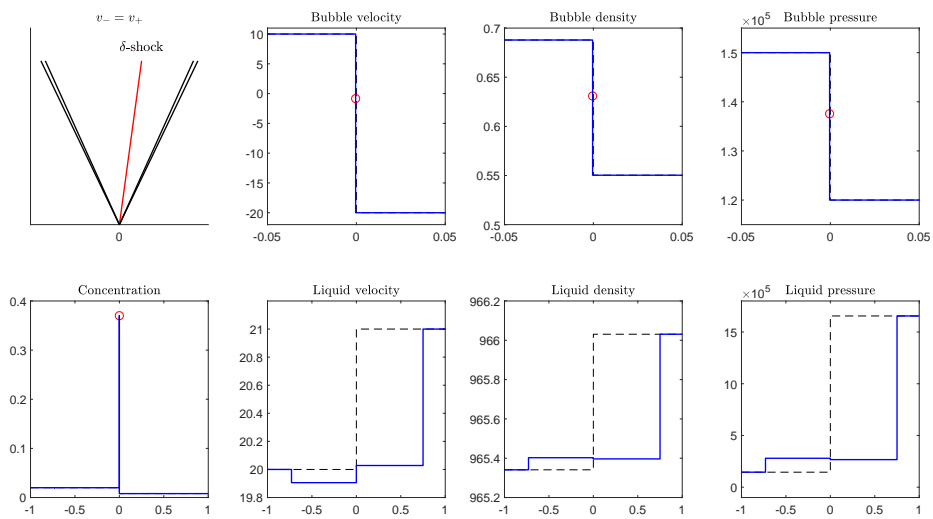


FIGURE 4.6: Initial data (dashed lines), exact solution (solid lines) and the quantities v_δ , ρ_δ , p_δ (circles) for a liquid carrier phase. The middle wave forms a δ -shock. Initial data is given by (4.42)

Numerical Concepts and Results

In this chapter, we want to show the results of some simple numerical simulations. The aim is not to give a complete introduction to the methods used but to show how well the analytical solution is approximated in a numerical simulation. This can only be done in one spatial dimension since we can not construct the analytical solution in higher dimensions. We will show numerical results for all the different cases of initial data that were discussed analytically in Chapter 4.

We assume the reader to be familiar with the basic concepts of numerics for partial differential equations, especially for hyperbolic ones. There are many very good textbook on the numerical treatment of hyperbolic conservation laws, see for example Godlewski and Raviart [30], LeVeque [52, 53], Kröner [47] or Toro [83] and the references therein.

We will start this chapter with a short summary of the finite volume methods used for the numerical simulations. Therefore, we will give a rather uncommon but very insightful introduction on finite volume methods based on a lecture given by Prof. Dr. Alina Chertock at the Oberwolfach Seminar 1948a on Structure-preserving methods for nonlinear hyperbolic problems.

5.1 The finite volume framework - Upwind and central schemes

Let us consider a system of one dimensional conservation laws

$$\frac{\partial}{\partial t} \mathbf{u} + \frac{\partial}{\partial x} \mathbf{f}(\mathbf{u}) = 0, \quad (5.1)$$

with $\mathbf{u} : \mathbb{R} \times \mathbb{R} \rightarrow \mathcal{U}$ and $\mathbf{f} : \mathcal{U} \rightarrow \mathbb{R}^m$. Here, the open set $\mathcal{U} \subseteq \mathbb{R}^m$ with $\mathbf{u} \in \mathcal{U}$ is the state space. Again, $t \in [0, t_{max}) \subseteq \mathbb{R}_{\geq 0}$ denotes the time variable and $x \in \Omega \subseteq \mathbb{R}$ the space variable. The set of unknowns $u_i : \mathbb{R} \times \mathbb{R} \rightarrow \mathbb{R}$ is called conserved quantities and the functions $f_i : \mathbb{R} \rightarrow \mathbb{R}$ the (nonlinear) fluxes. This system is subject to prescribed initial data

$$\mathbf{u}(0, x) = \mathbf{u}_0(x). \quad (5.2)$$

To get a basic understanding of the numerical concepts, one often discusses the concepts on scalar conservation laws, as we have done in the theoretical part of this work, too. At this point we want to skip a discussion of basic numerical concepts for scalar conservation laws and hope that the reader is familiar with numerical concepts for the advection equation $u_t + au_x = 0$ or Burger's equation $u_t + \frac{1}{2}(u^2)_x = 0$. Due to the nonlinearity of the flux function, the latter one is already a very good example of the difficulties appearing in the construction of suitable numerical methods.

Starting from the initial value problem (IVP) consisting of (5.1) together with (5.2) we have already seen in Chapter 3 that solutions may break down and develop such nonsmooth structures as shock waves, contact discontinuities, rarefaction waves and singular δ -shocks even when the initial data are infinitely smooth. These nonsmooth solutions are nonclassical and they are to be understood in a weak sense, that is, in the sense of distributions. We want to recall Definition 3.2.7, which reads as follows:

We say that \mathbf{u} is a weak solution of the IVP if it satisfies the following weak formulation

$$\int_0^{t_{\max}} \int_{-\infty}^{\infty} (\mathbf{u}(t, x) \cdot \boldsymbol{\phi}_t(t, x) + \mathbf{f}(\mathbf{u}(t, x)) \cdot \boldsymbol{\phi}_x(t, x)) dx dt + \int_{-\infty}^{\infty} \mathbf{u}_0(x) \cdot \boldsymbol{\phi}(0, x) dx = 0,$$

for every test function $\boldsymbol{\phi} \in [C_0^\infty([0, t_{\max}) \times \mathbb{R})]^m$.

We have also seen that weak solutions are not unique and in order to single out the unique physically relevant solution, one needs to impose certain additional criteria.

The question is now how we can find a numerical approximation of a solution of the considered IVP. Therefore we start from the system of conservation laws (5.1)

$$\frac{\partial}{\partial t} \mathbf{u} + \frac{\partial}{\partial x} \mathbf{f}(\mathbf{u}) = 0,$$

and introduce small scales in both space Δx and time Δt and integrate the system of conservation laws w.r.t. x and t over the space-time control volume $[t, t + \Delta t] \times [x - \frac{\Delta x}{2}, x + \frac{\Delta x}{2}]$, which gives

$$\int_t^{t+\Delta t} \int_{x-\frac{\Delta x}{2}}^{x+\frac{\Delta x}{2}} \mathbf{u}_\tau(\tau, \xi) d\xi d\tau + \int_t^{t+\Delta t} \int_{x-\frac{\Delta x}{2}}^{x+\frac{\Delta x}{2}} \mathbf{f}(\mathbf{u}(\tau, \xi))_{\xi} d\xi d\tau = 0.$$

Using the fundamental theorem of calculus we get

$$\begin{aligned} & \int_{x-\frac{\Delta x}{2}}^{x+\frac{\Delta x}{2}} \mathbf{u}(t+\Delta t, \xi) d\xi - \int_{x-\frac{\Delta x}{2}}^{x+\frac{\Delta x}{2}} \mathbf{u}(t, \xi) d\xi \\ & + \int_t^{t+\Delta t} \left[\mathbf{f}\left(\mathbf{u}\left(\tau, x + \frac{\Delta x}{2}\right)\right) + \mathbf{f}\left(\mathbf{u}\left(\tau, x - \frac{\Delta x}{2}\right)\right) \right] d\tau = 0. \end{aligned}$$

Rearranging these terms leads to

$$\begin{aligned} & \int_{x-\frac{\Delta x}{2}}^{x+\frac{\Delta x}{2}} \mathbf{u}(t+\Delta t, \xi) d\xi = \int_{x-\frac{\Delta x}{2}}^{x+\frac{\Delta x}{2}} \mathbf{u}(t, \xi) d\xi \\ & - \int_t^{t+\Delta t} \left[\mathbf{f}\left(\mathbf{u}\left(\tau, x + \frac{\Delta x}{2}\right)\right) + \mathbf{f}\left(\mathbf{u}\left(\tau, x - \frac{\Delta x}{2}\right)\right) \right] d\tau. \end{aligned}$$

We introduce the *sliding averages* of \mathbf{u} as

$$\bar{\mathbf{u}}(t, x) := \frac{1}{\Delta x} \int_{x-\frac{\Delta x}{2}}^{x+\frac{\Delta x}{2}} \mathbf{u}(t, \xi) d\xi \quad (5.3)$$

and divide both side of the above equation by Δx to get

$$\bar{\mathbf{u}}(t+\Delta t, x) = \bar{\mathbf{u}}(t, x) - \frac{1}{\Delta x} \int_t^{t+\Delta t} \left[\mathbf{f}\left(\mathbf{u}\left(\tau, x + \frac{\Delta x}{2}\right)\right) + \mathbf{f}\left(\mathbf{u}\left(\tau, x - \frac{\Delta x}{2}\right)\right) \right] d\tau.$$

Next, we define the averaged fluxes as

$$\hat{\mathbf{f}}(t, x) := \frac{1}{\Delta t} \int_t^{t+\Delta t} \mathbf{f}(\mathbf{u}(\tau, x)) d\tau \quad (5.4)$$

to finally obtain

$$\bar{\mathbf{u}}(t+\Delta t, x) = \bar{\mathbf{u}}(t, x) - \frac{\Delta t}{\Delta x} \left[\hat{\mathbf{f}}\left(t, x + \frac{\Delta x}{2}\right) - \hat{\mathbf{f}}\left(t, x - \frac{\Delta x}{2}\right) \right]. \quad (5.5)$$

Note that up to now, we have not discussed any numerical approximations. The relation above only uses exact averages of the analytical solution \mathbf{u} and the given flux function $\mathbf{f}(\mathbf{u})$. Although it is relatively easy to get spatially averaged values of \mathbf{u} from initial data or previous time steps, the question of how to compute time averaged fluxes is far from trivial. Furthermore, we have not specified up to now around which point x the spatial part of our control volume is centered. We will see in the following how this choice will

distinguish upwind and central schemes.

For simplicity we will consider a uniform discretization of the computational grid from now on and introduce

- a spatial grid x_j such that

$$x_{j+1} - x_j = \Delta x, \quad x_{j-\frac{1}{2}} = x_j - \Delta x/2, \quad x_{j+\frac{1}{2}} = x_j + \Delta x/2, \quad \forall j,$$

- computational cells $C_j := [x_{j-\frac{1}{2}}, x_{j+\frac{1}{2}}]$,
- for any time $t = t^n$, we also define $t^{n+1} = t^n + \Delta t$.

With this at hand, we now have to specify the space-time control volumes, which leads to the following distinction.

5.1.1 First-order upwind schemes

In this case we choose a space-time control volume $[t^n, t^{n+1}] \times [x_{j-\frac{1}{2}}, x_{j+\frac{1}{2}}]$, see Figure 5.1.

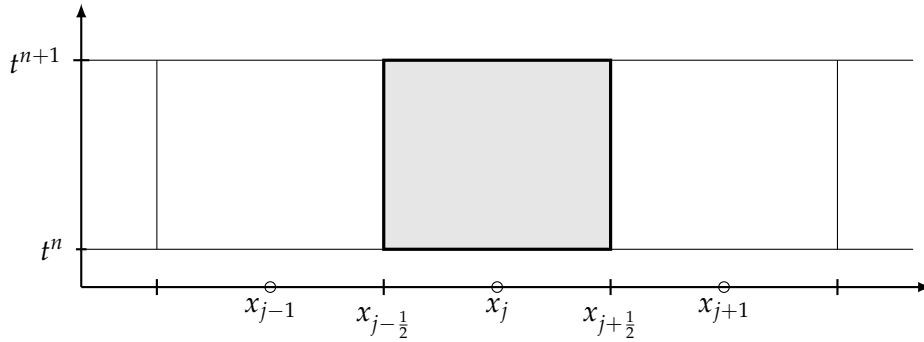


FIGURE 5.1: Space-time control volume for upwind type schemes

With this choice, the update of the conserved quantities \mathbf{u} in cell C_j reads

$$\bar{\mathbf{u}}(t^{n+1}, x_j) = \bar{\mathbf{u}}(t^n, x_j) - \frac{\Delta t}{\Delta x} \left[\hat{\mathbf{f}}(t^n, x_{j+\frac{1}{2}}) - \hat{\mathbf{f}}(t^n, x_{j-\frac{1}{2}}) \right], \quad (5.6)$$

compare to Equation (5.5). Let \mathbf{U}_j^n be an approximation of the average value of the j -th computational cell C_j at time t^n

$$\mathbf{U}_j^n \approx \bar{\mathbf{u}}(t^n, x_j) = \frac{1}{\Delta x} \int_{x_{j-\frac{1}{2}}}^{x_{j+\frac{1}{2}}} \mathbf{u}(t^n, \xi) d\xi \quad (5.7)$$

and $\mathbf{F}_{j+\frac{1}{2}}^n$ some approximation to the average flux along $x = x_{j+\frac{1}{2}}$

$$\mathbf{F}_{j+\frac{1}{2}}^n \approx \widehat{\mathbf{f}}(t^n, x_{j+\frac{1}{2}}) = \frac{1}{\Delta t} \int_{t^n}^{t^{n+1}} \mathbf{f}(\mathbf{u}(\tau, x_{j+\frac{1}{2}})) d\tau. \quad (5.8)$$

With these notations, we get numerical methods from Equation (5.6) of the form

$$\mathbf{U}_j^{n+1} = \mathbf{U}_j^n - \frac{\Delta t}{\Delta x} \left[\mathbf{F}_{j+\frac{1}{2}}^n - \mathbf{F}_{j-\frac{1}{2}}^n \right]. \quad (5.9)$$

Note that the conservation property is built into numerical schemes of this form. The change of the cell average is given by the difference in fluxes across the boundaries of the cell. The outgoing flux of one cell and the incoming flux of the neighboring cell are identical due to the definition of the fluxes, see (5.8).

A generic first-order upwind scheme then reads as follows

- Assume that the numerical solution is given in terms of its cell averages at time $t = t^n$

$$\mathbf{U}_j^n \approx \frac{1}{\Delta x} \int_{C_j} \mathbf{u}(t^n, x) dx, \quad C_j := [x_{j-\frac{1}{2}}, x_{j+\frac{1}{2}}], \quad \forall j. \quad (5.10)$$

- Compute the numerical fluxes

$$\mathbf{F}_{j+\frac{1}{2}}^n \approx \frac{1}{\Delta t} \int_{t^n}^{t^{n+1}} \mathbf{f}(\mathbf{u}(\tau, x_{j+\frac{1}{2}})) d\tau, \quad \forall j. \quad (5.11)$$

- Update the cell averages according to the numerical scheme (5.9)

$$\mathbf{U}_j^{n+1} = \mathbf{U}_j^n - \frac{\Delta t}{\Delta x} \left[\mathbf{F}_{j+\frac{1}{2}}^n - \mathbf{F}_{j-\frac{1}{2}}^n \right]. \quad (5.12)$$

Note, that the last step can be interpreted as a representation of a semi-discrete form

$$\frac{d}{dt} \mathbf{U}_j(t) = - \frac{\mathbf{F}_{j+\frac{1}{2}}(t) - \mathbf{F}_{j-\frac{1}{2}}(t)}{\Delta x}, \quad (5.13)$$

which allows the usage a Runge-Kutta type solver for the time stepping. This is in contrast to the central schemes as we will see later. The problem of the algorithm presented is the determination of exact or approximated fluxes in the second step. The first finite-volume upwind scheme with an ingenious idea to determine fluxes was proposed by Godunov in 1959 [31].

5.1.2 The Godunov method

Even if most people working on hyperbolic PDEs today are very familiar with Godunov's method, it was quite revolutionary at the time it was invented. During the International Conference "Mathematics and its Applications" in honor of the 90th birthday of Sergei K. Godunov, Godunov himself told the story of how he could barely convince the members of his PhD commission, containing for example Sergei L. Sobolev, of his idea to solve a PDE without any conventional approximation of the derivatives. But today, many finite-volume methods are based on Godunov's ideas. It became one of the most important building blocks of numerical schemes. We will also use a Godunov-type numerical method for the system of conservation laws considered in this thesis.

The question at hand is still how to get an approximation for the intercell boundary fluxes

$$\mathbf{F}_{j+\frac{1}{2}}^n \approx \frac{1}{\Delta t} \int_{t^n}^{t^{n+1}} \mathbf{f}(\mathbf{u}(\tau, x_{j+\frac{1}{2}})) d\tau. \quad (5.14)$$

Note, that the fluxes $\mathbf{f}(\mathbf{u}(t, x_{j+\frac{1}{2}}))$ may vary along the integration interval. But Godunov observed, that the cell averages \mathbf{U}_j^n are constant in each cell C_j at each time level t^n and therefore form a Riemann problem at each cell interface $x_{j+\frac{1}{2}}$

$$\begin{aligned} \mathbf{u}_t + \mathbf{f}(\mathbf{u})_x &= 0 \\ \mathbf{u}(t^n, x) &= \tilde{\mathbf{U}}_j^n(x) = \begin{cases} \mathbf{U}_j^n, & x < x_{j+\frac{1}{2}} \\ \mathbf{U}_{j+1}^n, & x > x_{j+\frac{1}{2}}. \end{cases} \end{aligned} \quad (5.15)$$

This Riemann problem, which we will call RP $(\mathbf{U}_j^n, \mathbf{U}_{j+1}^n)$, can then be solved analytically in terms of elementary waves emanating from each intercell interface. See Chapter 3 for an introduction to the analytical solution of Riemann problems for scalar and systems of conservation laws.

The Riemann problem RP $(\mathbf{U}_j^n, \mathbf{U}_{j+1}^n)$ centered at $x_{j+\frac{1}{2}}$ has a self-similar solution $\mathbf{U}_{j+\frac{1}{2}}^*$ which is constant along rays $(x - x_{j+\frac{1}{2}})/(t - t^n)$

$$\mathbf{U}_{j+\frac{1}{2}}^*(t, x) = \mathbf{U}_{j+\frac{1}{2}}^* \left(\frac{x - x_{j+\frac{1}{2}}}{t - t^n} \right), \quad \xi = \frac{x - x_{j+\frac{1}{2}}}{t - t^n}.$$

Since we are interested in the flux along the vertical line at $x = x_{j+\frac{1}{2}}$ we only need the solution of the Riemann problem along $(x - x_{j+\frac{1}{2}})/(t - t^n) = 0$. Therefore we can approximate the analytical solution by the constant solution of the Riemann problem (5.15)

$$\mathbf{u} \left(t, x_{j+\frac{1}{2}} \right) \approx \mathbf{U}_{j+\frac{1}{2}}^* \left(t, x_{j+\frac{1}{2}} \right) = \mathbf{U}_{j+\frac{1}{2}}^* \left(\frac{x_{j+\frac{1}{2}} - x_{j+\frac{1}{2}}}{t - t^n} \right) \equiv \mathbf{U}_{j+\frac{1}{2}}^*(0).$$

At this interface the flux can then be calculated using this constant value

$$\mathbf{F}_{j+\frac{1}{2}}^n = \frac{1}{\Delta t} \int_{t^n}^{t^{n+1}} \mathbf{f} \left(\mathbf{U}_{j+\frac{1}{2}}^*(0) \right) dt = \mathbf{f} \left(\mathbf{U}_{j+\frac{1}{2}}^*(0) \right), \quad \forall j.$$

That is, one has to evaluate the flux function at the so called *Godunov state* $\mathbf{U}_{j+\frac{1}{2}}^*(0)$ at each intercell boundary.

Regarding the size of time steps, one also has to impose a restriction. Waves from neighboring Riemann problems can intersect after some time, which is depicted in Figure 5.2. However, each wave has a finite speed

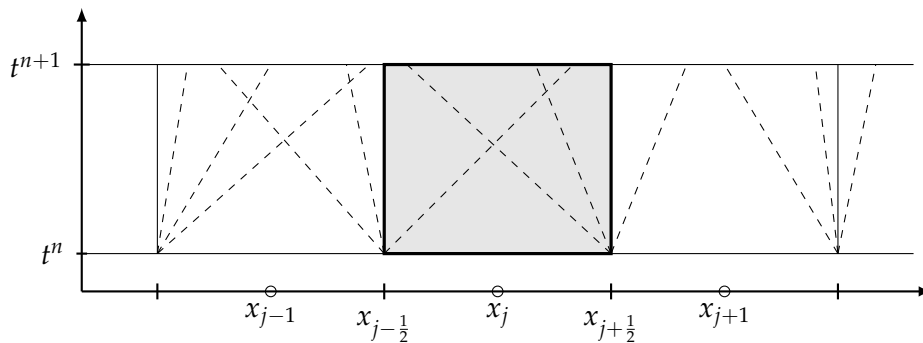


FIGURE 5.2: Waves emanating from intercell Riemann problems

of propagation and the maximum wave speed of any Riemann problem is bounded by

$$\max_{i,j} \left| \lambda_i \left(\mathbf{U}_j^n \right) \right|,$$

where the $\lambda_i(\mathbf{u})$ are the Eigenvalues of the Jacobian of the flux vector $\mathbf{A}(\mathbf{u}) = \mathbf{Df}(\mathbf{u})$. Hence, imposing the so-called CFL condition

$$\max_{i,j} \left| \lambda_i \left(\mathbf{U}_j^n \right) \right| \frac{\Delta t}{\Delta x} \leq \frac{1}{2} \quad (5.16)$$

ensures that waves from neighboring Riemann problems do not interact before reaching the next time level. Note that the bound $\frac{1}{2}$ may be replaced by 1 and the Godunov state is not altered by waves emanating from neighboring Riemann problems. The condition (5.16) with a bound of 1 is named after Richard Courant, Kurt Friedrichs and Hans Lewy, who first introduced this condition in 1928, see [12]. The dimensionless number

$$C_{CFL} = \max_{i,j} \left| \lambda_i \left(\mathbf{U}_j^n \right) \right| \frac{\Delta t}{\Delta x} \quad (5.17)$$

is called the *Courant number*. From linear stability analysis for explicit time stepping one gets the restriction $C_{CFL} \leq 1$.

Even though the Godunov scheme has many desirable properties like the conservation property, it possesses a few problems, too.

The only information needed to determine the numerical fluxes is the value of the fluxes at the cell interfaces. Solving the entire Riemann problem on each interface seems unnecessary. Furthermore, this relies on the availability of an explicit formula for the solution of the Riemann problem. We have such formulas at hand in the case of scalar conservation laws or linear systems of conservation laws. However, more complicated systems of conservation laws may not yield such formulas. Even in the scalar case for complicated flux functions with a large number of extremal points, one may need to solve an optimization problem. Such a problem might be computationally very costly.

Therefore, the numerical fluxes are determined from approximate solutions to Riemann problems at intercell boundaries in many cases. Methods derived in this way include the Roe solver, the Osher scheme, the HLL solver, as well as the HLLC solver. We will only comment shortly on the Roe scheme in the following subsection to show the basic idea and on the HLL approaches later on.

5.1.3 The Roe scheme

This scheme is a standard method for solving nonlinear equations. The basic idea is just to linearize them, see Roe [71]. For simplicity, we will present the method for a scalar conservation law

$$u_t + f(u)_x = 0 \quad \Rightarrow \quad u_t + f'(u)u_x = 0 \quad \Rightarrow \quad \hat{A}(u) \approx f'(u).$$

Here, $\hat{A}(u)$ is a constant state around which the nonlinear flux function is linearized. There are different choices, for example

$$\hat{A}_{j+\frac{1}{2}}^n = f' \left(\frac{U_j^n + U_{j+1}^n}{2} \right) \quad \text{or} \quad \hat{A}_{j+\frac{1}{2}}^n = \begin{cases} \frac{f(U_{j+1}^n) - f(U_j^n)}{U_{j+1}^n - U_j^n}, & U_j^n \neq U_{j+1}^n, \\ f'(U_j^n), & U_j^n = U_{j+1}^n. \end{cases}$$

Then, solving the linear Riemann problem

$$\begin{aligned} u_t + \hat{A}_{j+\frac{1}{2}}^n u_x &= 0, \\ u(x, t^n) &= \begin{cases} U_j^n, & x < x_{j+\frac{1}{2}}, \\ U_{j+1}^n, & x > x_{j+\frac{1}{2}}, \end{cases} \end{aligned}$$

becomes very easy. The solution is given by the solution of the advection equation, so it depends only on the velocity $\hat{A}_{j+\frac{1}{2}}^n$. It reads

$$F_{j+\frac{1}{2}}^n = F^{\text{Roe}}(U_j^n, U_{j+1}^n) = \begin{cases} f(U_j^n), & \hat{A}_{j+\frac{1}{2}}^n \geq 0, \\ f(U_{j+1}^n), & \hat{A}_{j+\frac{1}{2}}^n < 0. \end{cases} \quad (5.18)$$

In the case of systems of conservation laws, the linearization is given by the well known Roe matrix. The solution depends then on the eigenstructure of this matrix. Since for the system considered in this work an eigenvector is missing, we can not use this idea. Most of the time we will use the HLL approximate Riemann solver presented in the next section.

5.1.4 First-order central schemes

The starting point for the first-order central scheme is exactly the same finite volume evolution equation as in the case of upwind schemes, namely Equation (5.5)

$$\bar{\mathbf{u}}(t + \Delta t, x) = \bar{\mathbf{u}}(t, x) - \frac{\Delta t}{\Delta x} \left[\hat{\mathbf{f}} \left(t, x + \frac{\Delta x}{2} \right) - \hat{\mathbf{f}} \left(t, x - \frac{\Delta x}{2} \right) \right],$$

but now evaluated at the set of points $(t^n, x_{j+\frac{1}{2}})$ instead of (t^n, x_j) . In comparison to the upwind scheme the control volumes will be shifted by $\Delta x/2$ and now are $[t^n, t^{n+1}] \times [x_j, x_{j+1}]$, see Figure 5.3. Note, that while the data at

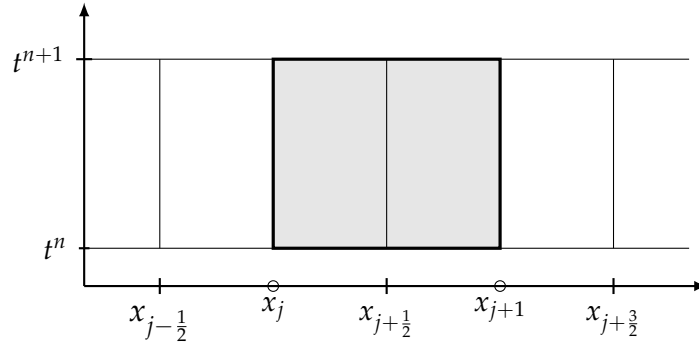


FIGURE 5.3: Space time control volume for central schemes

$t = t^n$ are given on the original grid $[x_{j-\frac{1}{2}}, x_{j+\frac{1}{2}}]$ the new computed solution will be obtained over the staggered grid $[x_j, x_{j+1}]$.

Using the central space time control volume for the numerical update, we get

$$\mathbf{U}_{j+\frac{1}{2}}^{n+1} = \frac{1}{\Delta x} \int_{x_j}^{x_{j+1}} \tilde{\mathbf{U}}_j^n(x) dx - \frac{1}{\Delta x} \int_{t^n}^{t^{n+1}} [\mathbf{f}(\mathbf{u}(t, x_{j+1})) - \mathbf{f}(\mathbf{u}(t, x_j))] dt. \quad (5.19)$$

Here $\tilde{\mathbf{U}}_j^n(x)$ is a piecewise constant function built from the given cell averages at time $t = t^n$. But both integrals in (5.19) can be calculated straight forward. The space integral can be exactly evaluated, since the $\tilde{\mathbf{U}}_j^n(x)$ is a piecewise constant function

$$\tilde{\mathbf{U}}_j^n(x) = \begin{cases} \mathbf{U}_j^n, & x \in [x_j, x_{j+\frac{1}{2}}), \\ \mathbf{U}_{j+1}^n, & x \in [x_{j+\frac{1}{2}}, x_{j+1}]. \end{cases}$$

Therefore we get

$$\frac{1}{\Delta x} \int_{x_j}^{x_{j+1}} \tilde{\mathbf{U}}_j^n(x) dx = \frac{\mathbf{U}_{j+1}^n + \mathbf{U}_j^n}{2}.$$

As long as a proper CFL condition is chosen, no waves generated at the cell interface can reach the vertical segments of the control volume. The solution then remains constant at the interfaces $x = x_j$. The time integral therefore

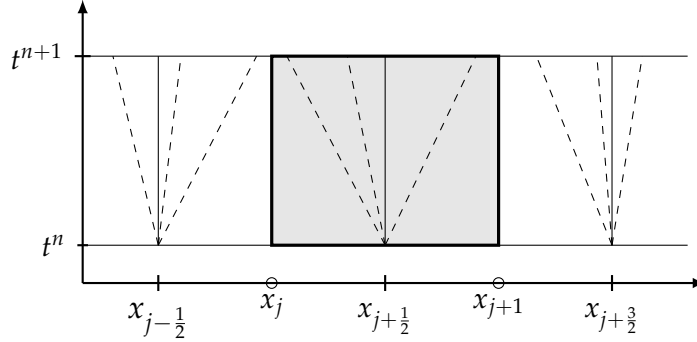


FIGURE 5.4: Waves emanating from intercell Riemann problems in the case of central schemes

becomes

$$\int_{t^n}^{t^{n+1}} [\mathbf{f}(\mathbf{u}(t, x_{j+1})) - \mathbf{f}(\mathbf{u}(t, x_j))] dt = \Delta t [\mathbf{f}(\mathbf{U}_{j+1}^n) - \mathbf{f}(\mathbf{U}_j^n)].$$

Inserting these results into Equation (5.19) leads to

$$\mathbf{U}_{j+\frac{1}{2}}^{n+1} = \frac{\mathbf{U}_{j+1}^n + \mathbf{U}_j^n}{2} - \frac{\Delta t}{\Delta x} [\mathbf{f}(\mathbf{U}_{j+1}^n) - \mathbf{f}(\mathbf{U}_j^n)].$$

But this is nothing else than the staggered Lax-Friedrichs scheme. Averaging this result over the cells $[x_{j-\frac{1}{2}}, x_{j+\frac{1}{2}}]$ gives the Lax-Friedrichs scheme in its typical form

$$\mathbf{U}_j^{n+1} = \mathbf{U}_j^n - \frac{\Delta t}{\Delta x} [\mathbf{F}_{j+\frac{1}{2}}^n - \mathbf{F}_{j-\frac{1}{2}}^n], \quad (5.20)$$

with the Lax-Friedrichs flux

$$\mathbf{F}_{j+\frac{1}{2}}^n = \mathbf{F}^{\text{LxF}}(\mathbf{U}_j^n, \mathbf{U}_{j+1}^n) = \frac{\mathbf{f}(\mathbf{U}_j^n) + \mathbf{f}(\mathbf{U}_{j+1}^n)}{2} - \frac{\Delta x}{2\Delta t} (\mathbf{U}_{j+1}^n - \mathbf{U}_j^n). \quad (5.21)$$

Due to the fact that no Riemann problem has to be solved, this is an extremely simple and universal tool for solving hyperbolic systems of conservation laws. On the other hand, this scheme has excessive numerical diffusion. It is not well suited for resolving shock waves or contact discontinuities. Due to that reason, we will use an upwind-type Godunov method for

our numerical simulations.

One can also improve the Lax-Friedrichs scheme to have less numerical diffusion. For example, one can replace the global value $\Delta x/\Delta t$ by a local approximation of the fastest wave speed $\lambda_{\max}(\mathbf{U}_j^n)$, which leads then to the local Lax-Friedrichs method or Rusanov's method. There are also entirely different choices for the numerical fluxes like the Engquist-Osher flux. We do not want to present any details of these methods here and refer the reader to the literature on numerical methods for conservation laws mentioned before.

Furthermore, these types of numerical schemes also lack a semi-discrete version. This makes the construction of higher-order methods complicated as one would like to do a high order reconstruction in space and a high order Runge-Kutta type method for the time stepping.

5.1.5 First-order finite volume schemes - Summary

A general first-order finite volume scheme can be summarized in the following three steps. Assume for a time $t = t^n$ we have given cell averages \mathbf{U}_j^n on the grid cells C_j

$$t = t^n : \quad \mathbf{U}_j^n \approx \frac{1}{\Delta x} \int_{C_j} \mathbf{u}(t^n, x) dx, \quad C_j := \left[x_{j-\frac{1}{2}}, x_{j+\frac{1}{2}} \right], \quad \forall j.$$

- **Reconstruct** the global approximate solution $\tilde{\mathbf{U}}_j^n(x)$ from the given cell averages
- **Evolve** the reconstructed function in time using either an exact or approximate solution algorithm.
 - For **upwind schemes** solve the Riemann problems

$$\mathbf{u}_t + \mathbf{f}(\mathbf{u})_x = 0, \quad \mathbf{u}(t^n, x) = \tilde{\mathbf{U}}_j^n(x), \quad \forall j, \quad (5.22)$$

either exact or with an approximate Riemann solver.

- For **central schemes** compute the shifted averages

$$\mathbf{U}_{j+\frac{1}{2}}^{n+1} = \frac{1}{\Delta x} \int_{x_j}^{x_{j+1}} \tilde{\mathbf{U}}_j^n(x) dx - \frac{1}{\Delta x} \int_{t^n}^{t^{n+1}} [\mathbf{f}(\mathbf{u}(t, x_{j+1})) - \mathbf{f}(\mathbf{u}(t, x_j))] dt.$$

- **Average** the solution at the next time level $t = t^{n+1}$ over each cell C_j .

These steps can then be repeated one after another to advance a certain number of time steps. As long as the reconstructed solution $\tilde{\mathbf{U}}_j^n(x)$ is a piecewise constant function built from the cell averages, these schemes are only first-order schemes. We will comment on higher-order schemes in the following subsection.

There are also central-upwind schemes that combine both of the above ideas. These methods are then Godunov-type finite volume methods that do not require solving Riemann problems at each cell interface. They also work in the three steps presented above, that is, reconstruction, evolution and averaging (REA). The key idea is to select space-time control volumes in the evolution step adaptively depending on the size of Riemann fans generated at each cell interface. We refer the interested reader to Kurganov and Tadmor [49] or Kurganov, Noelle and Petrova [48].

5.1.6 Second-order finite volume methods

The idea of improving the aforementioned algorithm is straightforward. The piecewise constant functions only lead to a first-order method. Therefore in the reconstruction step, the piecewise constant function is replaced by a piecewise linear function. To achieve a second-order approximation in space, we reconstruct the global piecewise linear solution $\tilde{\mathbf{U}}_j^n(x)$ in the first step of the REA algorithm

$$\tilde{\mathbf{U}}_j^n(x) = \mathbf{U}_j^n + \sigma_j^n (x - x_j), \quad \forall x \in C_j, \quad (5.23)$$

where \mathbf{U}_j^n is the cell average of the solution at time step n on the grid cell C_j and σ_j^n an appropriate slope. To achieve a higher-order spatial approximation, one has to choose the order of the reconstruction polynomial accordingly. The following steps of the REA algorithm, namely the evolution and averaging steps, are then carried out almost as before in the first-order case, see (5.22).

Note that the conservation property of the Godunov method is still valid since we have

$$\frac{1}{\Delta x} \int_{x_{j-\frac{1}{2}}}^{x_{j+\frac{1}{2}}} \tilde{\mathbf{U}}_j^n(x) dx = \mathbf{U}_j^n.$$

The slopes in a second-order reconstruction can be chosen in different ways, for example the central slopes

$$\sigma_j^n = \frac{\mathbf{U}_{j+1}^n - \mathbf{U}_{j-1}^n}{2\Delta x}, \quad (5.24)$$

backward slopes

$$\sigma_j^n = \frac{\mathbf{U}_j^n - \mathbf{U}_{j-1}^n}{\Delta x}, \quad (5.25)$$

or forward slopes

$$\sigma_j^n = \frac{\mathbf{U}_{j+1}^n - \mathbf{U}_j^n}{\Delta x}. \quad (5.26)$$

Independently of the choice of slopes, such a method will produce oscillations near discontinuities or sharp gradients of the solution. That is due to

Godunov's Theorem, which states that a monotone and linear scheme will be at most of first-order, see [31].

To avoid generating spurious oscillations, nonlinear solution-adaptive schemes must be constructed, which lead to so called *Total Variation Diminishing* (TVD) Methods. There are many different approaches to get rid of spurious oscillations. One well established approach is the usage of flux limiters like the *MINBEE* or *SUPERBEE* limiters. Other ideas include the *ENO* (Essentially Non-Oscillatory) and *WENO* (Weighted Essentially Non-Oscillatory) reconstructions by Harten, Engquist, Osher [38] and Liu, Osher, Chan [61], respectively.

Giving a comprehensive overview of this very active field of research is not possible within the scope of this work. We will comment on the methods used for this work in the next section.

Having achieved a second- or higher-order spatial reconstruction with an appropriate order of the reconstruction polynomial, one has to achieve a high-order approximation in time as well. Otherwise, the method constructed is not truly of high order. By integrating the conservation law over space

$$\frac{1}{\Delta x} \int_{x_{j-\frac{1}{2}}}^{x_{j+\frac{1}{2}}} [\mathbf{u}_t + \mathbf{f}(\mathbf{u})_x] dx = 0$$

one gets the semi-discrete formulation

$$\frac{d}{dt} \bar{\mathbf{u}}(t, x_j) + \frac{\mathbf{f}(\mathbf{u}(t, x_{j+\frac{1}{2}}^-)) - \mathbf{f}(\mathbf{u}(t, x_{j-\frac{1}{2}}^+))}{\Delta x} = 0,$$

where we have used $\mathbf{u}(t, x_{j+\frac{1}{2}}^-)$ and $\mathbf{u}(t, x_{j-\frac{1}{2}}^+)$ to indicate the one-sided limits of \mathbf{u} at the cell boundaries of cell j . Again, let $\mathbf{U}_j(t)$ be an approximation of the average value of the j -th computational cell C_j at time t and $\mathbf{F}_{j+\frac{1}{2}}(t)$ some numerical flux, that is

$$\mathbf{U}_j(t) \approx \bar{\mathbf{u}}(t, x_j) \quad \text{and} \quad \mathbf{F}_{j+\frac{1}{2}}(t) \approx \mathbf{f}(t, x_{j+\frac{1}{2}}^-).$$

Then the evolution step of the REA algorithm reads

$$\frac{d}{dt} \mathbf{U}_j(t) + \frac{\mathbf{F}_{j+\frac{1}{2}}(t) - \mathbf{F}_{j-\frac{1}{2}}(t)}{\Delta x} = 0,$$

compare to (5.13), where we mentioned the semi-discrete formulation before. This can be rewritten in the following form

$$\frac{d}{dt} \mathbf{U}_j(t) = \mathcal{L}(\mathbf{U}_j(t)). \tag{5.27}$$

The operator \mathcal{L} acts on the vector $\mathbf{U}_j(t)$ as

$$\mathcal{L}(\mathbf{U}_j(t)) := -\frac{\mathbf{F}_{j+\frac{1}{2}}(t) - \mathbf{F}_{j-\frac{1}{2}}(t)}{\Delta x}. \quad (5.28)$$

To achieve a fully high-order method in combination with the high-order spatial reconstruction, one has to solve this ODE-system with a stable ODE solver of an appropriate order, for example a Runge-Kutta type solver. Nonetheless, these semi-discrete methods have a disadvantage when used for hyperbolic conservation laws. We will comment on this later. So instead, we will use a fully discrete method for the simulations presented in this work, which we will describe in the following section.

5.2 The MUSCL Method

This section is based on the presentation of the MUSCL method given in Toro [83, Chapter 13/14]. We will only give a sufficiently brief overview of the methods used for an understanding of the results presented later. We would like to refer the reader to the book of Toro and the references therein for further reading.

The idea of improving the first-order Godunov method by replacing the piecewise constant function with a higher-order polynomial goes back to a series of papers by van Leer, see e.g. [85]. MUSCL stands for Monotone Upstream-centered Scheme for Conservation Laws. It is possible to construct high-order methods of fully discrete, semi-discrete and also implicit types. In the last section, we have already seen how one can construct a semi-implicit second-order MUSCL method.

We will start again from the reconstruction step of the REA algorithm and show in which way we implemented the MUSCL idea in a fully discrete manner. We will limit ourselves to the construction of a second-order method. In abuse of notation but in accordance to Toro [83] we will call the Δ_j slope vectors even if they are actually differences of \mathbf{U}_j^n . We choose them according to

$$\Delta_j = \frac{1}{2}(1 + \omega)\Delta_{j-\frac{1}{2}} + \frac{1}{2}(1 - \omega)\Delta_{j+\frac{1}{2}}, \quad (5.29)$$

where the differences are given by

$$\Delta_{j-\frac{1}{2}} = \mathbf{U}_j^n - \mathbf{U}_{j-1}^n, \quad \Delta_{j+\frac{1}{2}} = \mathbf{U}_{j+1}^n - \mathbf{U}_j^n. \quad (5.30)$$

Here, $\omega \in [-1, 1]$ is a parameter and can be chosen freely. Note, that for $\omega = 0$ we acquire the central slopes, for $\omega = 1$ the backward slopes and for $\omega = -1$ the forward slopes, respectively, compare to (5.24), (5.25) and (5.26).

The replacement of the piecewise constant function $\tilde{\mathbf{U}}_j^n(x)$ with a piecewise linear one is done in the following way

$$\tilde{\mathbf{U}}_j^n(x) = \mathbf{U}_j^n + \frac{(x - x_j)}{\Delta x} \Delta_j, \quad \forall x \in C_j = [x_{j-\frac{1}{2}}, x_{j+\frac{1}{2}}], \quad (5.31)$$

where the slope σ_j^n is given by $\sigma_j^n = \frac{\Delta_j}{\Delta x}$.

Again, one can see immediately that the integral of $\tilde{\mathbf{U}}_j^n(x)$ and \mathbf{U}_j^n over C_j are identical and therefore the conservation property holds. Also, higher orders of the reconstruction are possible.

By modifying the data in the reconstruction step, we no longer have ordinary Riemann problems at each cell interface. Instead, we get a so called *generalized Riemann problem* (GRP)

$$\begin{aligned} \mathbf{u}_t + \mathbf{f}(\mathbf{u})_x &= 0 \\ \mathbf{u}(t^n, x) &= \begin{cases} \tilde{\mathbf{U}}_j^n(x), & x < x_{j+\frac{1}{2}} \\ \tilde{\mathbf{U}}_{j+1}^n(x), & x > x_{j+\frac{1}{2}} \end{cases} \end{aligned} \quad (5.32)$$

From this GRP we have to determine the flux $\mathbf{F}_{j+\frac{1}{2}}(t)$ on the cell interface. Note that the calculation of a Godunov state $\mathbf{U}_{j+\frac{1}{2}}^*(0)$ may not be feasible, since for a GRP the wave curves do not have to be straight lines separated by constant states as in the case of a classical Riemann problem. We will not present any details of the solution of generalized Riemann problems. A MUSCLE-type scheme based on the solution of GRPs was developed by Ben–Artzi and Falcovitz, see [4]. Since the solution of the GRP is very complicated for nonlinear systems, we will rely on a different method. There are many different schemes based on the MUSCLE reconstruction idea, including other fully discrete methods like the Piecewise Linear Method (PLM) by Colella [11], the Eno/Weno reconstructions as semi-discrete methods or implicit methods, see Yee et al. [91].

5.2.1 The MUSCL-Hancock method

We will now present the method used in all simulations if not stated otherwise. The name MUSCL-Hancock method goes back to van Leer [86], who gave the name due to private communications with Hancock.

The method itself consists of three steps very similar to the first order REA algorithm.

- **Reconstruction** of the local approximate solution $\tilde{\mathbf{U}}_j^n(x)$ from the given cell averages

$$\tilde{\mathbf{U}}_j^n(x) = \mathbf{U}_j^n + \frac{(x - x_j)}{\Delta x} \Delta_j, \quad \forall x \in C_j, \quad (5.33)$$

where Δ_j is the slope vector given by (5.29). From this reconstruction we calculate the values of $\tilde{\mathbf{U}}_j^n(x)$ on the cell boundary. They are given by

$$\mathbf{U}_j^- = \mathbf{U}_j^n - \frac{1}{2} \Delta_j, \quad \mathbf{U}_j^+ = \mathbf{U}_j^n + \frac{1}{2} \Delta_j \quad (5.34)$$

and called *boundary extrapolated values*.

- **Evolution** of the boundary extrapolated values \mathbf{U}_j^- and \mathbf{U}_j^+ , see (5.34), in each cell C_j to an intermediate time level $t^{n+\frac{1}{2}} = t^n + \frac{1}{2}\Delta t$ using the numerical flux function

$$\begin{aligned}\bar{\mathbf{U}}_j^- &= \mathbf{U}_j^- + \frac{1}{2} \frac{\Delta t}{\Delta x} \left[\mathbf{F}(\mathbf{U}_j^-) - \mathbf{F}(\mathbf{U}_j^+) \right], \\ \bar{\mathbf{U}}_j^+ &= \mathbf{U}_j^+ + \frac{1}{2} \frac{\Delta t}{\Delta x} \left[\mathbf{F}(\mathbf{U}_j^-) - \mathbf{F}(\mathbf{U}_j^+) \right].\end{aligned}\quad (5.35)$$

In obtaining these values, the interaction between cells is ignored entirely. The evolution of these values is fully contained in the cell C_j . To achieve a second-order method with this form of the evolution step leads to a drastic simplification compared to other methods mentioned in the last subsection and goes back to Hancock, see [86].

Note, that there is no longer a single value for the flux at the intercell boundary as before in the first-order algorithm. At the intercell boundary there are now two genuinely distinct fluxes, namely $\mathbf{F}(\mathbf{U}_j^+)$ and $\mathbf{F}(\mathbf{U}_{j+1}^-)$.

- **Solution** of the Riemann problem. One can solve now the conventional Riemann problem with the evolved boundary extrapolated values given by (5.35) as constant initial datum

$$\begin{aligned}\mathbf{u}_t + \mathbf{f}(\mathbf{u})_x &= 0 \\ \mathbf{u}(t^n, x) &= \begin{cases} \bar{\mathbf{U}}_j^+, & x < x_{j+\frac{1}{2}} \\ \bar{\mathbf{U}}_{j+1}^-, & x > x_{j+\frac{1}{2}}. \end{cases}\end{aligned}\quad (5.36)$$

The intercell flux can then be determined exactly as in the first order algorithm by solving the Riemann problem exactly

$$\mathbf{F}_{j+\frac{1}{2}}^n = \mathbf{f}\left(\mathbf{U}_{j+\frac{1}{2}}^*(0)\right).$$

Since we do not have an explicit solution to the Riemann problem of the system under consideration in this work, we will use an approximate Riemann solver in this step, which is shown in the next section.

- **Update** the cell averages with the first-order upwind formula

$$\mathbf{U}_j^{n+1} = \mathbf{U}_j^n - \frac{\Delta t}{\Delta x} \left[\mathbf{F}_{j+\frac{1}{2}}^n - \mathbf{F}_{j-\frac{1}{2}}^n \right].\quad (5.37)$$

We already mentioned Godunov's theorem, that there are no monotone and linear schemes higher than first order. The scheme resulting from the above steps will be of second order accuracy and linear, but it will also produce spurious oscillations and is therefore not monotone. Since we want to keep the monotonicity property, we have to make the scheme nonlinear to keep a

higher order of approximation. Therefore, we will use the following nonlinear limiters of the slopes in the reconstruction step of the algorithm

$$\bar{\Delta}_j = \begin{cases} \max \left[0, \min \left(\beta \Delta_{j-\frac{1}{2}}, \Delta_{j+\frac{1}{2}} \right), \min \left(\Delta_{j-\frac{1}{2}}, \beta \Delta_{j+\frac{1}{2}} \right) \right], & \Delta_{j+\frac{1}{2}} > 0 \\ \min \left[0, \max \left(\beta \Delta_{j-\frac{1}{2}}, \Delta_{j+\frac{1}{2}} \right), \max \left(\Delta_{j-\frac{1}{2}}, \beta \Delta_{j+\frac{1}{2}} \right) \right], & \Delta_{j+\frac{1}{2}} < 0 \end{cases}, \quad (5.38)$$

where the max and min functions are to be understood as componentwise operations on the slope vector. The parameter β can be chosen freely. If not stated otherwise, we will use the value $\beta = 1$ which corresponds to the MINMOD or MINBEE limiter.

5.3 The HLL and HLLC approximate Riemann solvers

The idea for these approximate Riemann solvers goes back to Harten, Lax and van Leer [39]. We will give a brief overview of the derivation of these Riemann solvers following Toro [83, Chapter 10].

The main idea of the HLL solver is the assumption that the wave structure consists out of only two waves separating three constant states. These waves travel with the fastest and slowest signal speed s_+ and s_- . All other waves are ignored and the intermediate states are lumped into one single state in the $*$ -region. Therefore, this solver can be accurate only for hyperbolic systems of two equations and are definitely an approximation in our case.

We will consider a control volume $V = [0, t_c] \times [x_L, x_R]$ including the whole wave pattern of one Riemann problem emanating from the origin, that is

$$x_L \leq t_c s_-, \quad x_R \geq t_c s_+.$$

The situation is depicted in Figure 5.5.

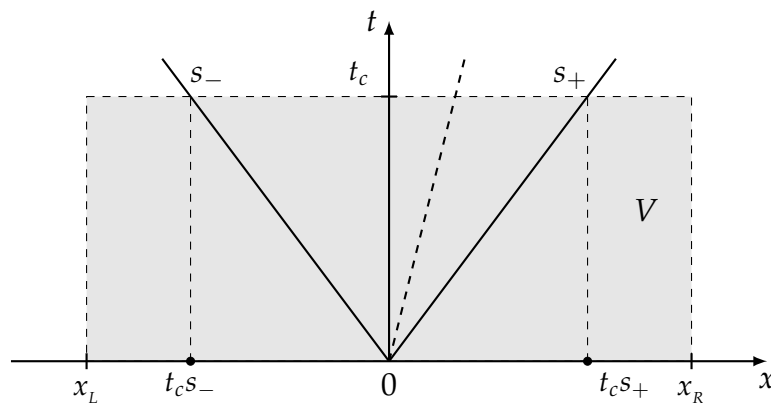


FIGURE 5.5: Control volume $V = [0, t_c] \times [x_L, x_R]$ with the Riemann problem emanating from the origin and the fastest signal speeds s_- and s_+ .

In analogy to Section 3.1.4 and 3.1.5, we will integrate the system of conservation laws with Riemann initial data

$$\begin{aligned} \mathbf{u}_t + \mathbf{f}_x(\mathbf{u}) &= 0 \\ \mathbf{u}(0, \mathbf{x}) &= \begin{cases} \mathbf{u}_- & \text{for } x < 0 \\ \mathbf{u}_+ & \text{for } x > 0, \end{cases} \end{aligned} \quad (5.39)$$

over the given control volume and get

$$\int_{x_L}^{x_R} \mathbf{u}(t_c, x) dx = \int_{x_L}^{x_R} \mathbf{u}(0, x) dx + \int_0^{t_c} \mathbf{f}(\mathbf{u}(t, x_L)) dt - \int_0^{t_c} \mathbf{f}(\mathbf{u}(t, x_R)) dt.$$

But the integrals on the right hand side can be evaluated straight forward since the integrands are constant or only have a single jump. This leads to

$$\int_{x_L}^{x_R} \mathbf{u}(t_c, x) dx = x_R \mathbf{u}_+ - x_L \mathbf{u}_- + t_c (\mathbf{f}_- - \mathbf{f}_+), \quad (5.40)$$

with $\mathbf{f}_- = \mathbf{f}(\mathbf{u}_-)$ and $\mathbf{f}_+ = \mathbf{f}(\mathbf{u}_+)$. But we can also split the integral on the left hand side in the following way

$$\int_{x_L}^{x_R} \mathbf{u}(t_c, x) dx = \int_{x_L}^{t_c s_-} \mathbf{u}(t_c, x) dx + \int_{t_c s_-}^{t_c s_+} \mathbf{u}(t_c, x) dx + \int_{t_c s_+}^{x_R} \mathbf{u}(t_c, x) dx.$$

Here we know, that the integrands in the first and third integral on the right hand side are constant. Therefore we can evaluate these integrals and get

$$\int_{x_L}^{x_R} \mathbf{u}(t_c, x) dx = \int_{t_c s_-}^{t_c s_+} \mathbf{u}(t_c, x) dx + (t_c s_- - x_L) \mathbf{u}_- + (x_R - t_c s_+) \mathbf{u}_+. \quad (5.41)$$

Comparing the right hand sides of (5.40) and (5.41) gives

$$\int_{t_c s_-}^{t_c s_+} \mathbf{u}(t_c, x) dx = t_c (s_+ \mathbf{u}_+ - s_- \mathbf{u}_- + \mathbf{f}_- - \mathbf{f}_+).$$

Dividing by the length of the integration interval we get the integral average of the intermediate state, which we will call \mathbf{U}^{hll} and reads

$$\mathbf{U}^{hll} = \frac{1}{t_c (s_+ - s_-)} \int_{t_c s_-}^{t_c s_+} \mathbf{u}(t_c, x) dx = \frac{s_+ \mathbf{u}_+ - s_- \mathbf{u}_- + \mathbf{f}_- - \mathbf{f}_+}{s_+ - s_-}. \quad (5.42)$$

Up to this point all calculations are exact. But we approximate the perhaps difficult solution to the Riemann problem by the following solution

$$\mathbf{U}(t, x) = \begin{cases} \mathbf{u}_-, & \frac{x}{t} \leq s_- \\ \mathbf{U}^{hll}, & s_- \leq \frac{x}{t} \leq s_+ \\ \mathbf{u}_+, & \frac{x}{t} \geq s_+, \end{cases} \quad (5.43)$$

and therefore ignore any internal structure in the *-region.

Finally, we need to calculate the numerical flux along the t -axis. We will not just put $\mathbf{F}^{hll} = \mathbf{f}(\mathbf{U}^{hll})$ but instead use some integral relations again. For this purpose, we will integrate the system of conservation laws (5.39) over the left half of the previous control volume, that is $[0, t_c] \times [x_L, 0]$. We obtain

$$\int_{t_c s_-}^0 \mathbf{u}(t_c, x) dx = -t_c s_- \mathbf{u}_- + t_c (\mathbf{f}_- - \mathbf{f}_0),$$

with \mathbf{f}_0 being the flux along the t -axis. We can rearrange this expression to get

$$\mathbf{f}_0 = \mathbf{f}_- - s_- \mathbf{u}_- - \frac{1}{t_c} \int_{t_c s_-}^0 \mathbf{u}(t_c, x) dx.$$

By substituting \mathbf{U}^{hll} into this relation and calling the corresponding flux along the t -axis \mathbf{F}^{hll} we get

$$\mathbf{F}^{hll} = \mathbf{f}_- + s_- (\mathbf{U}^{hll} - \mathbf{u}_-),$$

since \mathbf{U}^{hll} is again a constant integrand. Using the definition of \mathbf{U}^{hll} in this last expression leads to

$$\mathbf{F}^{hll} = \frac{s_+ \mathbf{f}_- - s_- \mathbf{f}_+ + s_- s_+ (\mathbf{u}_+ - \mathbf{u}_-)}{s_+ - s_-}. \quad (5.44)$$

We will then choose the numerical flux at an intercell boundary in the following way

$$\mathbf{F}_{j+\frac{1}{2}}^{hll} = \begin{cases} \mathbf{f}_-, & 0 \leq s_- \\ \mathbf{F}^{hll}, & s_- \leq 0 \leq s_+ \\ \mathbf{f}_+, & 0 \geq s_+. \end{cases} \quad (5.45)$$

Again, this flux ignores any internal structure of the exact solution. However, it is an easy to implement approximate Riemann solver we will use in the "Solution" step of the MUSCL-Hancock algorithm, provided one has the slowest and fastest signal speed. Since we have the exact wave speeds for each wave of the system under consideration in this work, we can easily determine these speeds and use the HLL approximate Riemann solver.

Since the internal structure in the *-region is neglected in the HLL solver, any intermediate wave is not or only badly resolved. Therefore Toro, Spruce

and Speares [84] proposed the HLLC approximate Riemann solver, where the C stands for Contact. In this approach, a third wave was assumed to be present. This reflects the structure of the exact solution of Euler equations of gas dynamics, where one has two acoustic waves and a contact wave between them.

The derivation of the HLLC solver is almost identical to the one of the HLL solver presented above. We will not present it here. For details see again Toro [83, Chapter 10]. One has to split the integral over the *-region in two parts for the now two unknown states \mathbf{u}_-^* and \mathbf{u}_+^* . Together with the two unknown flux vectors in the *-region there are four unknown vectors in total. The integral relations only give three relations, though. So one has to impose some additional conditions. In the case of the Euler equations, the authors used properties of the exact solution, namely the invariance of pressure and velocity

$$\begin{aligned} p_-^* &= p_+^* = p^*, \\ u_-^* &= u_+^* = u^*. \end{aligned} \quad (5.46)$$

5.4 The GHLL approximate Riemann solver

For the system under consideration in this work, we only have an exact solution for the dispersed phase, see Chapter 4. Using the relations (5.46) above did not lead to an improvement over the HLL solver in the liquid phase. We therefore constructed an adapted solver called GHLL solver.

This section is based on the publication [36]. In order to construct the GHLL solver, we will make use of the analytical solution derived in Chapter 4. In general, the GHLL Flux reads

$$\mathbf{F}^{ghll} = \begin{pmatrix} \mathbf{F}^* \\ \mathbf{F}_c^{hll} \end{pmatrix}, \quad (5.47)$$

where \mathbf{F}_c^{hll} denotes an HLL-type solver for the carrier phase of the system. The GHLL flux is split into two parts, namely \mathbf{F}^* for the dispersed phase and \mathbf{F}_c^{hll} the part for the carrier phase, respectively. Due to the decoupling of the dispersed phase equations in system (2.5) from the rest, the flux can be split in the given manner. For the dispersed components, we make use of the exact solution given in Section 4.1:

$$\begin{aligned} \text{(i)} \quad v_- = v_+ =: v \quad \mathbf{F}^* &= \begin{cases} \mathbf{f}(\mathbf{u}_-), & v > 0 \\ \mathbf{f}(\mathbf{u}_+), & \text{otherwise} \end{cases} \\ \text{(ii)} \quad v_- < v_+ \quad \mathbf{F}^* &= \begin{cases} \mathbf{f}(\mathbf{u}_-), & v_- > 0 \\ \mathbf{f}(\mathbf{u}_+), & v_+ < 0 \\ 0 & \text{otherwise} \end{cases} \\ \text{(iii)} \quad v_- > v_+ \quad \mathbf{F}^* &= \begin{cases} \mathbf{f}(\mathbf{u}_-), & v_\delta > 0 \\ \mathbf{f}(\mathbf{u}_+), & \text{otherwise} \end{cases} \end{aligned} \quad (5.48)$$

where v_δ is given by

$$v_\delta = \frac{v_- \sqrt{c_- \rho_-} + v_+ \sqrt{c_+ \rho_+}}{\sqrt{c_- \rho_-} + \sqrt{c_+ \rho_+}},$$

compare to (4.23). We thus use the exact solution of the dispersed phase to determine the numerical fluxes in the MUSCL-Hancock scheme.

For the carrier phase, we do not have an explicit solution to the Riemann problem at hand. We therefore try to use the HLLC approach. But as stated before, one needs some extra relations in order to construct the HLLC solver. One would like to use the Riemann invariants at the contact wave for this purpose. However, it is impossible to determine the Riemann invariants for the carrier fluid across the middle wave/waves. Accordingly, the construction of an HLLC solver resp. HLLCC solver requires approximations across the waves corresponding to $\lambda = v$. Note that in the case of the right velocity exceeding the left one in the dispersed phase, the middle wave splits into two waves, creating a region without any dispersed phase material. This splitting of the middle wave into two contact waves leads to the name HLLCC solver. To derive the flux for the liquid components from the HLLC or HLLCC solver and since one can not determine the Riemann invariants exactly, we impose the following approximate Riemann Invariants across the corresponding wave: $I_1 = (1 - c)\rho_c$ and $I_2 = (1 - c)\rho_c v_c$. But the resulting scheme for the liquid components is then equivalent to an ordinary HLL solver.

In the following, we discuss several numerical examples for all the three cases: Case 1 - contact case, Case 2 - vaporless case, Case 3 - δ -shock case. We consider bubbles in liquid as well as droplets in gas. We use parameters noted in Table 5.1. These data correspond to $T = 293.15$ K.

	gas	liquid
a [$\frac{\text{m}}{\text{s}}$]	369	1478
d_0 [Pa]	0	$-2.18 \cdot 10^{-8}$

TABLE 5.1: Equations of state parameters

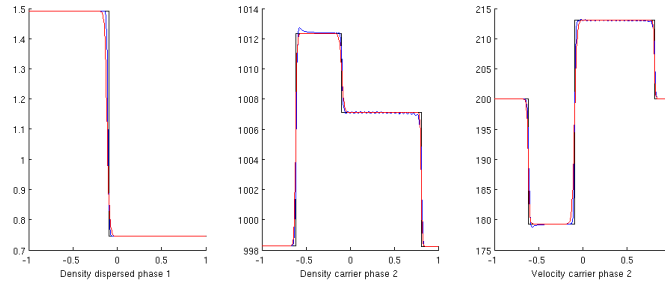
In order to give a condensed presentation for each test case, we only show three relevant pictures to discuss the properties of the solver and we neglect the equation describing the radius evolution.

We compare the GHLL solver to the second-order HLL solver and to the exact solution, presented by a blue, red and a black line, resp. All simulations are performed using the CFL number $C_{\text{CFL}} = 0.9$.

Example 1 - contact case, bubbles in liquid - uses the initial data given in Table 5.2.

We obtain the results shown in Figure 5.6. Obviously, the GHLL solver gives

	c	$\rho \left[\frac{\text{kg}}{\text{m}^3} \right]$	$v \left[\frac{\text{m}}{\text{s}} \right]$	$\rho_c \left[\frac{\text{kg}}{\text{m}^3} \right]$	$v_c \left[\frac{\text{m}}{\text{s}} \right]$
Left state	0.025	1.49	-200	998.29	-200
Right state	0.1	0.745	-200	998.24	200

TABLE 5.2: Initial data Example 1, $N = 200$ FIGURE 5.6: Contact case, bubbles in liquid, $N = 200$

- in contrast to the HLL solver - a quite good resolution for the contact wave, even on coarse grids. On the other hand, the GHLL solver produces small under- and overshoots near the contact in the carrier fluid, which lead to small oscillations. These oscillations completely disappear on finer grids. The resolution of shock waves is of the same quality for both solvers.

Example 2 - vaporless case, bubbles in liquid - uses the initial data given in Table 5.3.

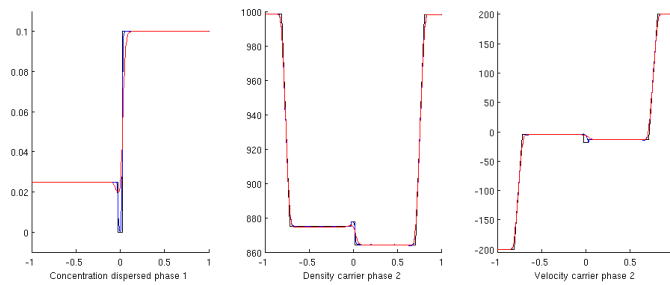
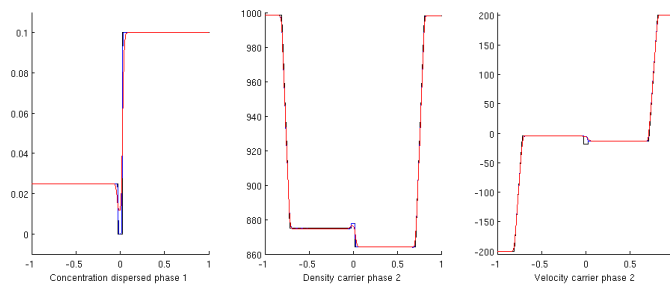
	c	$\rho \left[\frac{\text{kg}}{\text{m}^3} \right]$	$v \left[\frac{\text{m}}{\text{s}} \right]$	$\rho_c \left[\frac{\text{kg}}{\text{m}^3} \right]$	$v_c \left[\frac{\text{m}}{\text{s}} \right]$
Left state	0.025	1.49	-50	998.29	-200
Right state	0.1	0.745	50	998.24	200

TABLE 5.3: Initial data Example 2, $N = 200$, $N = 500$

We obtain the results presented in Figure 5.7 for the coarse grid and in Figure 5.8 for the finer grid.

Even on a coarse grid, the GHLL solver gives a quite good approximation of the vaporless state. Refining the mesh the GHLL solver gives a nearly exact solution, while the resolution of the vaporless state produced by the HLL solver is quite poor. One can clearly see that the tiny oscillations by the GHLL solver are totally disappeared on the finer grid.

Example 3 - δ -shock case, bubbles in liquid - uses the initial data given in Table 5.4.

FIGURE 5.7: Vaporless case, bubbles in liquid, $N = 200$ FIGURE 5.8: Vaporless case, bubbles in liquid, $N = 500$

	c	ρ [$\frac{\text{kg}}{\text{m}^3}$]	v [$\frac{\text{m}}{\text{s}}$]	ρ_c [$\frac{\text{kg}}{\text{m}^3}$]	v_c [$\frac{\text{m}}{\text{s}}$]
Left state	0.025	1.49	10	998.29	-200
Right state	0.1	0.745	-10	998.24	200

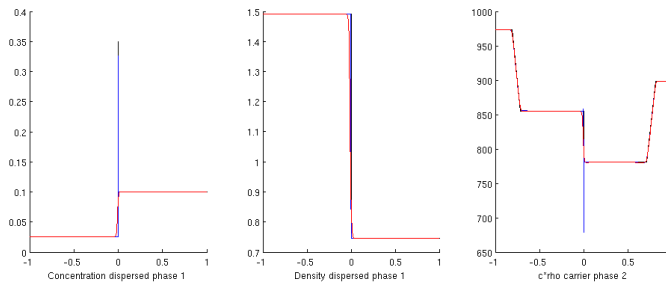
TABLE 5.4: Initial data Example 3, $N = 500$

Due to the formation of the singularity, the simulation for that example is performed on a finer grid. We obtain the result shown in Figure 5.9.

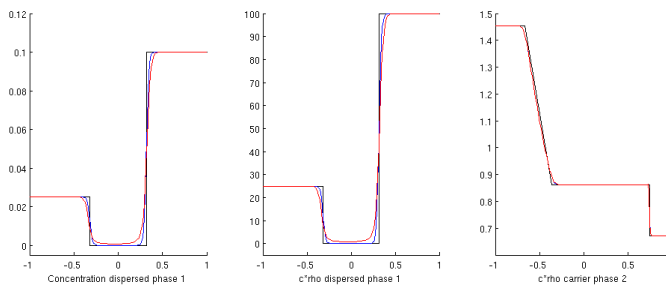
While the GHLL solver gives a very good approximation of the exact solution, the HLL solver fails to resolve the singularity.

Considering bubbles in a liquid, the GHLL solver always gives much better solutions than the HLL solver. In the following, we investigate the opposite case of droplets in gas. Because HLL and GHLL solver give nearly the same solution for the contact case even on a coarse grid ($N = 100$), we disclaim to present corresponding numerical results.

Example 4 - droplets in gas - uses the initial data given in Table 5.5. The results are shown in Figure 5.10. As in the opposite case of bubbles in a liquid, the GHLL solver gives a much better resolution of the middle state.

FIGURE 5.9: δ -shock case, bubbles in liquid, $N = 500$

	c	$\rho \left[\frac{\text{kg}}{\text{m}^3} \right]$	$v \left[\frac{\text{m}}{\text{s}} \right]$	$\rho_c \left[\frac{\text{kg}}{\text{m}^3} \right]$	$v_c \left[\frac{\text{m}}{\text{s}} \right]$
Left state	0.025	998.29	-200	1.49	-50
Right state	0.1	998.24	200	0.745	-50

TABLE 5.5: Initial data Example 4, $N = 100$ FIGURE 5.10: Vacuum case, droplets in gas, $N = 100$

Note that in the droplet case, the GHLL solver does not produce any over- and undershoots.

Example 5 - δ -shock case, droplets in gas - uses the initial given in Table 5.6.

	c	$\rho \left[\frac{\text{kg}}{\text{m}^3} \right]$	$v \left[\frac{\text{m}}{\text{s}} \right]$	$\rho_c \left[\frac{\text{kg}}{\text{m}^3} \right]$	$v_c \left[\frac{\text{m}}{\text{s}} \right]$
Left state	0.025	998.29	10	1.49	15
Right state	0.1	998.24	-10	0.745	-15

TABLE 5.6: Initial data Example 5, $N = 500$

Finally we present the results for the δ -shock case for droplets in Figure 5.11.

As before, the HLL solver is not able to resolve the singularity while the

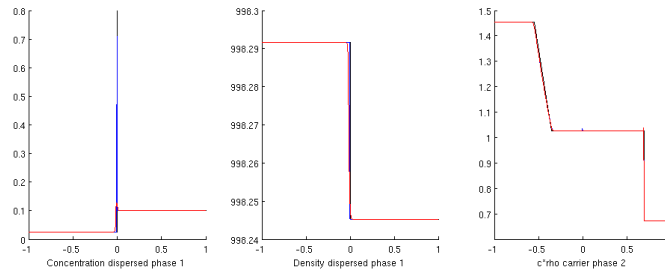


FIGURE 5.11: δ -shock case, droplets in gas, $N = 500$

GHLL solver gives a very good approximation.

In all the examples presented, the GHLL solver gives very good results for the dispersed phase, while the HLL solver cannot fairly resolve contact waves, vaporless states or singularities. If the carrier fluid is modeled as an ideal gas, the new GHLL solver always gives satisfactory results.

On the other hand, if the carrier fluid is modeled as a liquid, the GHLL solver produces small over- and undershoots in the solution of carrier fluid on coarse grids. The reason is that for parameter $|d_0| \gg 0$, the approximation used in the HLLCC solver is too imprecise. Accordingly, for that case, one should find a better approximation.

5.5 Method of modified equation analysis

In this section, we would like to comment on the properties of the numerical methods used or presented in this work. In particular, we are interested in stability, accuracy and diffusive or dispersive behavior of the methods. We will use the so called *modified equation analysis* which goes back to Warming and Hyett [88], also known as *method of differential approximations*. The second name goes back to Shokin [77].

As the model equation for a hyperbolic equation, we will consider the linear advection equation

$$L(u) = \frac{\partial u}{\partial t} + a \frac{\partial u}{\partial x} = 0. \quad (5.49)$$

A numerical method can then be described by an operator L_h acting on a discrete solution u_h , e.g. the upwind scheme

$$L_h(u_h) = u_i^{n+1} - u_i^n + \frac{a\Delta t}{\Delta x} (u_i^n - u_{i+1}^n) = 0 \quad \text{for } a > 0. \quad (5.50)$$

We will not perform the very similar *local truncation error analysis* we hope the reader is familiar with. The local truncation error comes from the truncation

of the infinite Taylor series to form the discrete algorithm. It is defined by

$$\tau = \frac{1}{\Delta t} L_h(u),$$

where one applies the operator L_h to the exact solution u satisfying $L(u) = 0$.

In the modified equation analysis one wants to find a continuous operator \tilde{L} such that $\tilde{L}(u_h) = 0$. To perform this analysis, we assume the existence of a continuously differentiable function $u_h(t, x)$ which coincides at the mesh points with the exact solution of the difference equation at least in some local sense, i.e.

$$u_h(t^n, x_i) = u_i^n. \quad (5.51)$$

In general, this numerical solution u_h will not satisfy (5.49) exactly, but only approximately

$$\frac{\partial u_h}{\partial t} + a \frac{\partial u_h}{\partial x} \neq 0.$$

We will therefore consider the *modified equation* or *equivalent differential equation*

$$\frac{\partial u_h}{\partial t} + a \frac{\partial u_h}{\partial x} = \sum_{l=2}^{\infty} c_l \frac{\partial^l u_h}{\partial x^l} \quad (5.52)$$

to quantify the errors. The numerical solution solves this modified equation exactly. This form is also called the Π -form of the differential approximation.

Let us consider the upwind scheme (5.50) to demonstrate how to get this form. We will start from

$$u_i^{n+1} = u_i^n - \frac{a\Delta t}{\Delta x} (u_i^n - u_{i+1}^n) \quad \text{for } a > 0,$$

and in a similar manner to the local truncation error analysis, we will expand the continuous numerical solution u_h in a Taylor series in space and time around x_i and t^n . We get

$$u_i^n + \Delta t u_t + \frac{\Delta t^2}{2} u_{tt} + \mathcal{O}(\Delta t^3) = u_i^n - \frac{a\Delta t}{\Delta x} \left(u_i^n - \left(u_i^n - \Delta x u_x + \frac{\Delta x^2}{2} u_{xx} + \mathcal{O}(\Delta x^3) \right) \right),$$

which is equivalent to

$$u_t + \frac{\Delta t}{2} u_{tt} + \mathcal{O}(\Delta t^2) = -a u_x + a \frac{\Delta x}{2} u_{xx} + \mathcal{O}(\Delta x^2).$$

Rearranging those terms, we finally obtain

$$u_t + a u_x = -\frac{\Delta t^1}{2} u_{tt} + a \frac{\Delta x^1}{2} u_{xx} + \mathcal{O}(\Delta t^2, \Delta x^2). \quad (5.53)$$

Equation (5.53) is called the Γ -form of the differential approximation. This form already gives us quite some information. From the terms on the right hand side, we can see that the upwind scheme is first-order accurate in space in time. Moreover, it is also consistent since for $\Delta x \rightarrow 0$ and $\Delta t \rightarrow 0$ the terms

vanish and the advection equation is satisfied.

The next objective is to replace the time-derivatives with space-derivatives using the so called *Cauchy-Kovalevskaya* procedure. The reader who is familiar with ADER schemes should be familiar with this procedure, too. We will take the Γ -form (5.53) and calculate the derivatives with respect to space and time to get

$$\begin{aligned} u_{tt} + au_{xt} &= -\frac{\Delta t}{2}u_{ttt} + a\frac{\Delta x}{2}u_{xxt} + \mathcal{O}(\Delta t^2, \Delta x^2) = \mathcal{O}(\Delta t, \Delta x), \\ u_{tx} + au_{xx} &= -\frac{\Delta t}{2}u_{ttx} + a\frac{\Delta x}{2}u_{xxx} + \mathcal{O}(\Delta t^2, \Delta x^2) = \mathcal{O}(\Delta t, \Delta x). \end{aligned}$$

Since both right hand sides are of order $\mathcal{O}(\Delta t, \Delta x)$ we get

$$u_{tt} = a^2u_{xx} + \mathcal{O}(\Delta t, \Delta x),$$

which we will insert into the Γ -form (5.53). This leads to

$$u_t + au_x = -\frac{\Delta t}{2}a^2u_{xx} + a\frac{\Delta x}{2}u_{xx} + \mathcal{O}(\Delta t^2, \Delta x^2).$$

which we can write in the form of the modified equation, see (5.52), as follows

$$u_t + au_x = a\frac{\Delta x}{2} \left(1 - a\frac{\Delta t}{\Delta x}\right) u_{xx} + \mathcal{O}(\Delta t^2, \Delta x^2), \quad (5.54)$$

which is the Π -form of the differential approximation. Here we can see that the leading error term is of dissipative nature because it is in front of the u_{xx} term, which could be interpreted as a heat coefficient. Since $a > 0$ we require for stability that $C_{CFL} = a\frac{\Delta t}{\Delta x} \leq 1$ to keep the coefficient in front of the leading error term non-negative. Note that this is a significant result. For a given spacing Δx , it is unnecessary to make the time step smaller and smaller to get better results. As long as the stability requirement is fulfilled, the diffusive error is smaller the larger the Courant number is. For $C_{CFL} = 1$ the leading error term vanishes and one can show that all higher-order terms vanish as well. Note that this is only true in the case of the linear advection equation since the numerical values are transported exactly on the uniform grid.

We would now like to compare this result for the explicit upwind scheme to implicit ones. Starting with the implicit upwind scheme

$$u_i^{n+1} = u_i^n - \frac{a\Delta t}{\Delta x} \left(u_i^{n+1} - u_{i+1}^{n+1}\right) \quad \text{for } a > 0,$$

and using the Taylor series expansion again, one gets the following Γ -form

$$u_t + au_x = -\frac{\Delta t}{2}u_{tt} + a\frac{\Delta x}{2}u_{xx} - a\Delta tu_{xt} + \mathcal{O}(\Delta t^2, \Delta x^2). \quad (5.55)$$

We can see that also this scheme is first-order accurate in space and time and consistent. Going again through the Cauchy-Kovalevskaya procedure

$$\begin{aligned} u_{tt} + au_{xt} &= \mathcal{O}(\Delta t, \Delta x), \\ u_{tx} + au_{xx} &= \mathcal{O}(\Delta t, \Delta x). \end{aligned}$$

to replace time-derivatives with space-derivatives on the right hand side. We get

$$\begin{aligned} u_{tt} &= a^2 u_{xx} + \mathcal{O}(\Delta t, \Delta x), \\ u_{xt} = u_{tx} &= -a u_{xx} + \mathcal{O}(\Delta t, \Delta x). \end{aligned}$$

Inserting these relations into the Γ -form (5.55), we obtain the Π -form again

$$\begin{aligned} u_t + au_x &= -\frac{\Delta t}{2} a^2 u_{xx} + \Delta t a^2 u_{xx} + a \frac{\Delta x}{2} u_{xx} + \mathcal{O}(\Delta t^2, \Delta x^2) \\ &= a \frac{\Delta x}{2} \left(1 + a \frac{\Delta t}{\Delta x} \right) u_{xx} + \mathcal{O}(\Delta t^2, \Delta x^2). \end{aligned} \quad (5.56)$$

This scheme is therefore unconditionally stable since the term in front of u_{xx} is always positive but at a very high cost. No matter how one chooses the CFL number, it is always more dissipative than the explicit upwind scheme, compare to Equation (5.54). Since we want to resolve shock waves and contact discontinuities, we want to avoid numerical dissipation at all costs and therefore, we will not use any implicit method in this work.

To analyze the physical meaning of the error terms, we will use the harmonic analysis of Fourier applied to the modified equation (5.52). We want to analyze the evolution of an isolated Fourier mode given as

$$u(t, x) = u_0 e^{i(kx - \omega t)},$$

where $k = \frac{2\pi}{\lambda}$ is the wave number and $\omega = \frac{2\pi}{T}$ is the angular frequency. To insert this ansatz into (5.52), we need to calculate the first derivative with respect to time and all orders of derivatives with respect to space. They read

$$u_t = -i\omega u, \quad u_x = ik u, \quad u_{xx} = (ik)^2 u \quad \text{and} \quad \frac{\partial^l u}{\partial x^l} = (ik)^l u. \quad (5.57)$$

Inserting these relations (5.57) into (5.52) gives the so called *dispersion relation*

$$-i\omega + aik = \sum_{l=2}^{\infty} c_l (ik)^l.$$

Rearranging those terms and using the following relation

$$i^l = \begin{cases} (-1)^m & \text{if } l = 2m, \\ i(-1)^m & \text{if } l = 2m + 1, \end{cases}$$

we get

$$\begin{aligned}\omega &= ak + i \sum_{l=2}^{\infty} c_l (ik)^l \\ &= ak + i \sum_{m=1}^{\infty} (-1)^m c_{2m} k^{2m} - \sum_{m=1}^{\infty} (-1)^m c_{2m+1} k^{2m+1}.\end{aligned}\quad (5.58)$$

Inserting this last relation (5.58) into the isolated Fourier mode ansatz, we obtain

$$\begin{aligned}u(t, x) &= u_0 \exp \left[i \left(kx - \left(ak + i \sum_{m=1}^{\infty} (-1)^m c_{2m} k^{2m} - \sum_{m=1}^{\infty} (-1)^m c_{2m+1} k^{2m+1} \right) t \right) \right] \\ &= u_0 \exp \left[ik \left(x - \left(a - \sum_{m=1}^{\infty} (-1)^m c_{2m+1} k^{2m} \right) t \right) \right] \\ &\quad \cdot \exp \left[\sum_{m=1}^{\infty} (-1)^m c_{2m} k^{2m} t \right].\end{aligned}\quad (5.59)$$

This can be rewritten in the form

$$u(t, x) = u_0 \cdot e^{ik(x-v(k)t)} \cdot e^{-dt}, \quad (5.60)$$

with

$$v(k) = a - \sum_{m=1}^{\infty} (-1)^m c_{2m+1} k^{2m}, \quad (5.61)$$

the wave number dependent wave speed and

$$d = \sum_{m=1}^{\infty} (-1)^m c_{2m} k^{2m}, \quad (5.62)$$

the diffusion error. We can clearly see that the velocity of the isolated Fourier mode (5.61) deviates from the exact wave speed $v(k) = a$ of the advection equation and depends on the wave number. Different wave numbers are therefore transported with different wave speeds, which causes dispersion. Note, that only the coefficients in front of odd orders of derivatives cause the dispersion errors, i.e. the coefficients c_3, c_5 etc. But they do not play any role for stability considerations.

On the other hand, we have the diffusion error, which does not influence the wave speeds but the amplitudes of the wave during propagation. To ensure linear stability we require $(-1)^m c_{2m} \leq 0$ in (5.62) as a sufficient condition. This guarantees that all Fourier modes are non-increasing over time. Note, that here only the coefficients in front of even orders of derivatives are responsible for diffusion errors, i.e. the coefficients c_2, c_4 , etc. Since there is an alternating sign in the conditions $(-1)^m c_{2m} \leq 0$ we require the sufficient conditions $c_2 \geq 0, c_4 \leq 0$ and so on for stability.

One can now perform this modified equation analysis for a fully discrete and a semi-discrete method of second-order accuracy. For the fully discrete method, we will analyze the second-order MUSCL-Hancock method again applied to the advection equation. Without going through the calculations, we will just state the results. The first three coefficients c_l are given as

$$\begin{aligned} c_2 &= 0, \\ c_3 &= \frac{1}{6}a\Delta x^2(C_{CFL} - 1)(C_{CFL} + 1), \\ c_4 &= \frac{1}{8}a\Delta x^3(C_{CFL} - 1)(C_{CFL} + 1)C_{CFL}. \end{aligned}$$

From c_2 we can see that this method is second-order accurate. And again, as for the first-order upwind scheme, this method is exact for $C_{CFL} = 1$. So there is no need to go for smaller and smaller time steps to achieve a better numerical result. Actually the error decreases for $C_{CFL} \rightarrow 1$.

One can also perform the modified equation analysis for a semi-discrete method. We will use a second-order upwind reconstruction combined with the second-order optimal TVD-Runge-Kutta scheme given by Gottlieb and Shu, see [32]. The coefficients c_l of the modified equation then read

$$\begin{aligned} c_2 &= 0, \\ c_3 &= \frac{1}{6}a\Delta x^2(C_{CFL} - 1)(C_{CFL} + 1), \\ c_4 &= \frac{1}{8}a\Delta x^3C_{CFL}^3. \end{aligned} \tag{5.63}$$

Despite the fact that this method is also second-order accurate and has the same coefficient c_3 in front of the dispersive terms, the coefficient c_4 is very problematic. Since $a > 0$, $\Delta x > 0$ and $C_{CFL} > 0$ we also have $c_4 > 0$ in contradiction to the sufficient requirements of linear stability. This could lead to a *linearly unconditionally unstable* method and only the application of limiters can save this method. This is why we did not use semi-implicit methods at all throughout this work, but instead the somewhat optimal MUSCL-Hancock method.

5.6 Numerical simulations

As the last part of this work, we want to present numerical simulations for the test cases given in Chapter 4. In the following, we will use the second-order MUSCL-Hancock scheme with MINBEE the limiter and the HLL approximate Riemann solver. The final time for all simulations is $0.5 \cdot 10^{-3}$ s.

In Chapter 4 we discussed the exact solutions for the three different cases for a liquid carrier phase depending on the initial velocities of the dispersed phase. All the initial data are given in Section 4.3, but we will state the corresponding ones here again at each of the following examples. We assumed the carrier phase to be liquid water and used a Tait equation of state (2.8) with

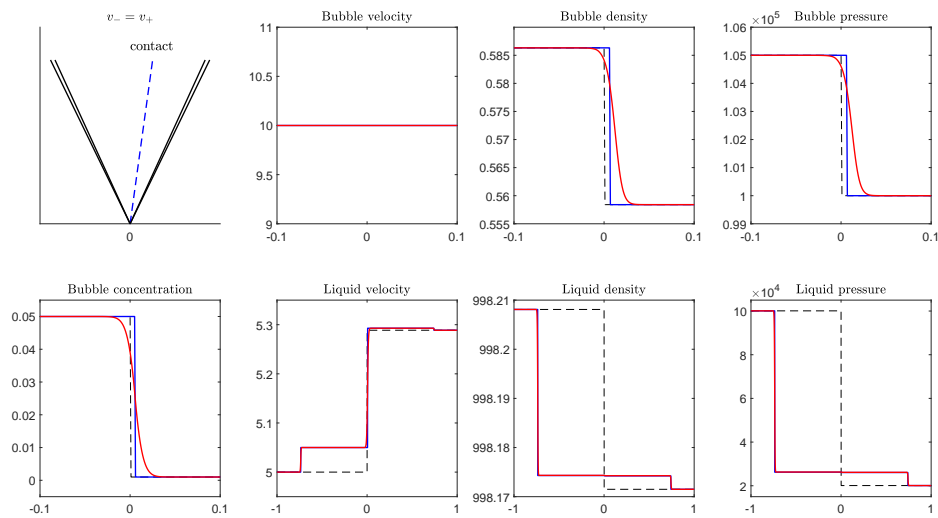


FIGURE 5.12: Initial data (dashed lines), exact solution (blue lines) and numerical simulation (red lines) for a liquid carrier phase. The middle wave is a contact wave. Initial data are given by (5.65)

the corresponding parameters from [87]. We state those parameters and the sound speed in the dispersed vapor phase a_v for the different Temperatures in Table (5.64).

T [K]	a_v [$\frac{\text{m}}{\text{s}}$]	$\bar{\rho}$ [$\frac{\text{kg}}{\text{m}^3}$]	\bar{p} [Pa]	\bar{K} [10^9 Pa]
293.15	423.18	1/0.00100184	2339.21	1/0.45836
309.15	434.07	1/0.00100639	5947.47	1/0.44271
363.15	466.98	1/0.00103594	70182.4	1/0.47316

Example 1 - contact case, bubbles in liquid The initial data of the contact case are given by

	c	ρ [$\frac{\text{kg}}{\text{m}^3}$]	v [$\frac{\text{m}}{\text{s}}$]	R	ρ_c [$\frac{\text{kg}}{\text{m}^3}$]	v_c [$\frac{\text{m}}{\text{s}}$]	p [Pa]
Left state	0.05	0.5863	10	0.001	998.2081	5	100000
Right state	0.001	0.5584	10	0.0005	998.1715	5.2887	20000

where we have assumed a temperature of 293.15 K, compare to (4.40). The initial data, the exact solution and the numerical solution are depicted in Figure 5.12.

In general, the numerical simulation matches the exact solution very well. Note that the first row and the first subfigure of the second row are magnified

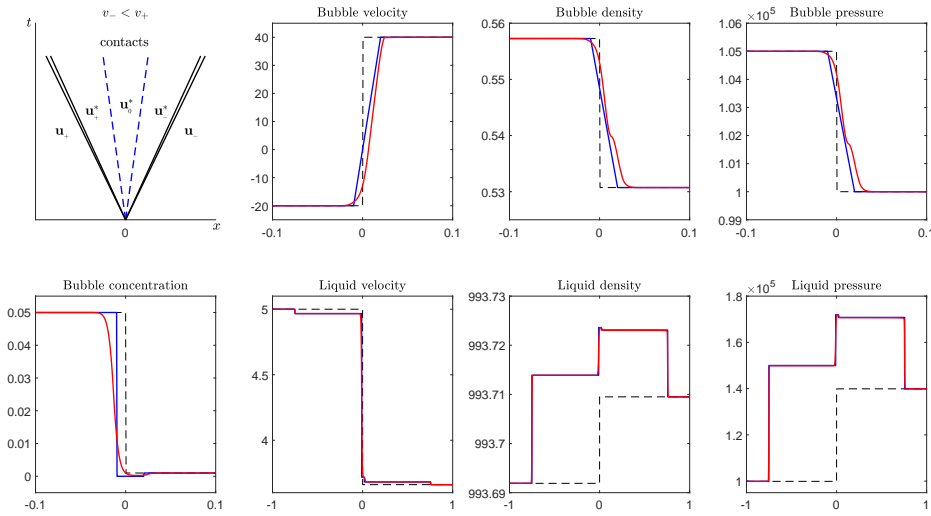


FIGURE 5.13: Initial data (dashed lines), exact solution (blue lines) and numerical simulation (red lines) for a liquid carrier phase. The middle wave splits in two contacts. Initial data are given by (5.66)

in x -direction by a factor of ten. Otherwise, the deviation of the simulation and the exact solution would be barely visible.

Example 2 - vaporless case, bubbles in liquid The initial data for the second case are

	c	$\rho \left[\frac{\text{kg}}{\text{m}^3} \right]$	$v \left[\frac{\text{m}}{\text{s}} \right]$	R	$\rho_c \left[\frac{\text{kg}}{\text{m}^3} \right]$	$v_c \left[\frac{\text{m}}{\text{s}} \right]$	$p \text{ [Pa]}$
Left state	0.05	0.5573	-20	0.0005	993.6919	5	100000
Right state	0.001	0.5307	40	0.001	993.7095	3.6612	140000

(5.66)

where we have assumed a temperature of 309.15 K, compare to (4.41). The numerical results are depicted in Figure 5.13. In this case the middle wave splits into two contact waves. Again, the numerical simulation is in very good agreement with the exact solution. From the first row in the figure, one could get the impression that the simulation slightly misses the exact wave speed. But keep in mind that the exact solution only requires a continuous connection between the initial states. For simplicity, we chose the linear connection of the initial states, but each continuous solution fulfills the sufficient condition. The numerical solution just does not follow a linear curve between the initial states, which is perfectly fine.

Again, the first row only depicts the interval $x \in [-0.1, 0.1]$. In the pictures for the liquid components, which are shown on the full numerical domain, one can barely see the small region between the two contact waves in the middle.

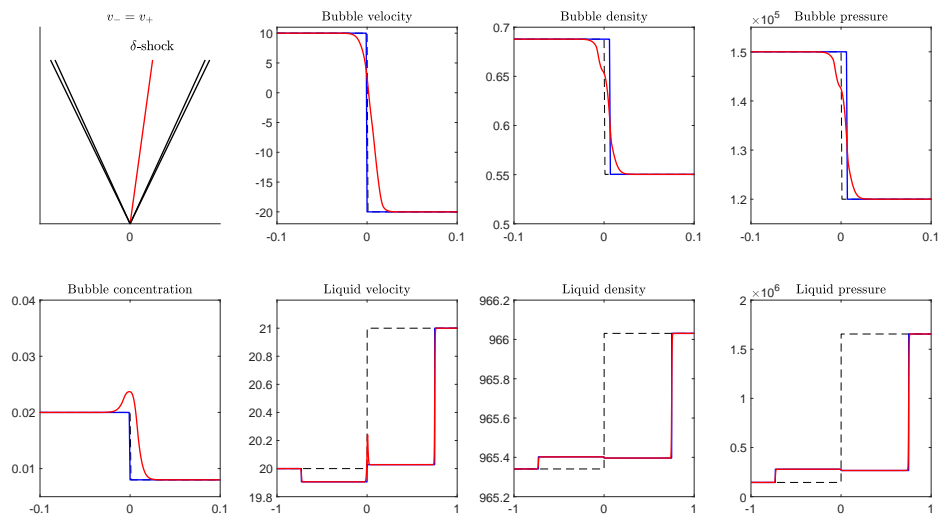


FIGURE 5.14: Initial data (dashed lines), exact solution (blue lines) and numerical simulation (red lines) for a liquid carrier phase. The middle wave forms a δ -shock. Initial data are given by (5.67)

Usually, vacuum states in a single fluid lead to numerical problems. Note that the absence of the dispersed phase is not a problem for the numerics of our model. Then the volume fraction of the carrier phase just becomes $c_c = 1 - c = 1$ and the problem reduces to a single-phase flow of the carrier phase. So this case is not to be compared to a vacuum case from other models.

Example 3 - δ -shock case, bubbles in liquid Next, we consider the case with a δ -shock. The volume fraction then becomes problematic. As we have stated before, for a volume fraction $c \rightarrow 1$ the model is not longer valid, since the assumption of the dispersed phase bubbles being separated by the carrier phase is no longer true. We considered the following initial data in this case to be

	c	ρ [$\frac{\text{kg}}{\text{m}^3}$]	v [$\frac{\text{m}}{\text{s}}$]	R	ρ_c [$\frac{\text{kg}}{\text{m}^3}$]	v_c [$\frac{\text{m}}{\text{s}}$]	p [Pa]
Left state	0.02	0.6879	10	0.0008	965.3410	20	145000
Right state	0.008	0.5503	-20	0.0006	966.0308	21	1655149.1033

(5.67)

where we have assumed a temperature of 363.15 K, compare to (4.42).

Again, the numerical simulation fits the exact solution quite well. As predicted by the exact solution, the values for velocity, density and pressure respectively are changing over the middle wave. Thus, assuming them to be constant as in the HLLC solver is not feasible. One can clearly see that the volume fraction of the dispersed phase increases right at the middle wave. If this concentration rises to values close to or higher than 1, the numerical simulation breaks down immediately. Note that the numerical approximation of

the δ -shock might look very smeared out in the subfigure for the bubble concentration. But we again depicted only a tenth of the numerical domain. In the subfigure for the liquid velocity, one can see the narrow peak due to the formation of the δ -shock.

Example 4 - droplets in gas In contrast to the cases presented before we will now perform a numerical simulation for a vapor carrier phase. In particular the carrier phase is assumed to be water vapor with an ideal gas equation of state at a temperature of 309.15 K. The case considered here is identical to Example 2 with exchanged equations of state for dispersed and carrier phase. The initial data are the following

	c	$\rho \left[\frac{\text{kg}}{\text{m}^3} \right]$	$v \left[\frac{\text{m}}{\text{s}} \right]$	R	$\rho_c \left[\frac{\text{kg}}{\text{m}^3} \right]$	$v_c \left[\frac{\text{m}}{\text{s}} \right]$	$p \text{ [Pa]}$
Left state	0.05	993.6941	-20	0.0005	0.5307	5	100000
Right state	0.001	993.6919	40	0.001	0.7430	-180.3256	140000

(5.68)

Due to the initial velocities of the dispersed phase, the middle wave splits into two contact waves. As predicted for the exact solution by (4.47), there should be no jump of the velocity across the two contact waves in the *-region. Note that the density and the pressure clearly are not constant across the contact waves, which is also in accordance with the theoretical results. However, the quantity $\hat{\rho}_c = (1 - c)\rho_c$ is predicted to be constant by (4.47) and therefore, the quantity $(1 - c)p_c$ must also be constant due to the linear dependence between pressure and density of the ideal gas. This can be seen in Figure 5.15. The first row depicts the primitive variables with the jump across the middle waves in the density and pressure. The second row shows the quantities which were predicted to be constant in the *-region by the theory.

In general, we wanted to depict physically relevant situations. Therefore, not all interesting features may be clearly visible in all of these figures. Nevertheless, we preferred to show some parts enlarged and to not always show the whole numerical domain instead of changing to arbitrary initial data. When doing these physically relevant simulations, the sound speed in the liquid carrier phase is much higher than in the gaseous dispersed phase, leading to much faster acoustic waves in the liquid phase compared to the middle waves in the vapor phase. Thus, when the whole numerical domain is depicted, the movement of the middle waves is barely visible.

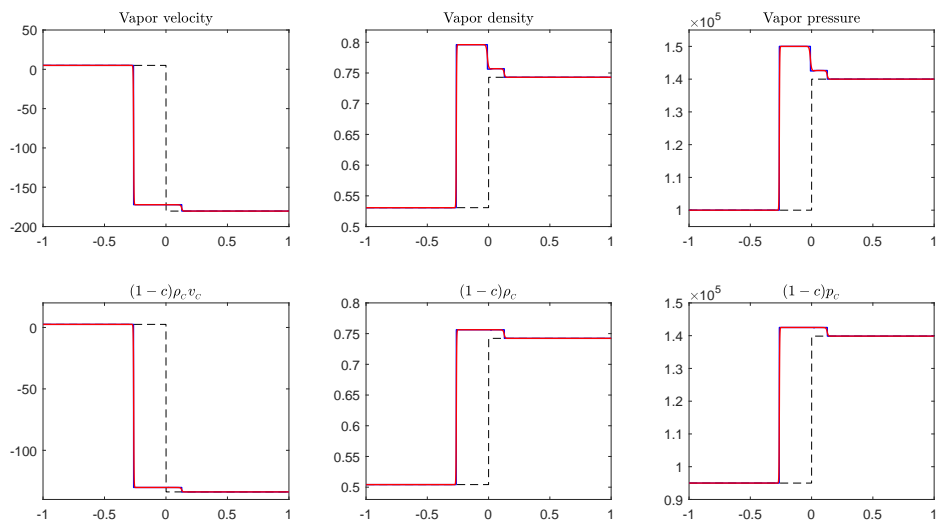


FIGURE 5.15: Initial data (dashed lines), exact solution (blue lines) and numerical simulation (red lines) for a liquid carrier phase. Note the difference between primitive and conserved variables in their behavior at the middle wave in accordance with (4.47). Initial data is given by (5.68)

Conclusion and Outlook

In this thesis, we studied the Riemann problem for the two-phase flow model proposed by Dreyer, Hantke and Warnecke [22] analytically. Although given as a system of balance laws, we focused on the isothermal system of conservation laws derived from it. We performed the eigenstate analysis on the dispersed phase alone as well as the full two-phase system of equation. The wave types and all possible wave patterns were found.

We had to consider Riemann initial data since we can not use any of the existing results for the Cauchy problem of systems of conservation laws. Nonetheless, these are quite important as the Riemann problem solution is not only a building block for existence results but also essential in some numerical methods.

Solutions to the Riemann problem were found by solving highly nonlinear systems of algebraic equations. All solutions are given implicitly and the uniqueness was shown using monotonicity arguments. The final result is a set of inequalities for the relative velocity between the two phases involved. The given bounds on the velocity are not sharp but give a sufficient criterion to ensure the uniqueness of the solution.

We studied bubbles in a liquid carrier as well as droplets or dust particles in a vapor carrier. In a gas, the equation of state (EOS) for isothermal flow yields the pressure as a linear function of the density. For a liquid, the simplest realistic assumptions lead to an affine function for the EOS. Therefore, commonly used affine linear equations of state like the Tait equation or the stiffened gas equation are included in our analysis. In the case of a liquid carrier phase, this leads to a considerable complication in the determination of the solutions to Riemann problems. Nonetheless, all possible wave configurations were discussed, the implicit functions to find a solution are given and the inequalities assuring monotonicity are stated as well.

Thus, this work includes a first analysis of the two-phase flow model considered. It takes a first step from a linear equation of state towards more general equations of state, which is very important with regard to applications. Initial data were given for all relevant cases. We chose, in particular, physically reasonable values.

There are still many open questions regarding the existence and uniqueness of solutions for the model considered. We will name a few here.

How can we get to arbitrary initial data? We have not done any work concerning this question up to now. However, it is very interesting if, with a Riemann solution at hand, one could generalize the results to arbitrary initial data as in the Glimm or front tracking scheme.

Is it possible to generalize the equation of state even further? The first drafts of this work specifically only considered bubbles in liquid. We then tried to work with a general equation of state $p = p(\rho)$ as far as possible. To solve the Riemann invariants at the acoustic waves, we needed the sound speed to be constant. Therefore, the form of the equation of state given in this work with a constant sound speed is the most general for which we could get an analytical solution. But it would be very interesting if other techniques could lead to a generalization of the results presented.

Considering the numerical part of this work, we obtained simulations for the cases considered in the analytical sections of this work. We used a second-order MUSCL-Hancock scheme with the MINBEE limiter and the HLL approximate Riemann solver.

Since we only have an analytical solution in the one dimensional case, we left out simulations of higher space dimensions, even though we have already obtained a few of them. Only in one space dimension, we can directly compare analytical and numerical results. The numerical simulations could be understood as a confirmation of the analytical calculations done. On the other hand, the analytical solution is a tool to verify numerical schemes in one space dimension and then generalize them to higher space dimensions in the hope that they will still approximate the exact solution.

Considering the order of convergence of the scheme, we right now work on the fourth-order ADER scheme introduced by Titarev and Toro [82] in the local space-time DG version proposed by Dumbser, Balsara, Toro and Munz [23]. We already implemented this solver for 2×2 systems of conservation laws. We hope that this scheme has a better performance when compared to the MUSCL-Hancock scheme.

We also tried to improve the classical HLL approximate Riemann solver by introducing the GHLL solver in [36]. This solver improved the resolution of δ -shocks and contacts in the dispersed phase using the information from the explicit analytical solution in this phase. However, it led to oscillations in the carrier phase quantities. The construction of an improved Riemann solver for the model considered is therefore still an open problem.

We would also like to use solvers which use the eigenstructure of the quasi-linear system of conservation laws like the Roe scheme. But since the system of conservation laws under consideration is only weakly hyperbolic, we lack an eigenvector, which does not allow the usage of such numerical schemes. At the moment, we have two different ideas of how to overcome this difficulty. One is to slightly modify the equations to end up with a hyperbolic model and the second one uses generalized eigenvectors.

To fully treat the numerical investigation of this model, we want to write a follow-up paper on this issue in the near future.



Calculations

To derive (4.6) we note that the system (4.5) implies that

$$\frac{c_- R_- v_- - c_+ R_+ v_+}{c_- R_- - c_+ R_+} = \frac{c_- v_- - c_+ v_+}{c_- - c_+} = \frac{c_- \rho_- v_- - c_+ \rho_+ v_+}{c_- \rho_- - c_+ \rho_+} = \frac{c_- \rho_- v_-^2 - c_+ \rho_+ v_+^2}{c_- \rho_- v_- - c_+ \rho_+ v_+} = \sigma. \quad (\text{A.1})$$

Equality of the first and second terms gives

$$\begin{aligned} 0 &= (c_- v_- - c_+ v_+) (c_- R_- - c_+ R_+) - (c_- - c_+) (c_- R_- v_- - c_+ R_+ v_+), \\ &= c_-^2 v_- R_- - c_- v_- c_+ R_+ - c_+ v_+ c_- R_- + c_+^2 v_+ R_+ - c_-^2 R_- v_- \\ &\quad + c_- c_+ R_+ v_+ + c_+ c_- R_- v_- - c_+^2 R_+ v_+, \\ &= -c_- v_- c_+ R_+ - c_+ v_+ c_- R_- + c_- c_+ R_+ v_+ + c_+ c_- R_- v_-, \\ &= c_- c_+ R_+ (v_+ - v_-) - c_- c_+ R_- (v_+ - v_-), \\ &= c_- c_+ (R_+ - R_-) (v_+ - v_-). \end{aligned} \quad (\text{A.2})$$

Similarly, equality of the second and third terms in (A.1) leads to

$$0 = c_- c_+ (\rho_+ - \rho_-) (v_+ - v_-). \quad (\text{A.3})$$

Finally, equality of the second and fourth terms in (A.1) implies that

$$0 = c_- c_+ (\rho_+ v_+ - \rho_- v_-) (v_+ - v_-). \quad (\text{A.4})$$

Clearly, if $c_- c_+ \neq 0$ the equations (A.3) and (A.4) give $v_- = v_+$ which is the required result in (4.6). Now suppose that $c_- = 0$. Our aim is to show that a shock wave can not connect the state with $c_- = 0$ to that with $c_+ \neq 0$. We will prove the result using a contradiction argument as follows. Suppose a shock wave connects the two states above. Then the shock speed is calculated from (A.1) as

$$\sigma = v_+.$$

This result violates the Lax entropy condition $v_- > \sigma > v_+$ for appearance of a shock wave. The case for $c_- \neq 0$ and $c_+ = 0$ leads to the same results. Therefore (4.6) holds in all cases.

We now solve the quadratic equation which leads to (4.23).

$$\begin{aligned}
v_\delta &= \frac{2[[c\rho v] \pm \sqrt{4[[c\rho v]^2 - 4[[c\rho][[c\rho v^2]]}]]}{2[[c\rho]]}, \\
&= \frac{(c_-\rho_-v_- - c_+\rho_+v_+) \pm \sqrt{(c_-\rho_-v_- - c_+\rho_+v_+)^2 - (c_-\rho_- - c_+\rho_+)(c_-\rho_-v_-^2 - c_+\rho_+v_+^2)}}{(c_-\rho_- - c_+\rho_+)} \\
&= \frac{(c_-\rho_-v_- - c_+\rho_+v_+) \pm \sqrt{-2c_-\rho_-v_-c_+\rho_+v_+ + c_+\rho_+c_-\rho_-v_-^2 + c_-\rho_-c_+\rho_+v_+^2}}{(c_-\rho_- - c_+\rho_+)} \\
&= \frac{(c_-\rho_-v_- - c_+\rho_+v_+) \pm (v_- - v_+) \sqrt{c_-\rho_-c_+\rho_+}}{(c_-\rho_- - c_+\rho_+)} \\
&= \frac{(c_-\rho_- \pm \sqrt{c_-\rho_-c_+\rho_+})v_- - (c_+\rho_+ \pm \sqrt{c_-\rho_-c_+\rho_+})v_+}{(c_-\rho_- - c_+\rho_+)} \\
&= \frac{(\sqrt{c_-\rho_-} \pm \sqrt{c_+\rho_+})v_- \sqrt{c_-\rho_-} - (\sqrt{c_+\rho_+} \pm \sqrt{c_-\rho_-})v_+ \sqrt{c_+\rho_+}}{(\sqrt{c_-\rho_-} - \sqrt{c_+\rho_+})(\sqrt{c_-\rho_-} + \sqrt{c_+\rho_+})} \\
&= \frac{\sqrt{c_-\rho_-}v_- \mp \sqrt{c_+\rho_+}v_+}{\sqrt{c_-\rho_-} \mp \sqrt{c_+\rho_+}}
\end{aligned}$$

Bibliography

- [1] N. Andrianov and G. Warnecke. On the solution to Riemann problem for compressible duct flow. *SIAM J. Appl. Math.*, 64:878 – 901, 2004.
- [2] N. Andrianov and G. Warnecke. The Riemann problem for the Baer–Nunziato two-phase flow model. *J. Comput. Phys.*, 195:434 – 464, 2004.
- [3] M.R. Baer and J.W. Nunziato. A two-phase mixture theory for the deflagration-to-detonation transition (DDT) in reactive granular materials. *Int. J. Multiphase Flows*, 12:861 – 889, 1986.
- [4] M. Ben-Artzi and J. Falcovitz. A second-order godunov-type scheme for compressible fluid dynamics. *Journal of Computational Physics*, 55(1):1–32, 1984.
- [5] F. Bouchut. On zero pressure gas dynamics. In B. Perthame, editor, *Advances in kinetic theory and computing - Selected papers*. World Scientific, Singapore, 1994.
- [6] A. Bressan. Global solutions to systems of conservation laws by wave-front tracking. *J. Math. Anal. Appl.*, 170:414 – 432, 1992.
- [7] A. Bressan. *Hyperbolic systems of conservation laws. The one-dimensional Cauchy problem*. Oxford Lecture Series in Mathematics and its Applications. Oxford University Press, 2000.
- [8] A. Bressan. Lecture notes on hyperbolic conservation laws. 04 2009.
- [9] G.Q. Chen, X.X. Ding, and P.Z. Luo. Convergence of the fractional step Lax-Friedrichs scheme and Godunov scheme for the isentropic system of gas dynamics. *Commun.Math. Phys.*, 121:63–84, 1989.
- [10] S. Cheng, J. Li, and T. Zhang. Explicit construction of measure solutions of cauchy problem for transportation equations. *Science in China (Series A)*, 40:1287 – 1299, 1997.

- [11] P. Colella. A Direct Eulerian MUSCL Scheme for Gas Dynamics. *Siam Journal on Scientific and Statistical Computing*, 6:104–117, 1985.
- [12] R. Courant, K. Friedrichs, and H. Lewy. Über die partiellen Differenzengleichungen der mathematischen Physik. *Math. Ann.*, 100:32–74, 1928.
- [13] C. Crowe, M. Sommerfeld, and Y. Tsuji. *Multiphase flows with droplets and particles*. CRC Press, Boca Raton, 1998.
- [14] C.M. Dafermos. The entropy rate admissibility criterion for solutions of hyperbolic conservation laws. *Journal of Differential Equations*, 14:202–212, 1973.
- [15] C.M. Dafermos. Admissible wave fans in nonlinear hyperbolic systems. In *Mechanics and Thermodynamics of Continua: A Collection of Papers Dedicated to B.D. Coleman on His Sixtieth Birthday*, pages 127–144. Springer Berlin Heidelberg, 1991.
- [16] C.M. Dafermos. *Hyperbolic Conservation Laws in Continuum Physics; 4th ed.* Grundlehren der mathematischen Wissenschaften. Springer-Verlag Berlin Heidelberg, Dordrecht, 2016.
- [17] K. Davitt, E. Rolley, F. Caupin, A. Arvengas, and S. Balibar. Equation of state of water under negative pressure. *Journal of Chemical Physics*, 133(17):1745071 – 1745078, 2010.
- [18] D.A. Drew and S.L. Passman. *Theory of multicomponent fluids*. Springer, New York, 1999.
- [19] W. Dreyer, F. Duderstadt, M. Hantke, and G. Warnecke. Bubbles in liquids with phase transition. part 1. on phase change of a single vapor bubble in liquid water. *Continuum Mech. Thermodyn.*, 24:461 – 483, 2012.
- [20] W. Dreyer, J. Giesselmann, and C. Kraus. A compressible mixture model with phase transition. *Physica D: Nonlinear Phenomena*, 273-274:1–13, 2014.
- [21] W. Dreyer, M. Hantke, and G. Warnecke. Exact solutions to the Riemann problem for compressible isothermal Euler equations for two phase flows with and without phase transition. *Quarterly of Applied Mathematics*, 71:509 – 540, 2013.
- [22] W. Dreyer, M. Hantke, and G. Warnecke. Bubbles in liquids with phase transition – part 2: on balance laws for mixture theories of disperse vapor bubbles in liquid with phase change. *Continuum Mech. Thermodyn.*, 26:521 – 549, 2014.
- [23] M. Dumbser, D. Balsara, E.F. Toro, and C.D. Munz. A unified framework for the construction of one-step finite volume and discontinuous Galerkin schemes on unstructured meshes. *Journal of Computational Physics*, 227(18):8209–8253, 2008.

- [24] J. Dymond and R. Malhotra. The tait equation: 100 years on. *International Journal of Thermodynamics*, 9(6):941–951, 1988.
- [25] W. E, Yu.G. Rykov, and Ya.G. Sinai. Generalized variational principles, global weak solutions and behavior with random initial data for systems of conservation laws arising in adhesion particle dynamics. *Commun. Math. Phys.*, 177:349 – 380, 1996.
- [26] M.H. Ernst, R.M. Ziff, and E.M. Hendriks. Coagulation processes with a phase transition. *J. Colloid Interface Sci.*, 97:266 – 277, 1984.
- [27] M. Escobedo, S. Mischler, and B. Perthame. Gelation in coagulation and fragmentation models. *Commun. Math. Phys.*, 231:157 – 188, 2002.
- [28] L.C. Evans. *Partial differential equations*, volume 19. Amer. Math. Soc. Providence, Rhode Island, 1998.
- [29] J. Glimm. Solutions in the large for nonlinear hyperbolic systems of equations. *Communications on Pure and Applied Mathematics*, 18(4):697–715, 1965.
- [30] E. Godlewski and P.-A. Raviart. *Numerical Approximation of Hyperbolic Systems of Conservation Laws*. Springer New York, 1996.
- [31] S.K. Godunov. and I. Bohachevsky. A Finite Difference Method for the Computation of Discontinuous Solutions of the Equations of Fluid Dynamics. *Matematičeskij sbornik, Steklov Mathematical Institute of Russian Academy of Sciences*, 47(89) (3):271–306, 1959.
- [32] S. Gottlieb and C.-W. Shu. Total variation diminishing Runge-Kutta schemes. *Mathematics of Computation*, 67(221):73–85, 1998.
- [33] E. Han, M. Hantke, and G. Warnecke. Exact Riemann solutions to compressible Euler equations in ducts with discontinuous cross-section. *J. Hyperbolic Diff. Eq.*, 9, No. 3:1 – 47, 2012.
- [34] M. Hantke, C. Matern, V. Ssemaganda, and G. Warnecke. Analytical results for the Riemann problem for a weakly hyperbolic two-phase flow model of a dispersed phase in a carrier fluid. In *Continuum Mechanics, Applied Mathematics and Scientific Computing: Godunov’s Legacy*, pages 169–175. Springer Nature Switzerland, 2020.
- [35] M. Hantke, C. Matern, V. Ssemaganda, and G. Warnecke. The Riemann problem for a weakly hyperbolic two-phase flow model of a dispersed phase in a carrier fluid. *Quart. Appl. Math.*, 78:431–467, 2020.
- [36] M. Hantke, C. Matern, and G. Warnecke. Numerical solutions for a weakly hyperbolic dispersed two-phase flow model. In *Hyperbolic Problems, Theory, Numerics, Applications*. Springer Proceedings in Mathematics and Statistics, 2016.

- [37] M. Hantke and F. Thein. Why condensation by compression in pure water vapor cannot occur in an approach based on Euler equations. *Quart. Appl. Math.*, 73(3):575–591, 2015. arXiv:1406.1377.
- [38] A. Harten, B. Engquist, S. Osher, and S.R. Chakravarthy. Uniformly high order accurate essentially non-oscillatory schemes, iii. *Journal of Computational Physics*, 71(2):231–303, 1987.
- [39] A. Harten, P. Lax, and B. van Leer. On Upstream Differencing and Godunov-Type Schemes for Hyperbolic Conservation Laws. *SIAM Rev*, 25:35–61, 01 1983.
- [40] P.C. Hohenberg and B.I. Halperin. Theory of dynamic critical phenomena. *Rev. Mod. Phys.*, 49:435–479, Jul 1977.
- [41] M. Ishii. *Thermal-fluid dynamic theory of two-phase flow*. Eyrolles, Paris, 1975.
- [42] A. Jeffrey. *Quasilinear Hyperbolic Systems and Waves*. Research notes in mathematics. Pitman, 1976.
- [43] I. Jeon. Existence of gelling solutions for coagulation-fragmentation equations. *Commun. Math. Phys.*, 194:541 – 567, 1998.
- [44] B.L. Keyfitz and H.C. Kranzer. The riemann problem for a class of hyperbolic conservation laws exhibiting a parabolic degeneracy. *Journal of Differential Equations*, 47(1):35 – 65, 1983.
- [45] B.L. Keyfitz and H.C. Kranzer. Spaces of weighted measures for conservation laws with singular shock solutions. *J. Diff. Eq.*, 118:420 – 451, 1995.
- [46] S. N. Kružkov. First Order Quasilinear Equations in Several Independent Variables. *Sbornik: Mathematics*, 10(2):217–243, February 1970. (English translation: *Math. USSR Sbornik* 10 (1970) 217–273).
- [47] D. Kröner. *Numerical Schemes for Conservation Laws*. Advances in numerical mathematics. Wiley, 1997.
- [48] A. Kurganov, S. Noelle, and G. Petrova. Semidiscrete central-upwind schemes for hyperbolic conservation laws and hamilton-jacobi equations. *SIAM J. Sci. Comput.*, 23(3):707–740, 2006.
- [49] A. Kurganov and E. Tadmor. New high-resolution central schemes for nonlinear conservation laws and convection–diffusion equations. *Journal of Computational Physics*, 160(1):241–282, 2000.
- [50] P.D. Lax. Hyperbolic systems of conservation laws ii. *Communications on Pure and Applied Mathematics*, 10(4):537–566, 1957.
- [51] P. LeFloch. An existence and uniqueness result for two nonstrictly hyperbolic systems. In *Nonlinear Evolution Equations That Change Type*, volume 27, pages 126–138. Springer New York, 1990.

- [52] R.J. LeVeque. *Numerical Methods for Conservation Laws*. Lectures in Mathematics ETH Zürich, Department of Mathematics Research Institute of Mathematics. Springer, 1992.
- [53] R.J. LeVeque, L.R. J, and D.G. Crighton. *Finite Volume Methods for Hyperbolic Problems*. Cambridge Texts in Applied Mathematics. Cambridge University Press, 2002.
- [54] J. Li and H. Yang. Delta-shocks as limits of vanishing viscosity for multi-dimensional zero-pressure gas dynamics. *Quart. J. Math.*, 59(2):315–342, 2001.
- [55] J. Li and T. Zhang. Generalized Rankine-Hugoniot relations of delta-shocks in solutions of transportation equations. In G.-Q. Chen, Y. Li, X. Zhu, and D. Cao, editors, *Nonlinear Partial Differential Equations and Related Areas*. World Scientific, Singapore, 1999.
- [56] T.P. Liu. The entropy condition and the admissibility of shocks. *Journal of Mathematical Analysis and Applications*, 53(1):78–88, 1976.
- [57] T.P. Liu. Solutions in the large for the equations of nonisentropic gas dynamics. *Indiana University Mathematics Journal*, 26(1):147–177, 1977.
- [58] T.P. Liu. Transonic gas flow in a duct of varying area. *Arch. Ration. Mech. Anal.*, 23:1 – 18, 1982.
- [59] T.P. Liu. Nonlinear resonance for quasilinear hyperbolic equation. *J. Math. Phys.*, 28:2593 – 2602, 1987.
- [60] T.P. Liu and J.A. Smoller. On the vacuum state for the isentropic gas dynamics equations. *Advances in Appl. Math.*, 1:345 – 359, 1980.
- [61] X.D. Liu, S. Osher, and T. Chan. Weighted essentially non-oscillatory schemes. *Journal of Computational Physics*, 115(1):200–212, 1994.
- [62] M. Mazzotti. Nonclassical composition fronts in nonlinear chromatography: Delta-shock. *Ind. Eng. Chem. Res.*, 48:7733 – 7752, 2009.
- [63] M. Mazzotti, A. Tarafder, J. Cornel, F. Gritti, and G. Guiochon. Experimental evidence of a delta-shock in nonlinear chromatography. *J. Chromatography A*, 1217:2002 – 2012, 2010.
- [64] R. Menikoff and B.J. Plohr. The Riemann problem for fluid flow of real materials. *Rev. Mod. Phys.*, 61:75 – 130, 1989.
- [65] I. Müller and T. Ruggeri. *Rational extended thermodynamics, volume 37 of Springer tracts in natural philosophy*. Springer, New York, 1998.
- [66] R. Nigmatulin. *Dynamics of multiphase media, volume 1*. Hemisphere Publ., New York-Washington-Philadelphia-London, 1991.
- [67] T. Nishida and J. Smoller. Mixed problems for nonlinear conservation laws. *J. Diff. Equ.*, 23:244–269, 1977.

- [68] O.A. Oleinik. Uniqueness and stability of the generalized solution of the cauchy problem for a quasi-linear equation. *Uspekhi Mat. Nauk*, 14:165 – 170, 1959.
- [69] J. Rauch. BV estimates fail for most quasilinear hyperbolic systems in dimensions greater than one. *Comm. Math. Phys.*, 106(3):481–484, 1986.
- [70] B. Riemann. Über die Fortpflanzung ebener Luftwellen von endlicher Schwingungsweite. *Abhandlungen der Königlichen Gesellschaft der Wissenschaften in Göttingen*, 8:43–66, 1860.
- [71] P.L. Roe. Approximate riemann solvers, parameter vectors, and difference schemes. *Journal of Computational Physics*, 43(2):357–372, 1981.
- [72] R. Saurel and R. Abgrall. A multiphase Godunov method for compressible multifluid and multiphase flows. *J. Comput. Phys.*, 150:425 – 467, 1999.
- [73] D. Serre. *Systems of Conservation Laws 1: Hyperbolicity, Entropies, Shock Waves*. Cambridge University Press, 1999.
- [74] D. Serre and I.N. Sneddon. *Systems of Conservation Laws 2: Geometric Structures, Oscillations, and Initial-Boundary Value Problems*. Systems of Conservation Laws. Cambridge University Press, 1999.
- [75] S.F. Shandarin and Ya.B. Zeldovich. The large scale structure of the universe: Turbulence, intermittency, structures in a self-gravitating medium. *Reviews of Modern Physics*, 61:185 – 220, 1989.
- [76] W. Sheng and T. Zhang. *The Riemann problem for the transportation equations in gas dynamics*, volume No. 654, 137. Mem. Amer. Math. Soc., 1999.
- [77] Y.I. Shokin. *The method of differential approximation*. Springer-Verlag, Berlin Heidelberg, 1983.
- [78] J. Smoller. *Shock Waves and Reaction-diffusion Equations*. Grundlehren der mathematischen Wissenschaften. Springer-Verlag, 1994.
- [79] H.B. Stewart and B. Wendroff. Two phase flow: models and methods. *J. Comput. Phys.*, 56:363 – 409, 1984.
- [80] D. Tan, T. Zhang, and Y. Zheng. Delta-shock waves as limits of vanishing viscosity for hyperbolic systems of conservation laws. *J. Diff. Eq.*, 112:1 – 32, 1994.
- [81] F. Thein. *Results for Two Phase Flows with Phase Transition*. Phd thesis, Otto-von-Guericke-Universität Magdeburg, 2018.
- [82] V.A. Titarev and E.F. Toro. ADER: Arbitrary High Order Godunov Approach. *Journal of Scientific Computing*, 17:609–618, 2002.
- [83] E.F. Toro. *Riemann solvers and numerical methods for fluid dynamics*. Springer-Verlag Berlin Heidelberg, 3rd edition, 2009.

- [84] E.F. Toro, M. Spruce, and W. Speares. Restoration of the contact surface in the HLL-Riemann solver. *Shock Waves*, 4:25–34, 1994.
- [85] B. van Leer. Towards the ultimate conservative difference scheme III. Upstream-centered finite-difference schemes for ideal compressible flow. *Journal of Computational Physics*, 23(3):263–275, 1977.
- [86] B. van Leer. On the Relation Between the Upwind-Differencing Schemes of Godunov, Enguist-Osher and Roe. *SIAM J. Sci. Stat. Comput.*, 5(1):1–20, 1985.
- [87] W. Wagner and H.-J. Kretzschmar. *International Steam Tables: Properties of Water and Steam Based on the Industrial Formulation IAPWS-IF97*. Springer-Verlag Berlin Heidelberg, 2008.
- [88] R.F. Warming and B.J. Hyett. The modified equation approach to the stability and accuracy analysis of finite-difference methods. *Journal of Computational Physics*, 14(2):159–179, 1974.
- [89] G. Warnecke. *Analytische Methoden in der Theorie der Erhaltungsgleichung*. B.G. Teubner, Stuttgart-Leipzig, 1999.
- [90] H. Yang. Riemann problems for a class of coupled hyperbolic systems of conservation laws. *J. Diff. Equations*, 159:447 – 484, 1999.
- [91] H.C. Yee, R.F. Warming, and A. Harten. Implicit total variation diminishing (TVD) schemes for steady-state calculations. *Journal of Computational Physics*, 57(3):327–360, 1985.
- [92] Y. Zheng. Systems of conservation laws with incomplete sets of eigenvectors everywhere. In G.-Q. Chen, Y. Li, X. Zhu, and D. Cao, editors, *Nonlinear Partial Differential Equations and Related Areas*. World Scientific, Singapore, 1999.